

INFORMATION TO USERS

While the most advanced technology has been used to photograph and reproduce this manuscript, the quality of the reproduction is heavily dependent upon the quality of the material submitted. For example:

- Manuscript pages may have indistinct print. In such cases, the best available copy has been filmed.
- Manuscripts may not always be complete. In such cases, a note will indicate that it is not possible to obtain missing pages.
- Copyrighted material may have been removed from the manuscript. In such cases, a note will indicate the deletion.

Oversize materials (e.g., maps, drawings, and charts) are photographed by sectioning the original, beginning at the upper left-hand corner and continuing from left to right in equal sections with small overlaps. Each oversize page is also filmed as one exposure and is available, for an additional charge, as a standard 35mm slide or as a 17"x 23" black and white photographic print.

Most photographs reproduce acceptably on positive microfilm or microfiche but lack the clarity on xerographic copies made from the microfilm. For an additional charge, 35mm slides of 6"x 9" black and white photographic prints are available for any photographs or illustrations that cannot be reproduced satisfactorily by xerography.

Ditolla, Robert John

**RANDOM VIBRATION ANALYSIS BY THE POWER SPECTRUM AND
RESPONSE SPECTRUM METHODS**

The University of Arizona

Ph.D.

1986

**University
Microfilms
International** 300 N. Zeeb Road, Ann Arbor, MI 48106

RANDOM VIBRATION ANALYSIS BY THE
POWER SPECTRUM AND RESPONSE SPECTRUM METHODS

by

Robert John DiTolla

A Dissertation Submitted to the Faculty of the

DEPARTMENT OF CIVIL ENGINEERING

In Partial Fulfillment of the Requirements
For the Degree of

DOCTOR OF PHILOSOPHY

In the Graduate College

THE UNIVERSITY OF ARIZONA

1 9 8 6

THE UNIVERSITY OF ARIZONA
GRADUATE COLLEGE

As members of the Final Examination Committee, we certify that we have read
the dissertation prepared by Robert John DiTolla

entitled "Random Vibration Analysis by the Power Spectrum and Response
Spectrum Methods"

and recommend that it be accepted as fulfilling the dissertation requirement
for the Degree of Doctor of Philosophy

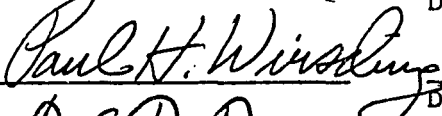
Ralph M. Richard



Date

6/10/86

Paul H. Wirsching



Date

6/11/86

Donald DaDeppo



Date

5/27/86

Date

Date

Final approval and acceptance of this dissertation is contingent upon the
candidate's submission of the final copy of the dissertation to the Graduate
College.

I hereby certify that I have read this dissertation prepared under my
direction and recommend that it be accepted as fulfilling the dissertation
requirement.


Dissertation Director

Date

6/10/86

STATEMENT BY AUTHOR

This dissertation has been submitted in partial fulfillment of requirements for an advanced degree at The University of Arizona and is deposited in the University Library to be made available to borrowers under rules of the Library.

Brief quotations from this dissertation are allowable without special permission, provided that accurate acknowledgement of source is made. Requests for permission for extended quotation from or reproduction of this manuscript in whole or in part may be granted by the head of the major department or the Dean of the Graduate College when in his or her judgment the proposed use of the material is in the interests of scholarship. In all other instances, however, permission must be obtained by the author.

SIGNED: Robert John Di Jolla

ACKNOWLEDGEMENTS

The author wishes to express his gratitude to the staff and faculty of the Departments of Civil Engineering and Optical Sciences for the opportunity to pursue advanced studies at the University of Arizona. In particular, to Dr. Ralph Richard for his continued instruction and guidance during the past several years.

The author would also like to acknowledge the inspiration and support which he has always received from his parents. In addition, special thanks to my wife, Maureen, for her support and assistance.

TABLE OF CONTENTS

	Page
LIST OF ILLUSTRATIONS	vi
LIST OF TABLES	x
ABSTRACT	xi
1. INTRODUCTION	1
2. THE POWER SPECTRUM METHOD AND RESPONSE	
SPECTRUM METHODS APPLIED TO SDOF SYSTEMS . .	6
A Random Process	6
Power Spectral Density	8
Autocorrelation Function	11
The Power Spectrum Method for	
SDOF Systems	13
Frequency Response Analysis of	
SDOF Systems	16
Example 2.1	19
Power Spectrum Method Using the	
Finite Element Method	21
The Response Spectrum Method for	
SDOF Systems	22
3. EVALUATION OF THE POWER SPECTRUM AND	
RESPONSE SPECTRUM METHOD FOR SDOF SYSTEMS . .	29
Response of a SDOF System to a	
White Noise Input	29
Response of a SDOF System to a Non-Uniform	
Spectral Density Input	34
4. RESPONSE OF MDOF SYSTEMS TO	
RANDOM EXCITATIONS	51
Modal Superposition Method For Decoupling	
MDOF Equations of Motion	51
Power Spectrum Method for MDOF Systems . . .	55
Calculating Internal Forces in the	
Power Spectrum Method	57

TABLE OF CONTENTS--Continued

	Page
Response Spectrum Method for MDOF Systems	61
Comparison of the Two Methods for Determining the Relative Displacements of MDOF Systems	64
5. APPLICATIONS	78
Design of the Support System for the SIRTF Primary Mirror	78
Modeling the Structure	80
Summary of Results	84
Example 5.1	93
Damping Evaluation with the White Noise Equation	98
Example 5.2	100
6. SUMMARY AND CONCLUSIONS	101
REFERENCES	104

LIST OF ILLUSTRATIONS

Figure		Page
2.1	A Record of a Random Time Function	7
2.2	An Ensemble of Random Time Functions . . .	7
2.3	Random Time Functions	9
2.4	Power Spectral Density Functions for Defining Random Time Functions . . .	12
2.5	A SDOF System Subjected to Support Excitation	18
2.6	Power Spectrum Method for a SDOF System	20
2.7	Vanmarcke's Illustration of the Mean-Square of a PSD Output Function	24
2.8	The Transfer Function for the Relative Displacement Response of a SDOF System	27
3.1	Relative Displacement Response Spectrum for White Noise Input . . .	31
3.2	Guidelines to the Use of the NASTRAN Numerical Integration Procedure	33
3.3a	Power Spectral Density Inputs With Positive Slopes	36
3.3b	Power Spectral Density Inputs With Negative Slopes	37

LIST OF ILLUSTRATIONS--Continued

Figure		Page
3.4	RMS Relative Displacement Response Spectra for Non-Uniform PSD Inputs	38
3.5a	Limitations of the Accuracy of the White Noise Approximation for PSD Inputs With Positive Slopes	42
3.5b	Limitations of the Accuracy of the White Noise Approximation for PSD Inputs With Negative Slopes	43
3.6	Comparison of PSD Output Functions Generated by the Power Spectrum Method and White Noise Approximation	45
3.7	The White Noise Approximation for Non-Constant PSD Input Functions	47
3.8	The White Noise Approximation for Large Fundamental Frequencies	48
3.9	The White Noise Approximation for Large Damping Ratios	49
4.1	A Three-Story Building Excited by a Random Ground Acceleration	59
4.2	Gain Functions for a Lightly Damped MDOF System	62
4.3	Correction Factor for Modal Interaction Using the RSS Method	66
4.4	Example 4.1a	70
4.5	Example 4.1b	71
4.6	Example 4.1c	72
4.7	Example 4.2a	73

LIST OF ILLUSTRATIONS--Continued

Figure		Page
4.8	Example 4.2b	74
4.9	Example 4.2c	75
4.10	Example 4.3a	76
4.11	Example 4.3b	77
5.1	Mounting the SIRTf Primary Mirror	79
5.2	Random Vibration y-axis and z-axis Interface Levels	81
5.3	Random Vibration x-axis Interface Levels	82
5.4	Complex Finite Element Model of the SIRTf Primary Mirror Support System	85
5.5	Free-Vibration Mode Shapes of the SIRTf Primary Mirror Support System	86
5.6	Simplified Finite Element Model of the SIRTf Primary Mirror Support System	88
5.7	SDOF Idealization of the SIRTf Primary Mirror Support System	90
5.8	Shear Forces and Bending Moments Applied to the Flexures About The Strong Axis	92
5.9	Shear Force Response Spectrum for y-axis Random Vibration	94
5.10	Bending Moment Response Spectrum for for y-axis Random Vibration	95
5.11	Maximum RMS Stress in the Flexures for Combined y-axis and z-axis Random Vibration	96

LIST OF ILLUSTRATIONS--Continued

Figure		Page
5.12	Dynamic Response at Resonant Frequency vs. Damping	99

LIST OF TABLES

		Page
Table		
3.1	Closed Form Solutions for the Gain Function and Variance of SDOF Systems Subjected to White Noise Inputs	30
5.1	Free Vibration Frequencies of the SIRT Primary Mirror Support System . . .	91

ABSTRACT

Determination of the stresses and displacements which occur in response to random excitations cannot be accomplished by traditional deterministic analysis methods. As the specification of the excitation and the response of the structure become more complex, solutions by direct, closed-form methods require extensive computations.

Two methods are presented which can be used in the analysis of structures which are subjected to random excitations. The Power Spectrum Method is a procedure which determines the random vibration response of the structure based upon a frequency response analysis of a structural model. The Response Spectrum Method is a method which is based upon specified forces or displacements as a function of time.

A derivation of each of the methods is presented and followed by comparisons of the results which were obtained for single and multiple-degree-of-freedom systems. Assumptions and limitations of the methods are discussed as well as their accuracy over ranges of frequency, damping and loading specification.

As a direct application and comparison of the two methods, an analysis of the support system for the primary mirror of the Space Infrared Telescope Facility (SIRTF) has been performed. In addition, a method for the evaluation of the critical damping in a single-degree-of-freedom structure is demonstrated.

CHAPTER 1

INTRODUCTION

All structures which possess mass and elasticity are capable of vibration. The study of vibration is concerned with the oscillatory motions of structures and the internal forces which develop as a consequence of these motions. Two basically different approaches can be used for the evaluation of the structural response to vibratory loadings. The choice of the method to be used depends upon the definition of the loading. If the entire time variation of the vibration is known, it is referred to as a prescribed dynamic loading. Computational methods for the determination of the stresses and displacements which result from prescribed dynamic loadings are called deterministic analyses. If the time variation of the vibration is not known but can be defined in a statistical sense, the loading is termed a random dynamic loading. A nondeterministic analysis method is used to provide statistical information about the motions which result from statistically defined random loadings.

Random vibration theory has become an important subject in the last 30 years, in part due to the advances

which have been made in high-speed flight vehicles. When application of the theory became necessary for design, it was not required to start from the beginning. Related problems such as those involving the response of a control system to random signals containing unwanted noise had been previously studied by Rice (1945), Laning (1956) and Bendat (1958). In addition, the mathematical basis of statistical mechanics was well understood and documented in works such as those by Cramer (1946), Feller (1950) and Davenport (1958). Another important contribution to the development of random vibration theory was in the studies of metal fatigue problems by Miner (1945), Miles (1954) and Powell (1958).

Based upon these and other similar studies, the mathematical theory of random vibrations was formulated and defined in works such as those by Thomson (1957), Crandall (1958) and Robson (1961). Advancement of random vibration theory was rapid as its application was spread to engineering analysis disciplines. All of the important developmental work in this discipline is numerous, however, the studies by Dyer (1961), Tack (1962) Clarkson (1962), Lyon (1962) and Hecker (1962) were among the most significant of the earlier works in which design methods for random vibration analysis were developed.

Early design methods for random vibration analysis relied heavily upon mathematical formulations of the

problem. Among the most often used of these methods for the analysis of linear structures which are subjected to a stationary and ergodic random process is referred to in this dissertation as the Power Spectrum Method. Documented by Crandall (1958), the Power Spectrum Method is important because it allows the statistical response of a linear structure to a stationary and ergodic random process to be evaluated by the methods of frequency response analyses.

Determination of the transfer function which is the goal of a frequency response analysis was often obtained experimentally for complex systems or analytically by solving the differential equations of motion. However, with the advent of high-speed computers and the development of the finite element method, numerical techniques for frequency response analysis for complex models have become available. Based upon the fundamentals of matrix algebra and energy methods in structural mechanics, the finite element method may be used to calculate the transfer function by the numerical evaluation of an analytical model which is subjected to a variable frequency harmonic loading (Kapur). The NASTRAN (NASA Structural Analysis) program is a current benchmark finite element program in the engineering profession which has the capability to perform frequency response analysis (Joseph).

Although the results from the Power Spectrum Method can be quite accurate, the cost and execution time of the method can be substantial for complex structural models, especially when performing parametric studies. Simpler and less costly alternatives to the Power Spectrum Method such as the Statistical Energy Method (Stearn) have been developed. Another method which has gained popularity as a less expensive approach to the solution of vibration problems, especially in the analysis of building structures to the random ground motion of earthquakes, is the Reponse Spectrum Method which is based on the work by Rosenblueth (1951). In the analysis of structures, the maximum displacement or force has the most practical value for design purposes. For a single-degree-of-freedom (SDOF) structure, this quantity is usually represented by the maximum force or relative displacement. Response spectra are plots of these peak response parameters as functions of natural frequency and damping.

Generation of response spectra are often made from an evaluation of vibration records by the Duhamel integral (Clough and Penzien). However, for a random excitation this type of deterministic approach is not valid. It has been suggested by Vanmarcke(1976) that response spectra can be generated from the power spectral density (PSD) functions which define the random excitation of a SDOF structure. These response spectra are obtained by the use

of the white noise approximation to the Power Spectrum Method as a solution for a SDOF structure which is subjected to a PSD input function.

As an approximate solution to problems which involve a non-uniform PSD input function, the white noise approximation (which is the basis of the Response Spectrum Method) is a valid approximation for certain ranges of damping, frequency and slope of the PSD input function. Although the white noise approximation has been used extensively (e.g. Hurty and Rubinstein) its limits of accuracy have not been documented. The primary goal of this dissertation is to quantify the limits of accuracy of the white noise approximation by comparing the approximate solutions using the Response Spectrum Method to solutions which were obtained by the Power Spectrum Method. No approximations or limitations with respect to frequency, damping or PSD slope were made in the development of the Power Spectrum Method (Crandall, 1958).

All random processes considered herein are assumed to be stationary and ergodic with a Gaussian (normal) probability distribution. The vibration response is assumed to be linear and the input functions are assumed to be non-correlated.

CHAPTER 2

THE POWER SPECTRUM METHOD AND RESPONSE SPECTRUM METHODS APPLIED TO SDOF SYSTEMS

Before the Power Spectrum and Response Spectrum Methods are discussed, it is important to define certain mathematical concepts and statistical terminology.

A Random Process

A number of physical phenomena occur by which an instantaneous value at any future time cannot be exactly predicted. Examples include the noise of a jet engine, the heights of waves in a choppy sea and the ground motion of an earthquake. Data of these types are known as random time functions. A typical continuous random time function is shown in Figure 2.1. Although the character of the function may be irregular, many continuous random phenomena exhibit some degree of statistical regularity whereby certain averaging procedures can be applied to establish useful engineering relationships.

In general, several records of the type shown in Figure 2.1 are necessary to establish statistical regularity for a random time function. The entire

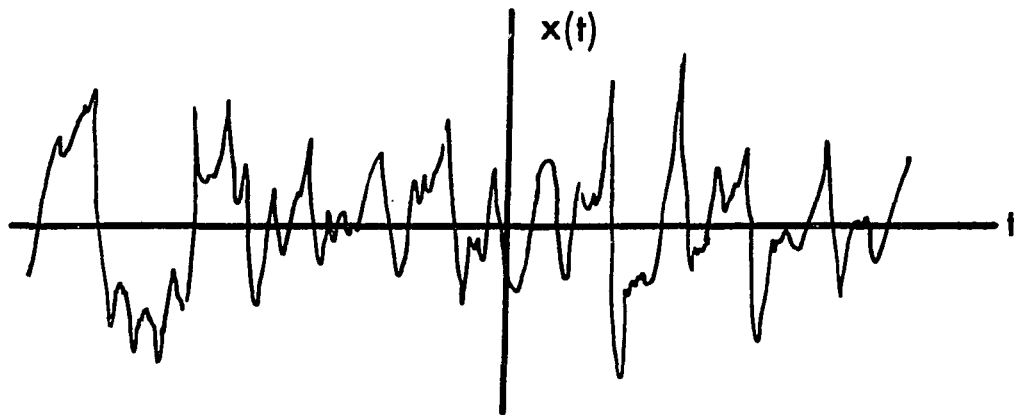


Figure 2.1. A Record of a Random Time Function

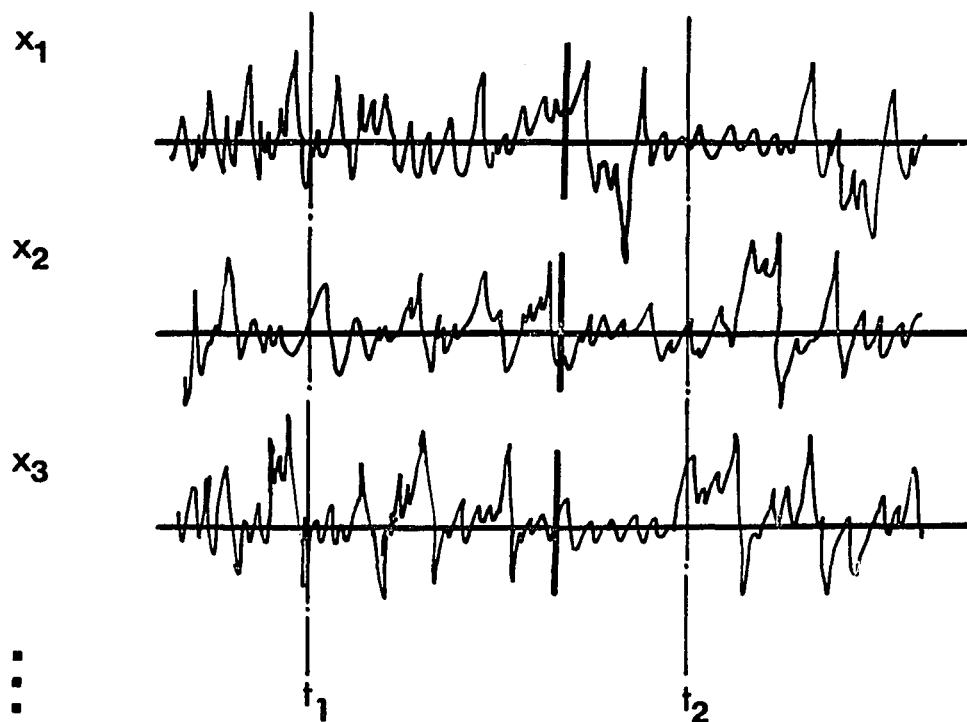


Figure 2.2. An Ensemble of Random Time Functions

collection of all such records is called an ensemble (Figure 2.2) and is said to constitute a random process. If at any time t , the values of the quantities $x_1(t_1)$, $x_2(t_1)$, ... , etc. are independent of t_1 the random process is said to be stationary. If the distribution of quantities $x_1(t_1)$, $x_1(t_2)$, ..., etc. at any one time is equal to the distribution with respect to time of any single random time function the random process is said to be ergodic. In this dissertaion all random processes are assumed to be continuous as well as both stationary and ergodic. These assumptions provide the capability to allow the statistical properties of a single random time function to define the statistical properties of the entire random process.

Power Spectral Density

An important statistical definition of a stationary and ergodic random process is known as the power spectral density (PSD). To develop the concept of power spectral density consider the continuous random time function $x(t)$ which has commenced at time $t = -\infty$ and continues until time $t = +\infty$ (Figure 2.3a). For a function of this type it is not possible to determine a Fourier transform (Robson). However, the Fourier transform of the function $x_T(t)$ shown in Figure 2.3b can be determined where $x_T(t)$ is defined to be identical with

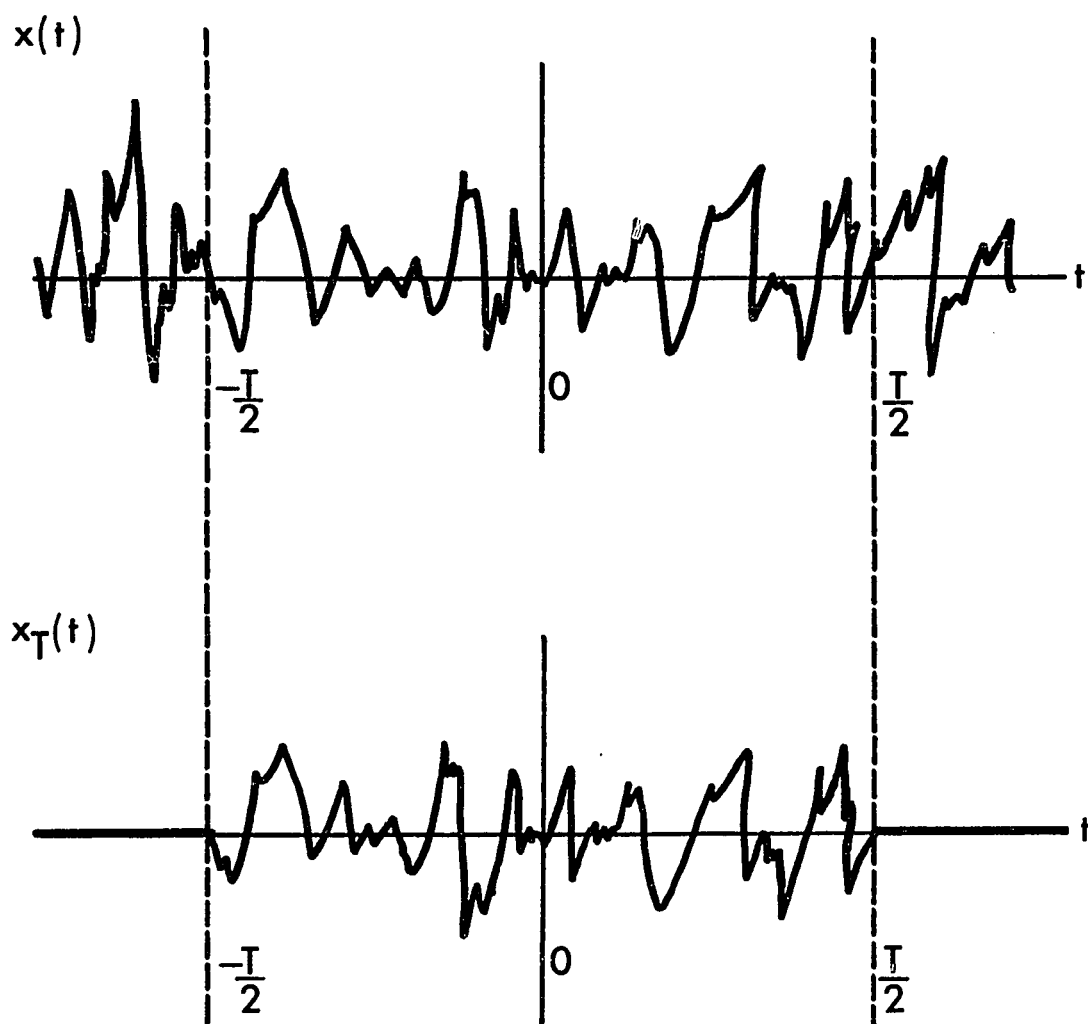


Figure 2.3. Random Time Functions

$x(t)$ over the interval $-T/2 < t < T/2$ and equal to zero at all other times. For the function $x_T(t)$ the mean-square value of x_T can be expressed in terms of the Fourier transform (Crandall, 1958) by the relationship:

$$\sigma_{x_T}^2 = \langle x_T^2(t) \rangle = \frac{1}{T} \int_{-T/2}^{T/2} x_T^2(t) dt \quad (2.1a)$$

$$= \frac{1}{T} \int_{-\infty}^{\infty} x_T^2(t) dt \quad (2.1b)$$

$$= \frac{2}{T} \int_0^{\infty} |A_T(if)|^2 df \quad (2.1c)$$

where:

$\sigma_{x_T}^2$ = mean-square value of the function x_T

$A_T(if)$ = Fourier transform of the function x_T .

As T approaches infinity, the mean-square value of the function $x(t)$ becomes:

$$\sigma_x^2 = \langle x^2(t) \rangle = \int_0^{\infty} \lim_{T \rightarrow \infty} \left[\frac{2}{T} |A_T(if)|^2 \right] df \quad (2.2a)$$

$$= \int_0^{\infty} S(f) df \quad (2.2b)$$

$$\text{where } S(f) = \lim_{T \rightarrow \infty} \left[\frac{2}{T} |A_T(if)|^2 \right]$$

The quantity $S(f)$ is called the power spectral density of the random time function $x(t)$. The power spectral density indicates the manner of distribution of the

harmonic content of the random time function over the frequency range from zero to infinity.

For illustration, typical PSD functions which have been generated from various random time functions are shown in Figure 2.4. The frequency content of the random time function in 2.4a is widely scattered and is characterized by a bounded PSD function which has its greatest values in the middle frequency range. In contrast, the PSD function shown in 2.4b is concentrated near a single frequency which reflects the narrow-band random time function. A limiting case is defined in 2.4c as the white noise condition which represents a random time function which contains a uniform spectrum over the full frequency range from zero to infinity. Additional information regarding the generation and measurement of PSD functions can be obtained from Crandall (1963) or Blackman (1958).

Autocorrelation Function

Another important statistical quantity which is necessary in the development of the theory of random vibration analysis is the autocorrelation function. For a random time function $x(t)$ such as that shown in Figure 2.1, the autocorrelation function $R(\tau)$ is defined as:

$$R(\tau) = \langle x(t) x(t + \tau) \rangle \quad (2.3)$$

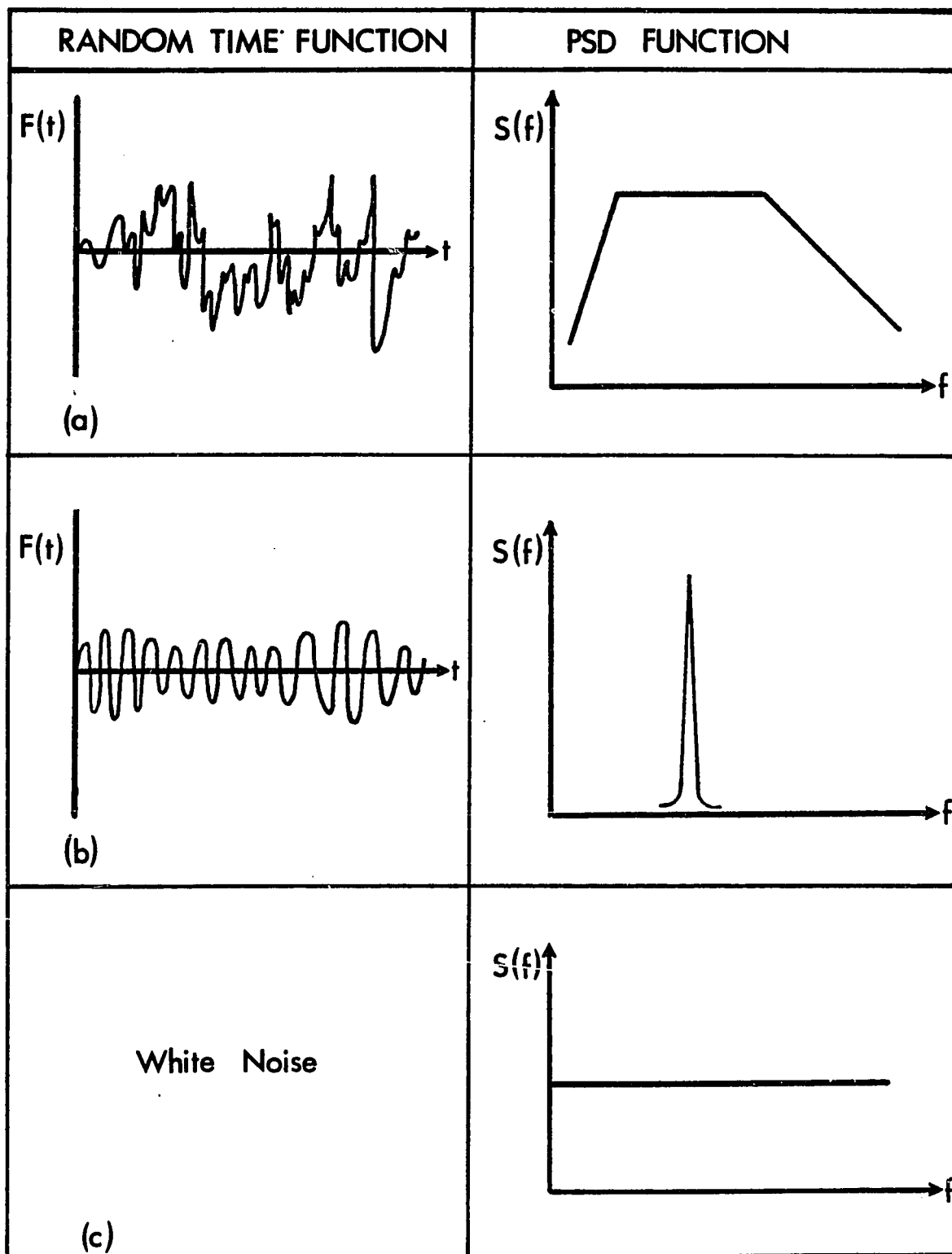


Figure 2.4. Power Spectral Density Functions for Defining Random Time Functions

The autocorrelation function can thus be determined by first multiplying the value of a quantity $x(t)$ at any time t by the value $x(t + \tau)$ when a time τ has elapsed. When all multiplications have been performed at all values of t , the mean value of all such products is taken and the result is the autocorrelation function.

To determine a relationship between two spectral density functions it is important to consider the Fourier transform relationship between the autocorrelation function and the power spectral density function. This important relationship has been developed in random vibration textbooks (e.g. Robson) and is given by:

$$S(\omega) = 2 \int_{-\infty}^{\infty} R(\tau) e^{-i\omega\tau} d\tau \quad (2.4)$$

The Power Spectrum Method for SDOF Systems

To determine the response of a linear SDOF structure to a stationary and ergodic random process by the Power Spectrum Method first consider the autocorrelation function of a response function $x(t)$. From equations 2.3 and 2.1:

$$\begin{aligned} R_x(\tau) &= \langle x(t) x(t + \tau) \rangle \\ &= \lim_{T \rightarrow \infty} \frac{1}{2T} \int_{-T}^T x(t) x(t + \tau) dt \end{aligned} \quad (2.5)$$

To evaluate equation 2.5 the following relationship for the response $x(t)$ is used (Crandall, 1958):

$$x(t) = \int_0^{\infty} h(\tau) f(t - \tau) d\tau \quad (2.6a)$$

where $h(\tau)$ is the unit impulse response function which is the Fourier transform of the transfer function, $H(\omega)$ and is given by:

$$h(\tau) = \frac{1}{2\pi} \int_{-\infty}^{\infty} H(\omega) e^{i\omega\tau} d\omega \quad (2.6b)$$

and $f(t)$ is the excitation function. Substitution of equation 2.6a into equation 2.5 and interchanging the order of integration produces:

$$R_x(\tau) = \int_0^{\infty} h(\tau_1) d\tau_1 \int_0^{\infty} h(\tau_2) d\tau_2 \lim_{T \rightarrow \infty} \frac{1}{2T} \int_{-T}^T f(t - \tau_1) f(t - \tau_1 - \tau_2) dt \quad (2.7)$$

Because $f(t)$ is a stationary random process, the third integral in equation 2.7 is the autocorrelation function for f and equation 2.7 becomes:

$$R_x(\tau) = \int_0^{\infty} h(\tau_1) d\tau_1 \int_0^{\infty} h(\tau_2) R_f(\tau + \tau_2 - \tau_1) d\tau_2 \quad (2.8)$$

A direct evaluation of equation 2.8 is extremely complex. It is usually easier to consider its Fourier transform equivalent. Substitution of equation 2.8 into equation 2.4 yields an expression for the power spectral density of the response:

$$S_x(\omega) = 2 \int_{-\infty}^{\infty} e^{-i\omega\tau} d\tau \int_0^{\infty} h(\tau_1) d\tau_1 \int_0^{\infty} h(\tau_2) R_x(\tau_1 - \tau_2 - \tau) d\tau_2 \quad (2.9)$$

Because $h(t)$ is identically zero for all $t < 0$ it is possible to lower the limits of integration in equation 2.9 from zero to $-\infty$. Interchanging the resulting equation yields:

$$S_x(\omega) = 2 \int_{-\infty}^{\infty} h(\tau_1) d\tau_1 \int_{-\infty}^{\infty} h(\tau_2) d\tau_2 \int_{-\infty}^{\infty} e^{-i\omega t} R_f(\tau + \tau_2 - \tau_1) d\tau \quad (2.10)$$

Letting $\tau + \tau_2 - \tau_1 = \tau_3$ and rearranging the exponentials produces:

$$S_x(\omega) = 2 \int_{-\infty}^{\infty} h(\tau_1) e^{-i\omega\tau_1} d\tau_1 \int_{-\infty}^{\infty} h(\tau_2) e^{i\omega\tau_2} d\tau_2 \int_{-\infty}^{\infty} R_f(\tau_3) e^{-i\omega\tau_3} d\tau_3 \quad (2.11)$$

Substitution of the Fourier transform relationship given by equation 2.4 into equation 2.11 and the substitution of the inverse of equation 2.6b which is given by:

$$H(\omega) = \int_{-\infty}^{\infty} h(t) e^{-i\omega t} dt \quad (2.12)$$

produces the following relationship

$$S_x(\omega) = H(\omega) H(-\omega) S_f(\omega) \quad (2.13a)$$

$$= H(\omega) \bar{H}(\omega) S_f(\omega) \quad (2.13b)$$

$$= |H(\omega)|^2 S_f(\omega) \quad (2.13c)$$

Equation 2.13c is the basis of the Power Spectrum Method. It defines the power spectral density of the response $S_x(\omega)$ as the product of the power spectral density of the excitation $S_f(\omega)$ and the square of the gain

function. The gain function, $|H(\omega)|$, is defined by:

$$H(\omega) = |H(\omega)| e^{i\psi} \quad (2.13d)$$

where: $|H(\omega)|$ = the amplitude of the transfer function
(gain function)

and ψ = the phase angle of the transfer function.

Of particular interest in the evaluation of the response of most structures to a random vibration is the variance or mean-square of the response. From equation 2.2b, the mean-square of the response is related to the PSD of the response by:

$$\sigma_x^2(\omega) = \int_0^\infty S_x(\omega) d\omega$$

and from equation 2.13:

$$\sigma_x^2(\omega) = \int_0^\infty |H(\omega)|^2 S_f(\omega) d\omega \quad (2.14)$$

The root-mean-square (RMS) is defined as σ , or as the square root of the expression defined in equation 2.14.

Frequency Response Analysis of SDOF Systems

The importance of the transfer function, $H(\omega)$ in random vibration analysis is apparent in the previous derivation of the Power Spectrum Method. For a SDOF system $H(\omega)$ can be determined from the frequency response solution to the dynamic equation of motion. Calculation of transfer functions are dependent upon the form of the

excitation and the type of output. As an example, the SDOF system shown in Figure 2.5 is subjected to an acceleration of its support and the output is the relative displacement of the mass. For this system, the equation of motion becomes:

$$m\ddot{x} + c\dot{x} + kx = -m\ddot{x}_g \sin \bar{\omega}t \quad (2.15)$$

where:

- m = mass of the system
- c = damping coefficient
- k = structural stiffness
- x_t = total displacement
- $= x_g + x$
- x_g = displacement of the support
- \ddot{x}_g = acceleration of the support applied to at a circular frequency ω .

The general solution to the second-order, linear differential equation (2.15) is the complementary solution to the homogeneous equation and a particular solution to the specified loading. The complementary solution is the transient, or the free-vibration response which will often damp out quickly and have a negligible effect upon the total solution (Clough and Penzien). The particular solution is the steady-state response at the frequency of the applied loading, but not in phase, is:

$$x(t) = \frac{m\ddot{x}_g}{k} \frac{1}{[(k - m\omega^2)^2 + (c\omega)^2]^{\frac{1}{2}}} \sin(\bar{\omega}t - \phi) \quad (2.16)$$

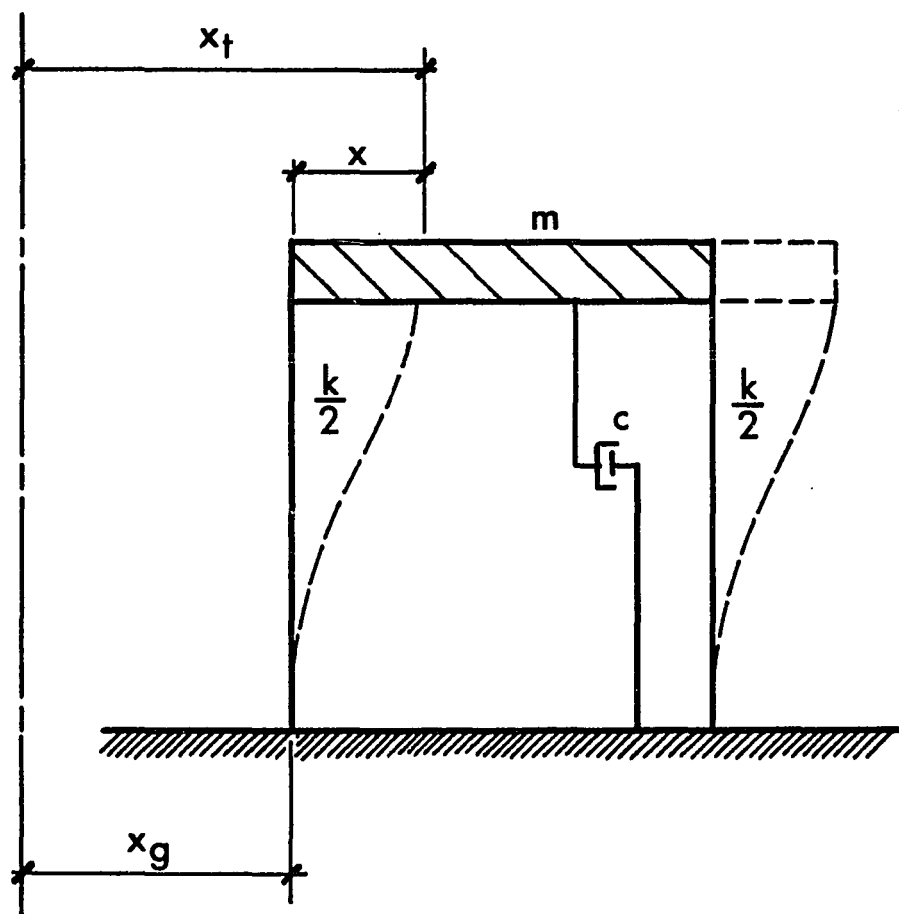


Figure 2.5. A SDOF System Subjected to Support Excitation

$$\text{or: } x(t) = \rho \sin(\bar{\omega}t - \theta) \quad (2.17)$$

where: ρ = amplitude of the steady-state response

$$= \frac{m\ddot{x}_g}{k} H(\omega)$$

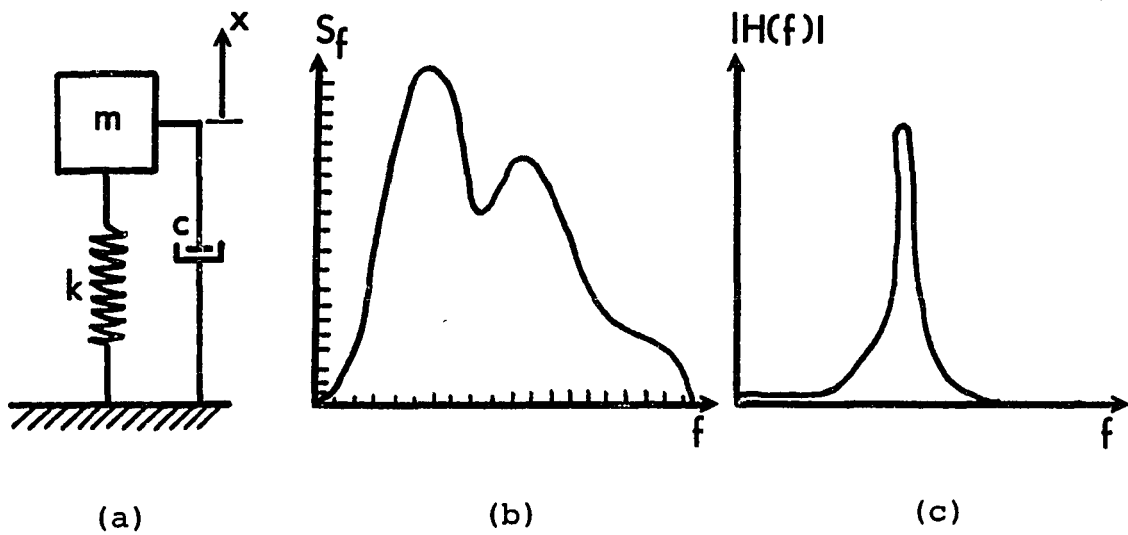
in which:

$$H(\omega) = \frac{m}{[(k - m\omega^2)^2 + (c\omega)^2]^{\frac{1}{2}}} = \text{transfer function.}$$

For this example, the transfer function can be thought of as a magnification factor which represents the ratio of the steady-state dynamic displacement to the displacement which results when the exciting force is applied statically (Hurty and Rubinstein).

Example 2.1

As an application of the Power Spectrum Method for the analysis of a linear SDOF system, consider the structure shown in Figure 2.6a which is subjected to the single-point random base acceleration input shown in Figure 2.6b. The transfer function has been calculated from equation 2.16 and is shown in Figure 2.6c. The mean-square value of the relative displacement of the mass is calculated numerically and is shown in the accompanying table.



f (Hz)	$S_f(f)$	$ H(f) $	$ H(f) ^2 \Delta f$	$S_f H(f) ^2 \Delta f$
0	0.	1.0	10.	0.
10	0.	1.0	10.	0.
20	0.2	1.0	10.	2.
30	0.6	1.0	10.	6.
40	1.2	1.0	10.	12.
50	1.8	1.2	14.4	25.92
60	1.8	1.6	25.6	46.08
70	1.1	2.0	40.0	44.9
80	0.9	3.7	136.9	123.21
90	1.1	5.4	291.6	320.76
100	1.2	3.0	90.0	108.
110	1.1	1.4	19.6	21.56
120	0.8	0.6	3.6	2.88
130	0.6	0.1	0.1	.06
140	0.3	0.	0.	0.
150	0.2	0.	0.	0.
160	0.2	0.	0.	0.
170	0.2	0.	0.	0.
180	0.1	0.	0.	0.
190	0.1	0.	0.	0.
200	0.5	0.	0.	0.
210	0.	0.	0.	0.
				$\sigma_x^2 = 712.47g^2$

Figure 2.6. Power Spectrum Method for a SDOF System

Power Spectrum Method Using the Finite Element Method

In Example 2.1 it was demonstrated that the PSD of the response can be calculated from the PSD of the input if the transfer function has been determined. The transfer function of a structure can often be obtained experimentally by applying to the base of the structure a variable frequency sinusoidal shaker with a constant input (Thomson 1981). Alternatively, for simple structural models analytical methods may be used to determine the transfer functions. For complex structures, frequency response analyses can be accomplished numerically by using the finite element method.

The finite element method is a well documented analysis method in structural mechanics (e.g. Cook, Gallagher, Zienkiewicz). To solve frequency response analysis problems by the finite element method, the dynamic equation of motion (equation 2.15) is solved numerically by either a direct or modal approach (Joseph). Details of the modal approach are presented in Chapter 4.

The final step in the Power Spectrum Method using the finite element method is a similar data reduction procedure that was applied to the results of the frequency response analysis shown in Example 2.1. In NASTRAN, this procedure is a numerical solution of equation 2.13 which is performed at user-selected frequencies. The

mean-square of the response is also calculated numerically by determining the area under the output spectral density curve by the trapezoidal rule (Joseph).

The Response Spectrum Method for SDOF Systems

In analyzing linear, elastic SDOF systems by the Response Spectrum Method, a response spectrum is calculated to predict the peak response of single-degree-of-freedom oscillators. Response spectra are plots of maximum response parameters for a SDOF structure as functions of the natural frequency and damping. For non-deterministic analysis, approximate response spectra can be generated by considering the white noise solution of equation 2.14 as the solution for the SDOF structure which is subjected to a stationary and ergodic random process which has been defined in terms of a PSD function.

An illustration of the white noise solution to equation 2.14 has been given by Vanmarcke (1976). This illustration shows the approximations which are inherent in the use of the white noise solution. Vanmarcke's illustration of the white noise solution to equation 2.14 is based upon the following representation of the integral in equation 2.14:

$$\sigma_x^2(\omega) = \int_0^\infty |H(\omega)|^2 S_f(\omega_n) d\omega + \int_0^{\omega_n} S_f(\omega) d\omega - \omega_n S_f(\omega_n) \quad (2.18)$$

where: ω_n = natural frequency of the system

$S_f(\omega_n)$ = value of the PSD input function at the natural frequency.

In Figure 2.7 the contribution of each of the three terms of Equation 2.18 is illustrated. For small damping, the value of the gain function squared is assumed to be unity at all frequencies less than the natural frequency and zero at all frequencies greater than the natural frequency.

The first term in Equation 2.18 is the area between zero and infinity which is obtained by multiplying the gain function squared by a constant spectral density (Figure 2.7a). The second term is the area obtained when the gain function squared is multiplied by the actual spectral density input function (Figure 2.7b). The third term is subtracted because that area would otherwise be added twice (Figure 2.7c).

As an example of the application of equation 2.18, a SDOF system was examined which was subjected to an acceleration of its base and the output was the relative displacement of the mass. The transfer function for this system is given by:

$$H(\omega) = \left[(\omega_n^2 - \omega^2)^2 + 4\xi^2 \omega_n^2 \omega^2 \right]^{-1/2} \quad (2.19)$$

where ξ = damping ratio in the system.

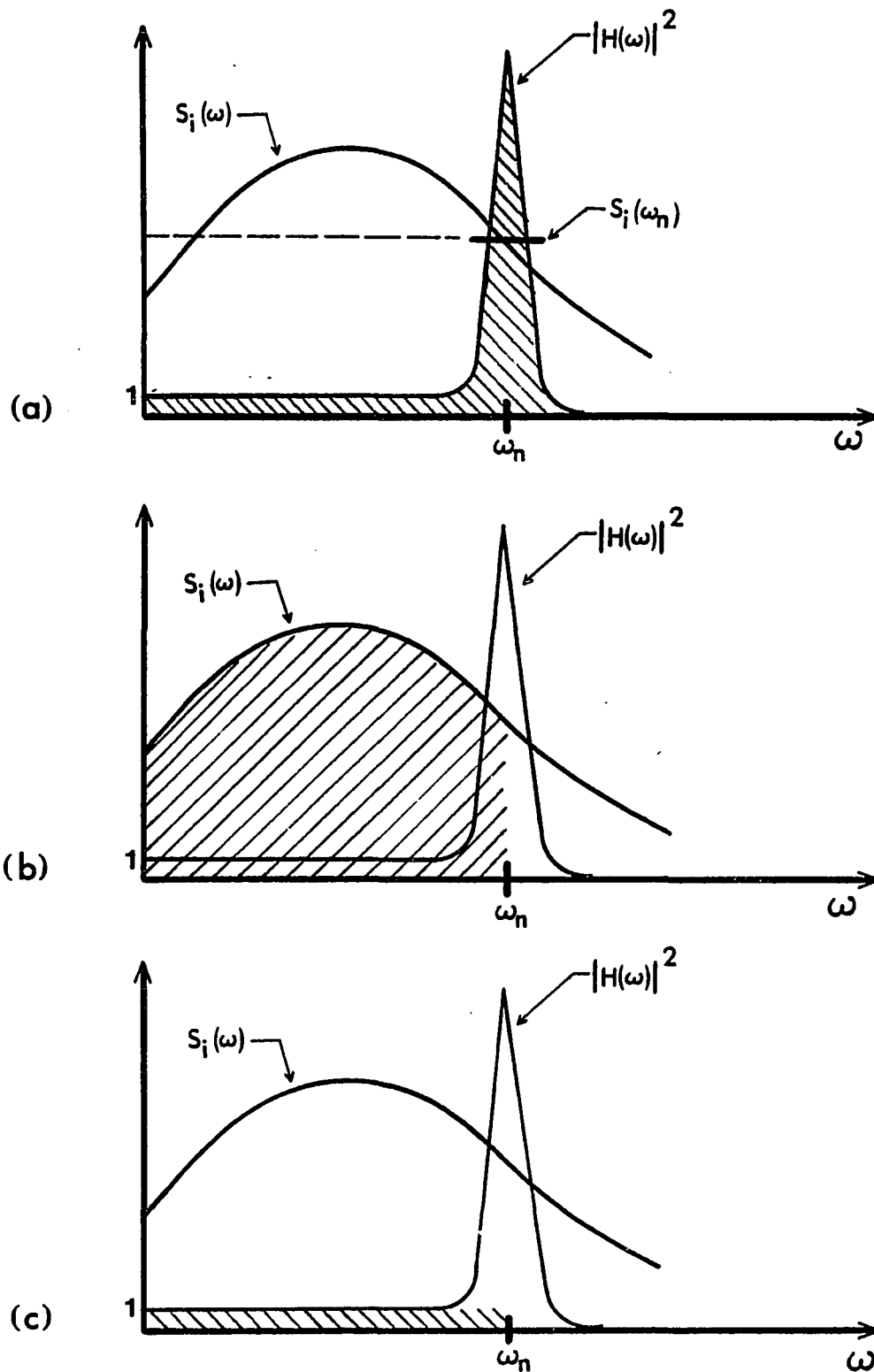


Figure 2.7. Vanmarcke's Illustration of the Mean-Square of a PSD Output Function

Substitution of equation 2.19 into the first term of equation 2.18 yields:

$$\int_0^{\infty} |H(\omega)|^2 S_f(\omega_n) d\omega = S_f(\omega_n) \int_0^{\infty} \left[(\omega_n^2 - \omega^2)^2 + 4\xi^2 \omega_n^2 \omega^2 \right]^{-\frac{1}{2}} d\omega \quad (2.20)$$

When the damping is small, the integral in equation 2.20 can be evaluated by the method of residues (Crandall, 1958) to obtain:

$$\int_0^{\infty} |H(\omega)|^2 S_f(\omega_n) d\omega = S_f(\omega_n) \frac{\omega_n \pi}{4\xi \omega_n^4} \quad (2.21a)$$

where $S_f(\omega_n)$ is given in units of g^2/ω , where g equals the acceleration of gravity which is 386 in/sec^2 in English units. Conversion to the more commonly used units of g^2/Hz produces:

$$\int_0^{\infty} |H(\omega)|^2 S_f(\omega_n) d\omega = \frac{1}{\omega_n^4} \left[\frac{S_f(f_n) \pi f_n}{4\xi} \right] \quad (2.21b)$$

Substitution of equation 2.21b into equation 2.18 yields:

$$\sigma_x^2(\omega) = \frac{1}{\omega_n^4} \left[\frac{S_f(f_n) \pi f_n}{4\xi} \right] + \int_0^{\infty} S_f(\omega) d\omega - \omega_n S_f(\omega_n) \quad (2.22)$$

For lightly damped systems, the first term in equation 2.22 will predominate (Vanmarcke, 1976). A further approximation is obtained by the substitution of $S_f(\omega_n)$ for $S_f(\omega)$ in the second term. This substitution

equalizes the last two terms and permits them to be cancelled from the equation. The resulting expression:

$$\sigma_x(\omega) = \frac{1}{\omega_n^2} \left[\frac{S_f(f_n) \pi f_n}{4\xi} \right]^{1/2} \quad (2.23)$$

is known as the white noise solution for a SDOF system with base acceleration input and relative displacement output.

Two of the approximations which were made in the development of equation 2.23 are extremely important and their consequences will be evaluated in the subsequent chapters when the approximation is applied to both single and multiple-degree-of-freedom systems. In general, the damped vibration frequency is given by:

$$\omega_D = \omega_n \sqrt{1 - \xi^2} \quad (2.24)$$

where ω_D = damped vibration frequency.

For structural systems with small damping ratios, the damped frequency differs very little from the undamped frequency. In the generation of equation 2.18, small levels of damping were assumed. This allowed the transfer function to be represented by a sharp peak at the resonant frequency, a value of unity for frequencies less than resonance and a value of zero for frequencies greater than resonance. Examination of Figure 2.8 demonstrates that there will be a practical limit to these assumptions.

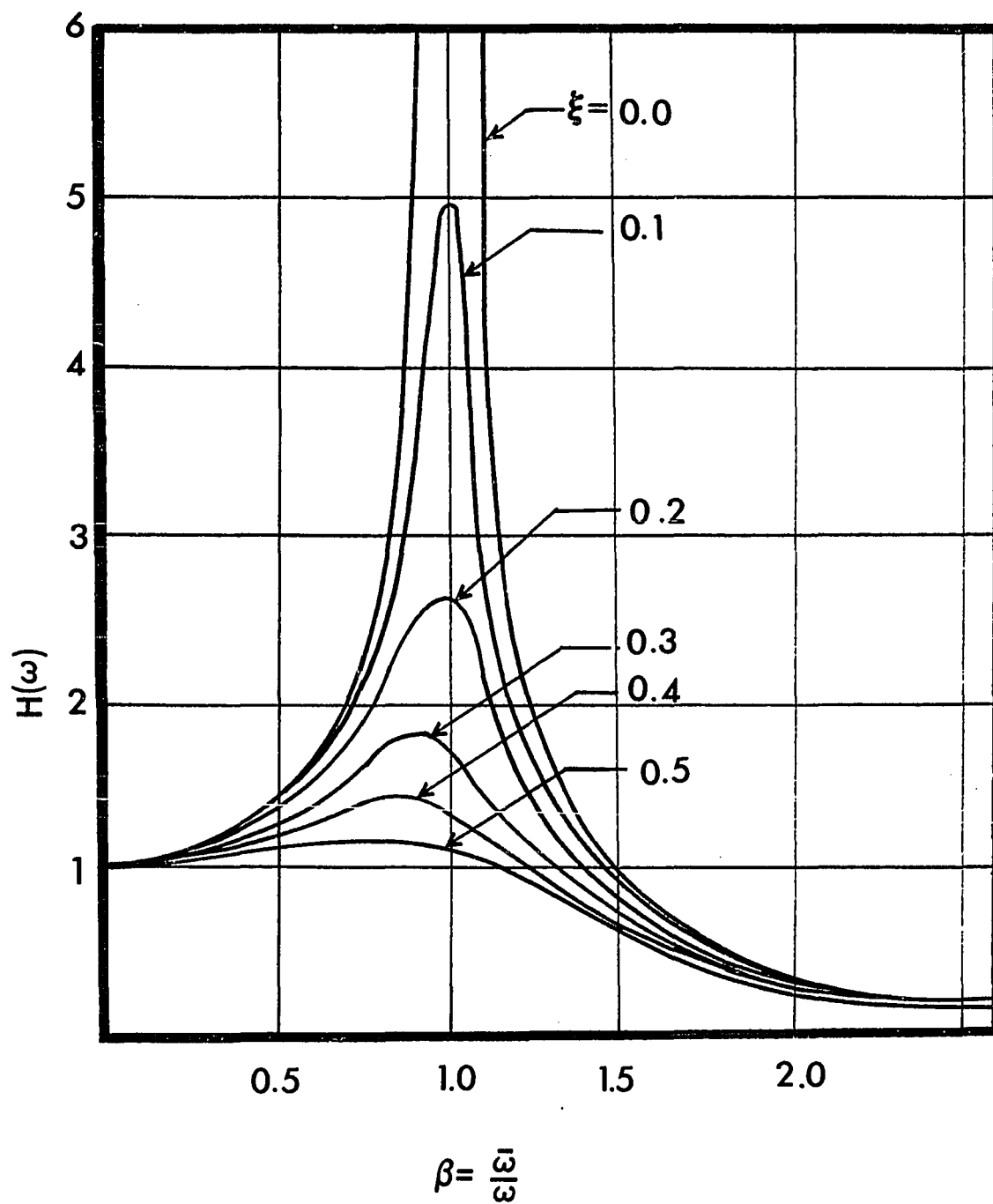


Figure 2.8. The Transfer Function for the Relative Displacement Response of a SDOF System

The reduction of equation 2.22 to equation 2.23 was made with the assumption that the value of the input power spectral density function $S_f(f)$ is constant. Indeed, for the white noise condition it will be shown that no approximation is introduced by the substitution of $S_f(f_n)$ for $S_f(f)$. However, for PSD input functions which are not constant an approximation results, and the difference between $S_f(f_n)$ and $S_f(f)$ becomes magnified in the higher frequency ranges.

CHAPTER 3

EVALUATION OF THE POWER SPECTRUM AND RESPONSE SPECTRUM METHODS FOR SDOF SYSTEMS

Response of a SDOF System to a White Noise Input

As was demonstrated in the previous chapter, the Response Spectrum Method is an approximation to the Power Spectrum Method and is based upon the white noise input for the calculation of the response spectrum for a SDOF oscillator. Therefore, the closed-form solutions for the responses which are summarized in Table 3.1 produce exact solutions for the response spectra of a SDOF system when it is subjected to white noise input. A typical response spectrum for the load case of a $1.0 \text{ g}^2/\text{Hz}$ white noise acceleration input and RMS relative displacement output has been computed using Equation 2.23 and is shown in Figure 3.1.

To gain confidence in the application of the Power Spectrum Method a series of SDOF models was analyzed using the NASTRAN finite element program. The finite element models were subjected to the same magnitude of white noise PSD base acceleration input as was used in the derivation of Figure 3.1. Excellent correlation between the Power

TABLE 3.1

Closed Form Solutions for the Gain Function and Variance of SDOF Systems
Subjected to White Noise Inputs

Type of loading	input spectral	output spectral density	gain function $ H(\omega) $	response
Force excited system	$p(t)$	$x(t)$	$[(k-m\omega^2)^2 + (c\omega)^2]^{-1/2}$	$\sigma_x^2 = 0.785 f_n S_f / \xi k^2$
	$p(t)$	$\ddot{x}(t)$	$\frac{\omega^2}{[(k-m\omega^2)^2 + (c\omega)^2]^{-1/2}}$	not finite
	$p(t)$	$F(t)$	$\left[\frac{k^2 + (c\omega)^2}{(k-m\omega^2)^2 + (c\omega)^2} \right]^{1/2}$	$\sigma_F^2 = 0.785 f_n S_f (1 + 4\xi^2) / \xi$
Base excited system	$y(t)$	$x(t)$	$\left[\frac{k^2 + (c\omega)^2}{(k-m\omega^2)^2 + (c\omega)^2} \right]^{1/2}$	$\sigma_x^2 = 0.785 f_n S_f (1 + 4\xi^2) / \xi$
	$\ddot{y}(t)$	$z(t)$	$\frac{m}{[(k-m\omega^2)^2 + (c\omega)^2]^{1/2}}$	$\sigma_z^2 = S_f / 1984 \xi f_n^3$
	$\ddot{y}(t)$	$\ddot{z}(t)$	$\frac{m\omega^2}{[(k-m\omega^2)^2 + (c\omega)^2]^{1/2}}$	not finite

$x(t)$ = absolute displacement of mass

$y(t)$ = base displacement

$z(t)$ = displacement of mass relative to ground

$F(t)$ = force on system

k = stiffness

m = mass

c = damping coefficient

σ^2 = mean-square of the response

S_f = PSD input function

ξ = damping ratio

f_n = natural frequency

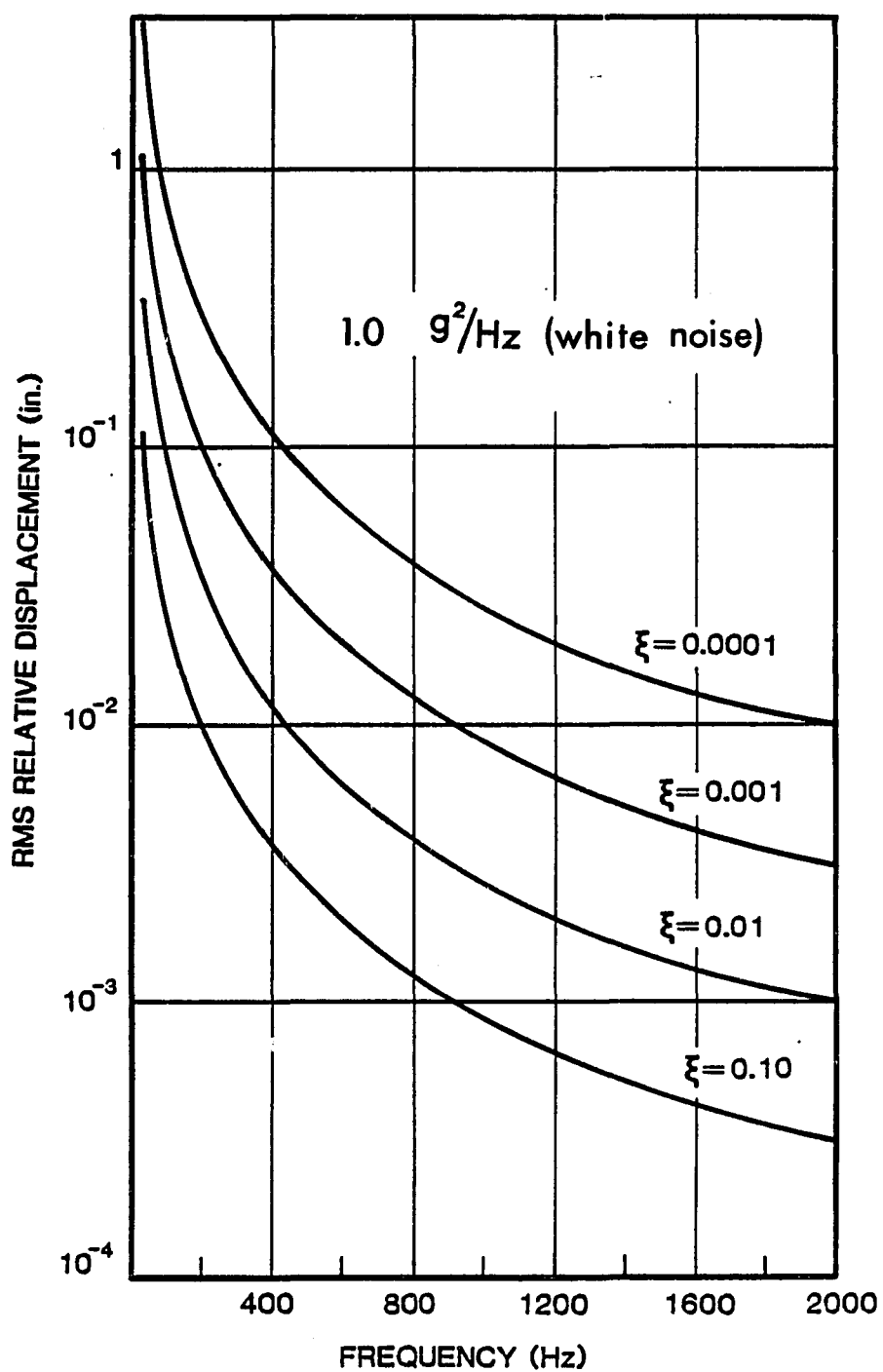


Figure 3.1. Relative Displacement Response Spectrum for White Noise Input

Spectrum Method and the white noise solution was obtained. Differences of less than 0.1 percent in the value of the root-mean-square (RMS) relative displacements were obtained. Each of the other loading cases in Table 3.1 (for which a finite response has been defined) was also tested for a white noise PSD input by the Power Spectrum Method with equal success in correlation with the white noise equation. In the execution of the Power Spectrum Method, the bandwidth of the PSD input was approximately five times the natural frequency of the system. This was done to obtain the high level of accuracy.

Results from the Power Spectrum Method were obtained with a numerical integration procedure contained within the NASTRAN program. This integration procedure uses the trapezoidal rule and is sensitive to the parameters which must be specified in the input to the program. The use of these parameters is not well documented by the program literature.

Shown in Figure 3.2 are typical PSD output curves. Accurate solutions with the NASTRAN numerical integration method for determining the mean-square of a response variable by calculating the area underneath a PSD output curve can be obtained by observing the following conditions. This study was made as part of a numerical testing procedure to ascertain the performance of the NASTRAN program.

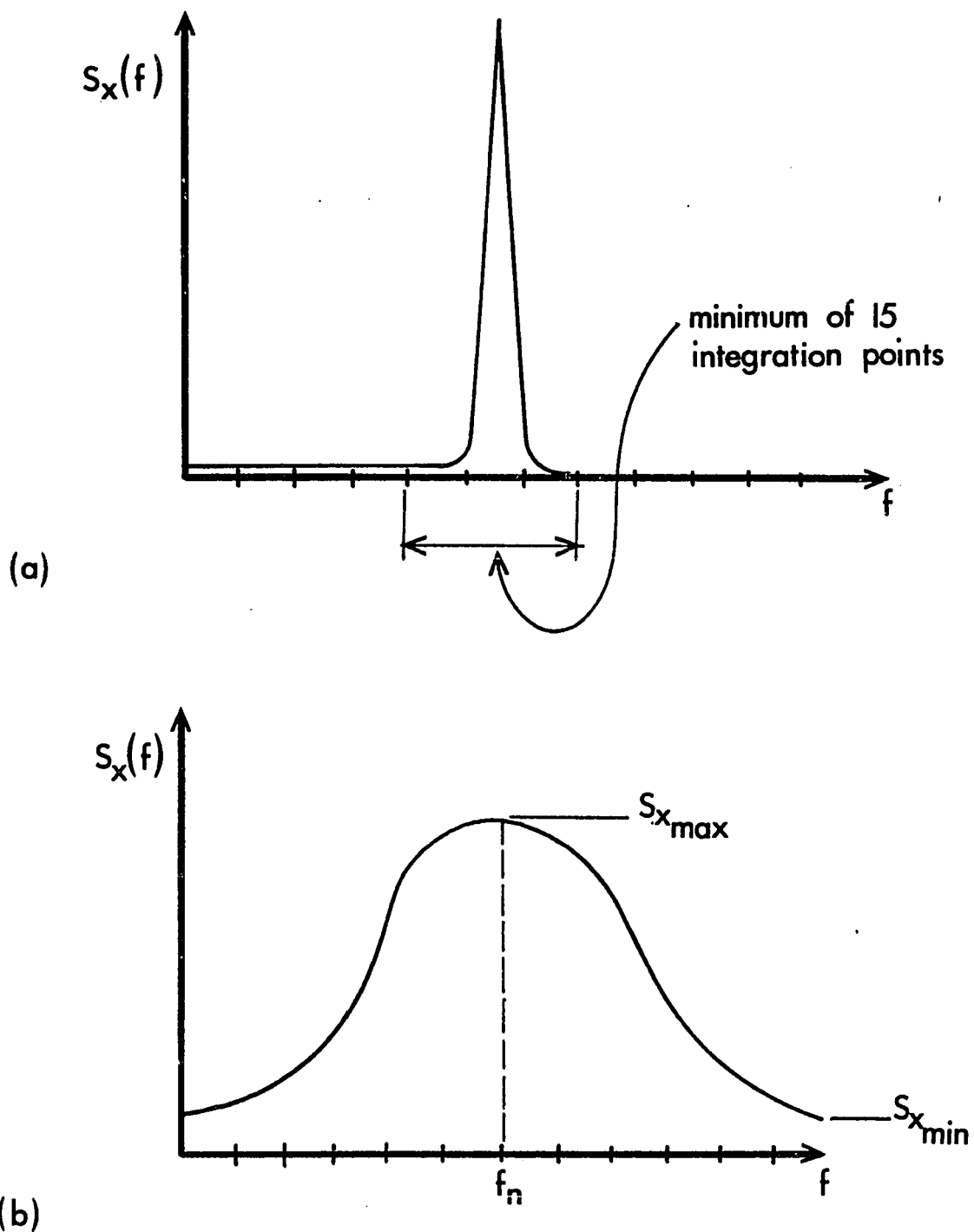


Figure 3.2. Guidelines to the Use of the NASTRAN Numerical Integration Procedure

- 1) The shape of the curve is dependent upon the fundamental frequency of the system and the damping ratio. If the number of integration points for a sharply-peaked curve is too few (resulting in a wide integration interval), the calculated area will be too large. At least 15 to 20 points should be defined within the points where $S_x(f) \approx 0$ as shown in (Figure 3.2a).
- 2) The points where $S_x(f) \approx 0$ must be included within the limits of integration. The value of $S_x(f)_{\max}$ should be at least 3 orders of magnitude greater than $S_f(f)_{\min}$ (Figure 3.2b).
- 3) Since specific integration points may be input in the program, the fundamental frequency, f_n should be one of these specified points.

Response of a SDOF System to a Non-Uniform Spectral Density Input

For a general PSD function, certain approximations were introduced by adopting the white noise solution (see Chapter 2). The accuracy of the white noise equation in predicting the response of a SDOF system to a non-uniform spectral density input is limited by these approximations. Using the Power Spectrum Method as a basis of comparison, the validity of the white noise approximation was tested

for limiting values of frequency, damping and slope of the input spectral density curve.

Application of the white noise approximation to SDOF systems was made with base acceleration input spectral density functions having the slopes as shown in Figures 3.3a and 3.3b. Calculations of the response spectra of the RMS relative displacement were made and are presented in Figure 3.4a thru 3.4h. Ranges of damping and frequency were based on values which often occur in engineering problems.

Solutions for the same spectral density inputs to the SDOF systems were also obtained by the Power Spectrum Method and are indicated by the dashed lines in Figures 3.4a thru 3.4h. For curves in which only solid lines are shown, the RMS relative displacements obtained by the two methods differed by less than 1% for all frequencies less than 2000 Hz. As demonstrated by these figures, the accuracy of the white noise approximation depends upon a combination of damping, frequency and the slope of the PSD input function.

To quantify the limits of accuracy of the white noise approximation, Figures 3.5a and 3.5b were constructed from the response spectrum curves. Using these figures, one can estimate the maximum value of the damping ratio for which the white noise approximation produces a difference of less than 5% with the Power

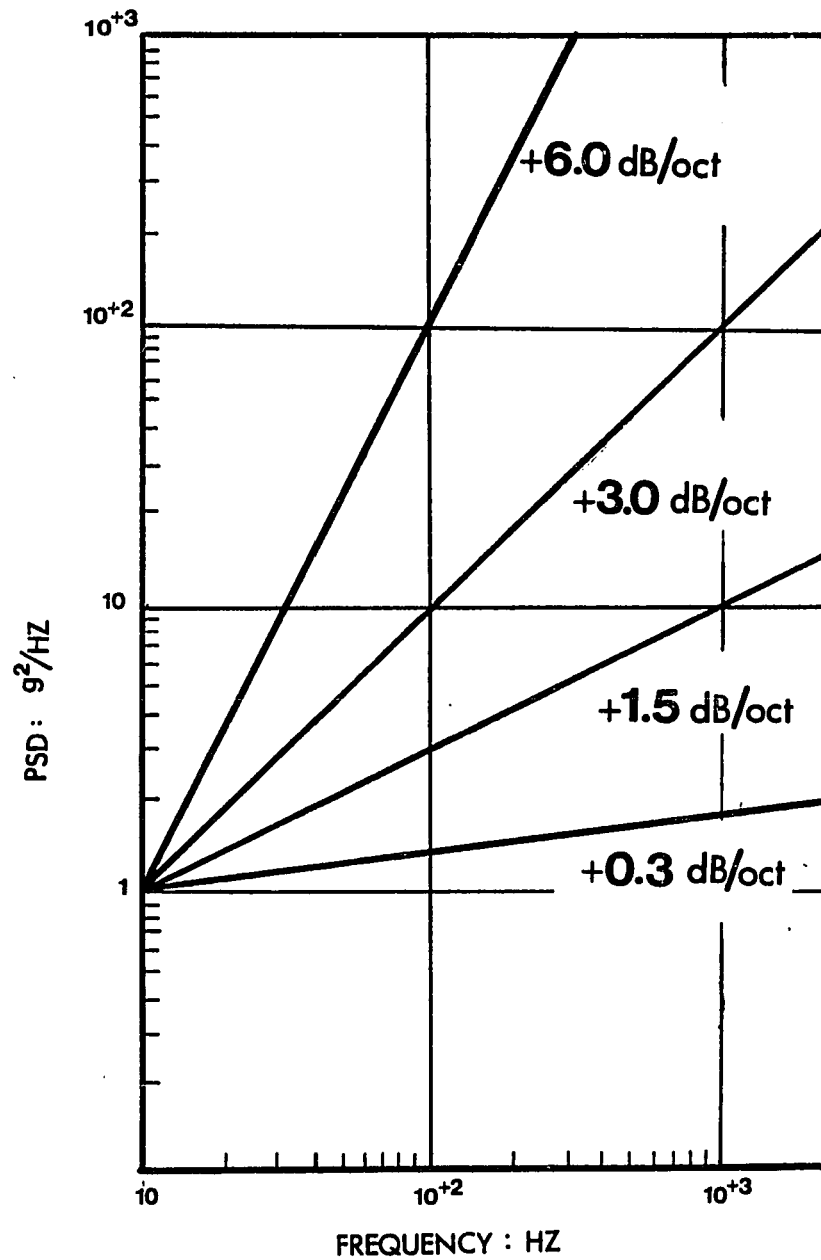


Figure 3.3a. Power Spectral Density Inputs With Positive Slopes

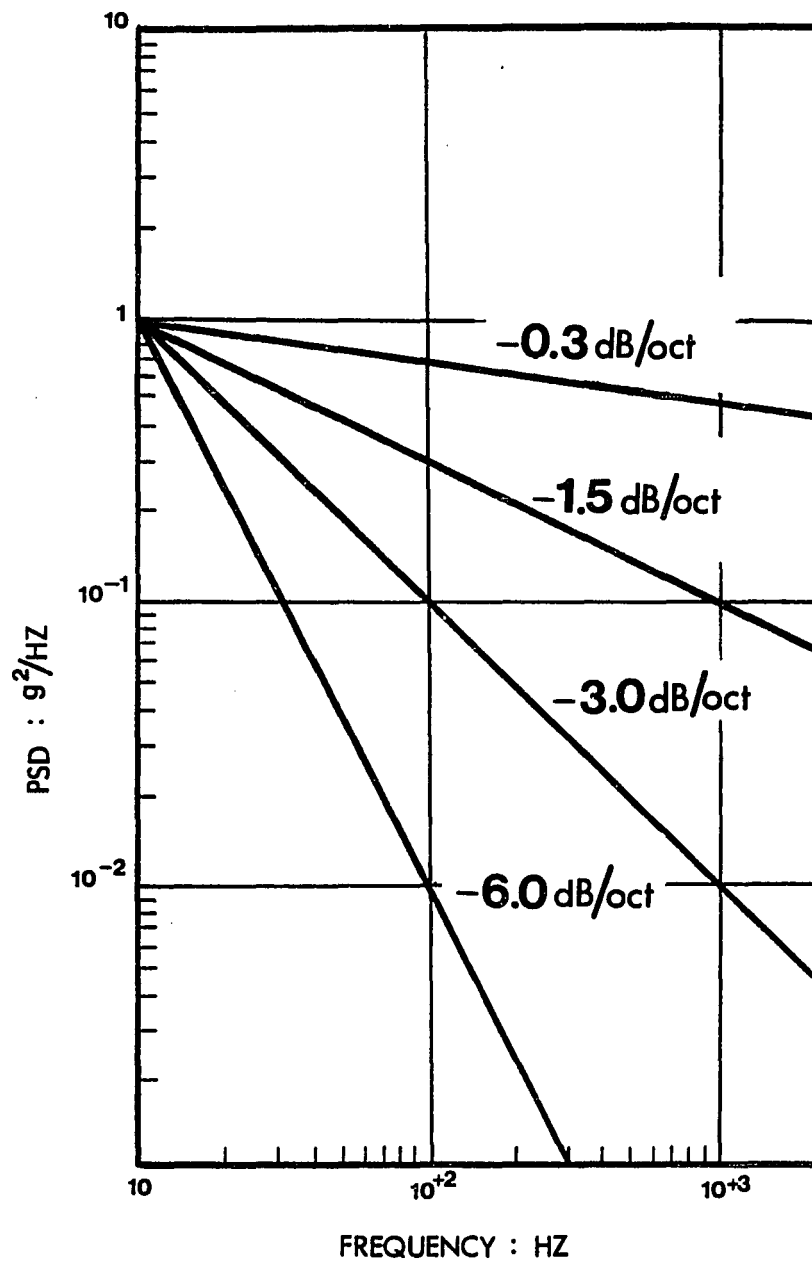
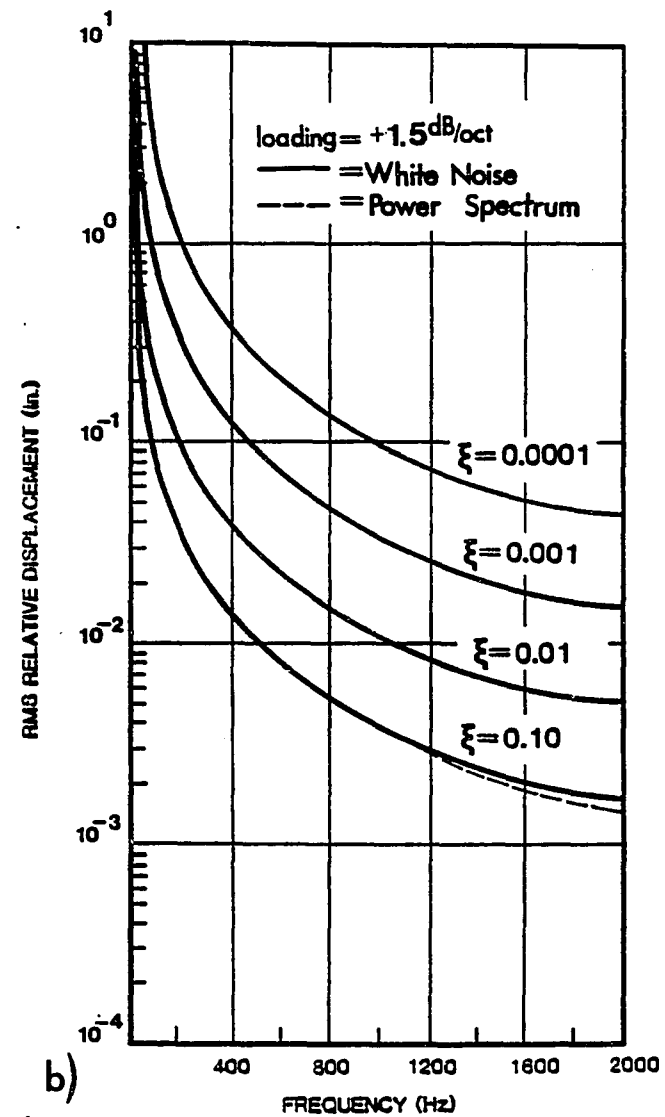
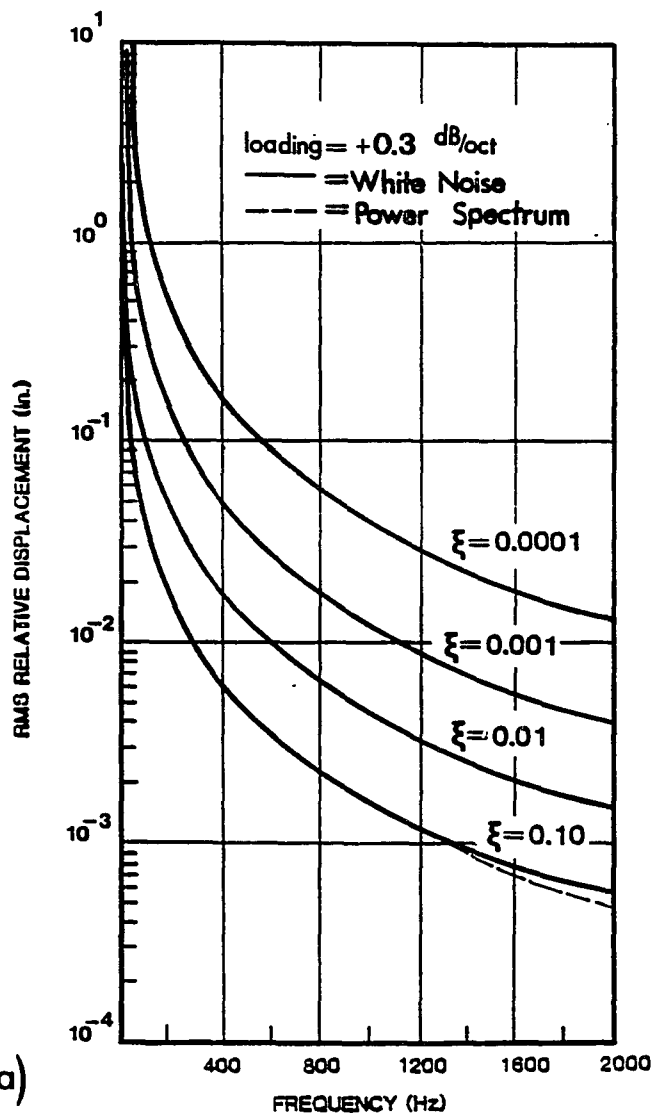
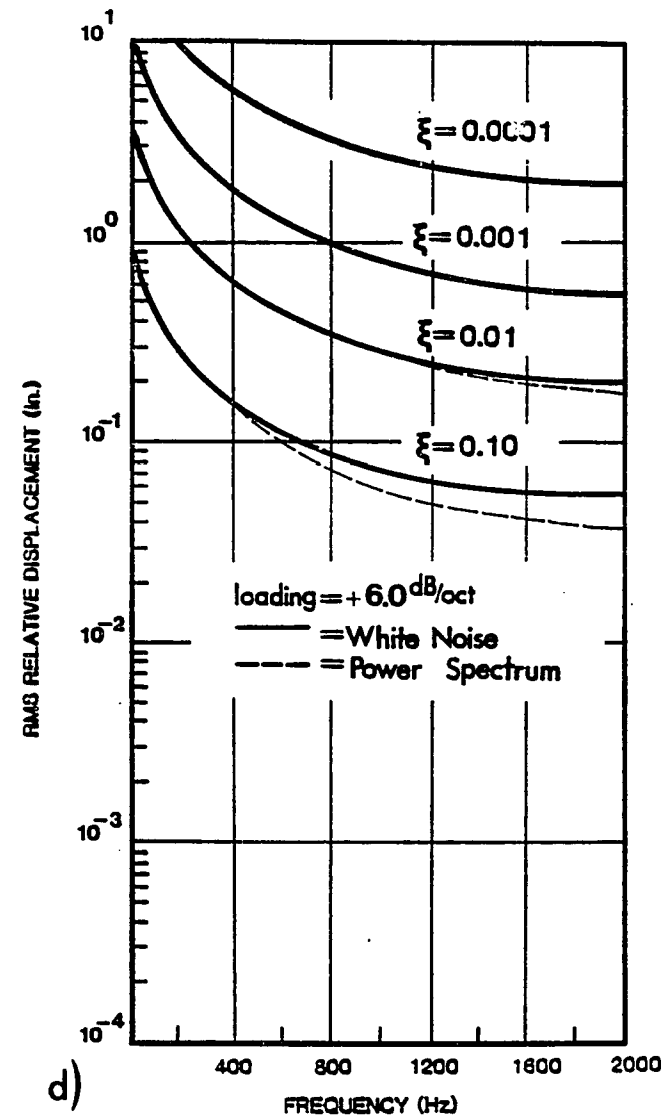
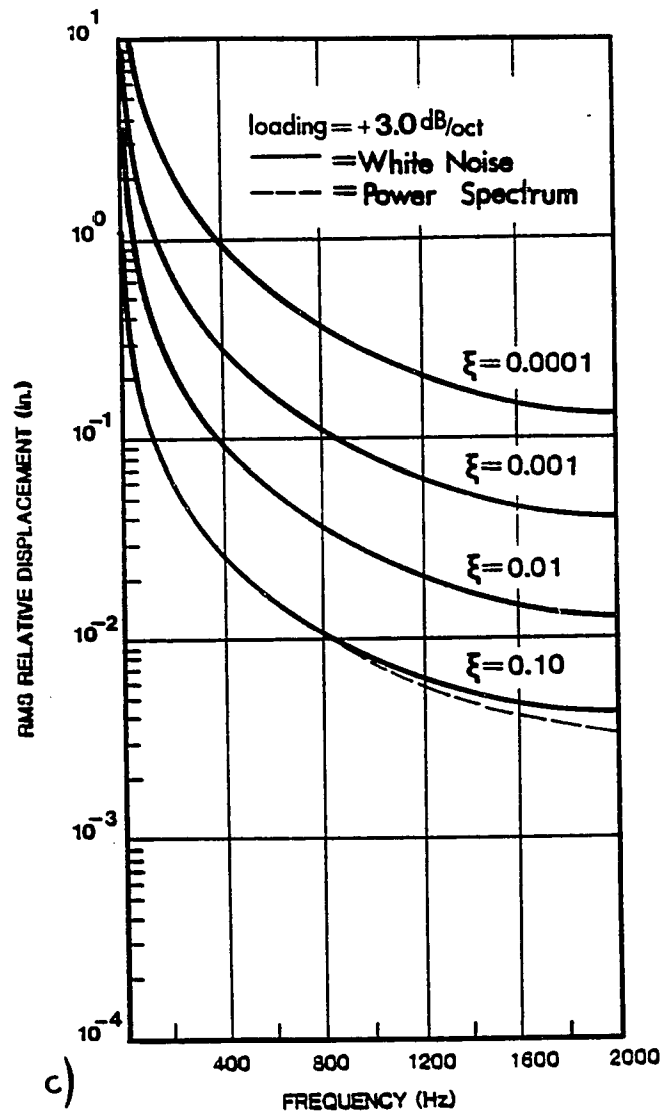


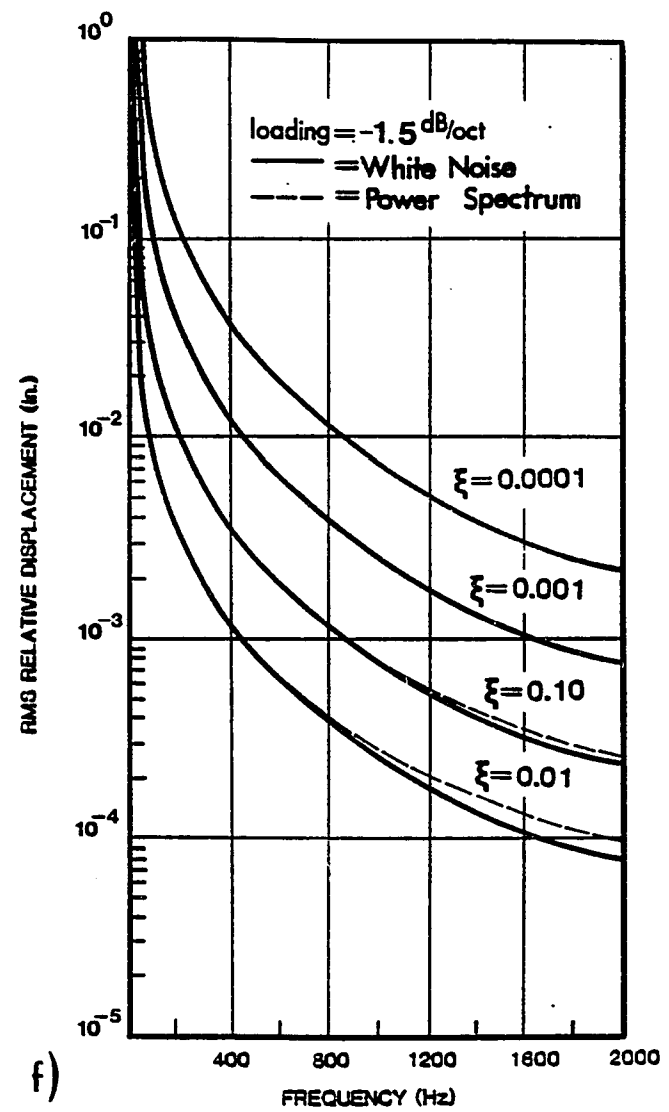
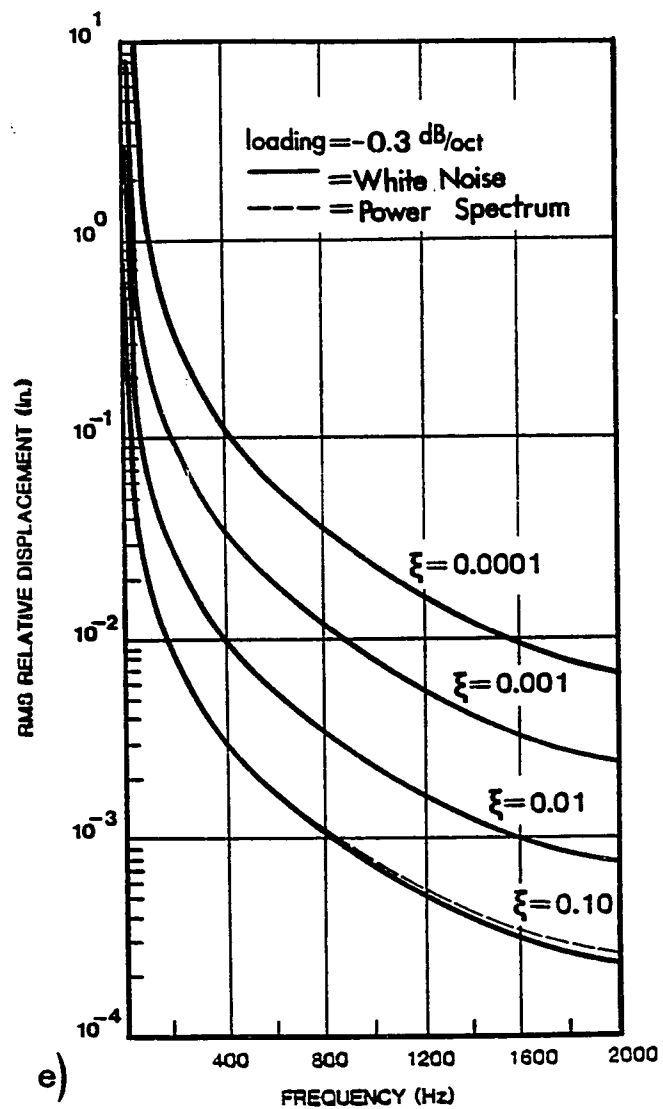
Figure 3.3b. Power Spectral Density Inputs With Negative Slopes



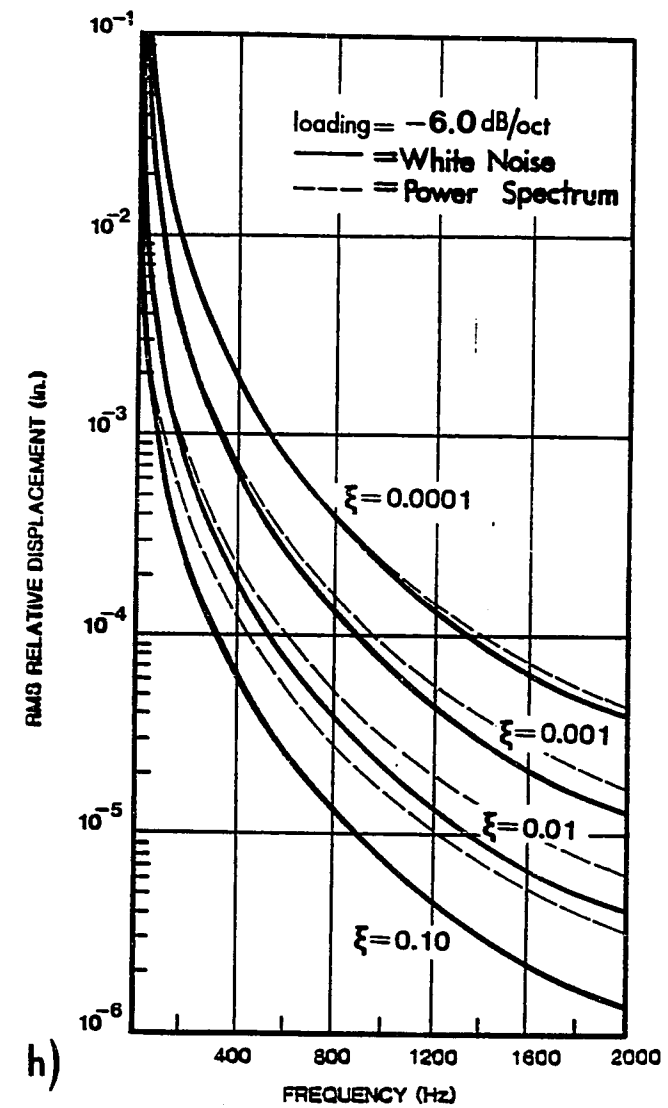
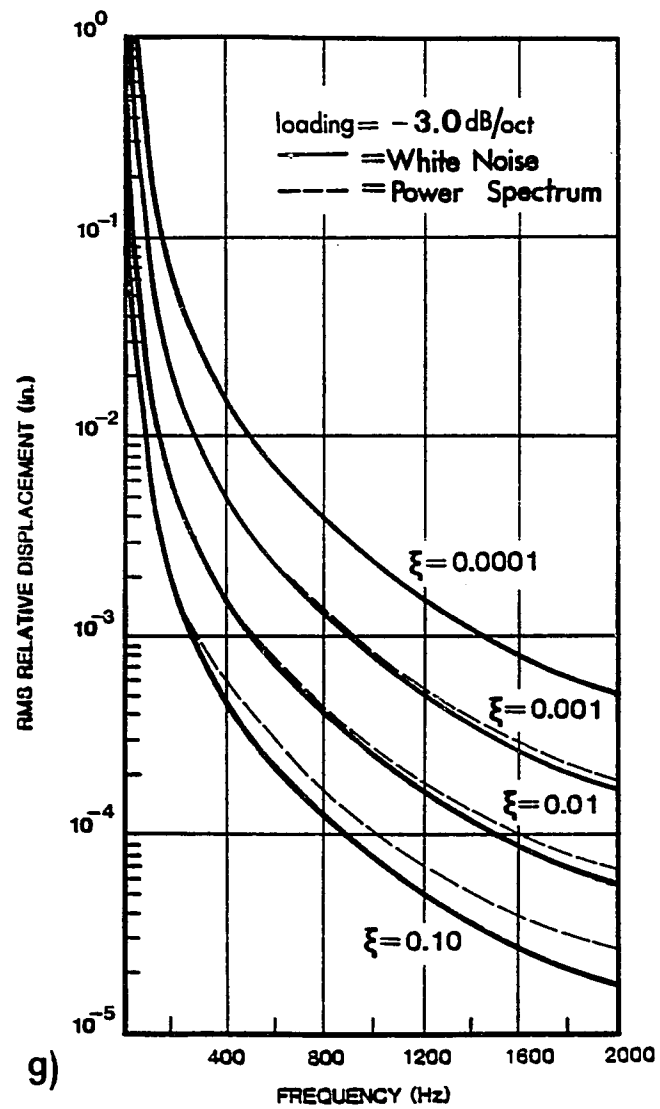
Figures 3.4a and 3.4b. RMS Relative Displacement Response Spectra for Non-Uniform PSD Inputs



Figures 3.4c and 3.4d. RMS Relative Displacement Response Spectra for Non-Uniform PSD Inputs



Figures 3.4e and 3.4f. RMS Relative Displacement Response Spectra for Non-Uniform PSD Inputs



Figures 3.4g and 3.4h. RMS Relative Displacement Response for Non-Uniform PSD Inputs

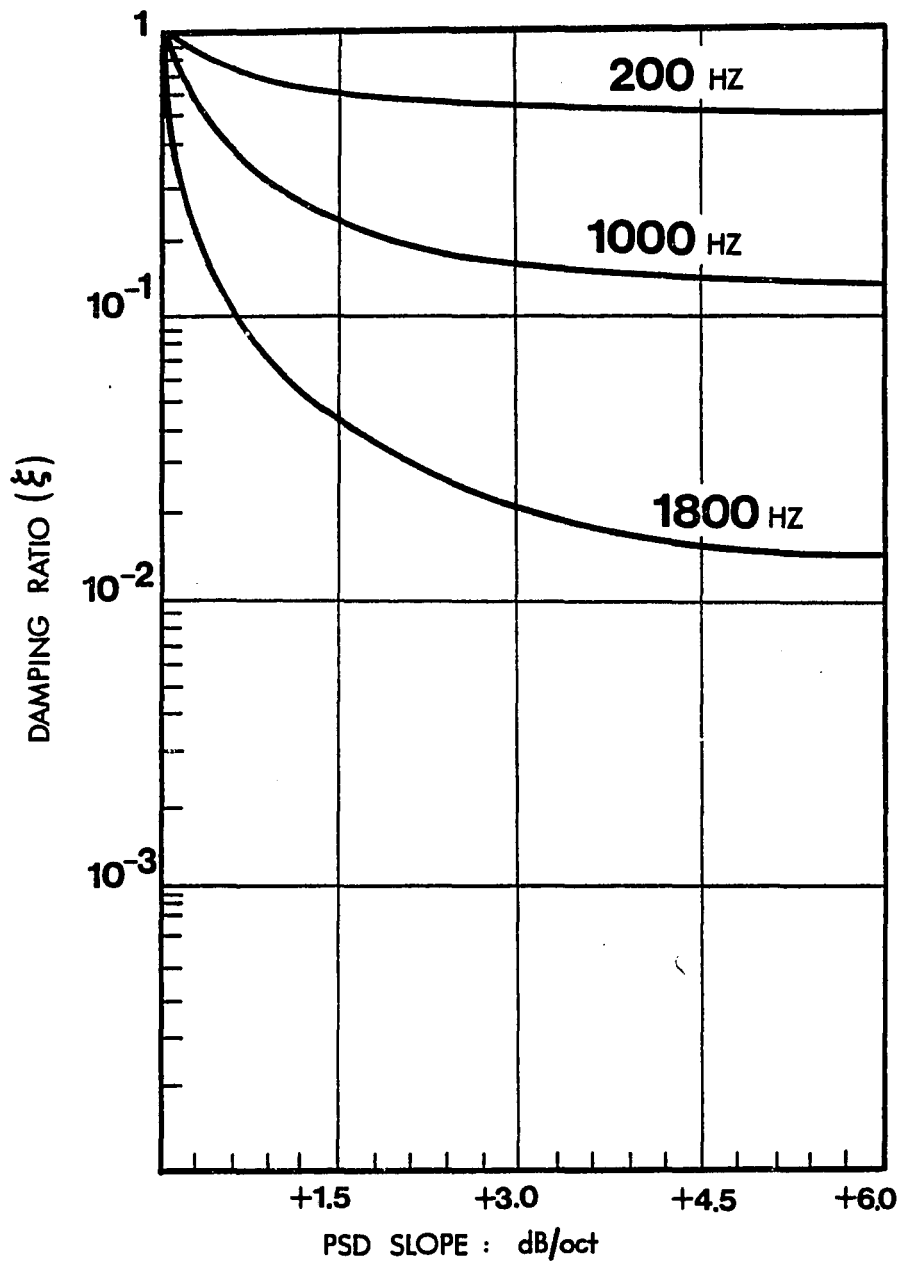


Figure 3.5a. Limitations of the Accuracy of the White Noise Approximation for PSD Inputs With Positive Slopes

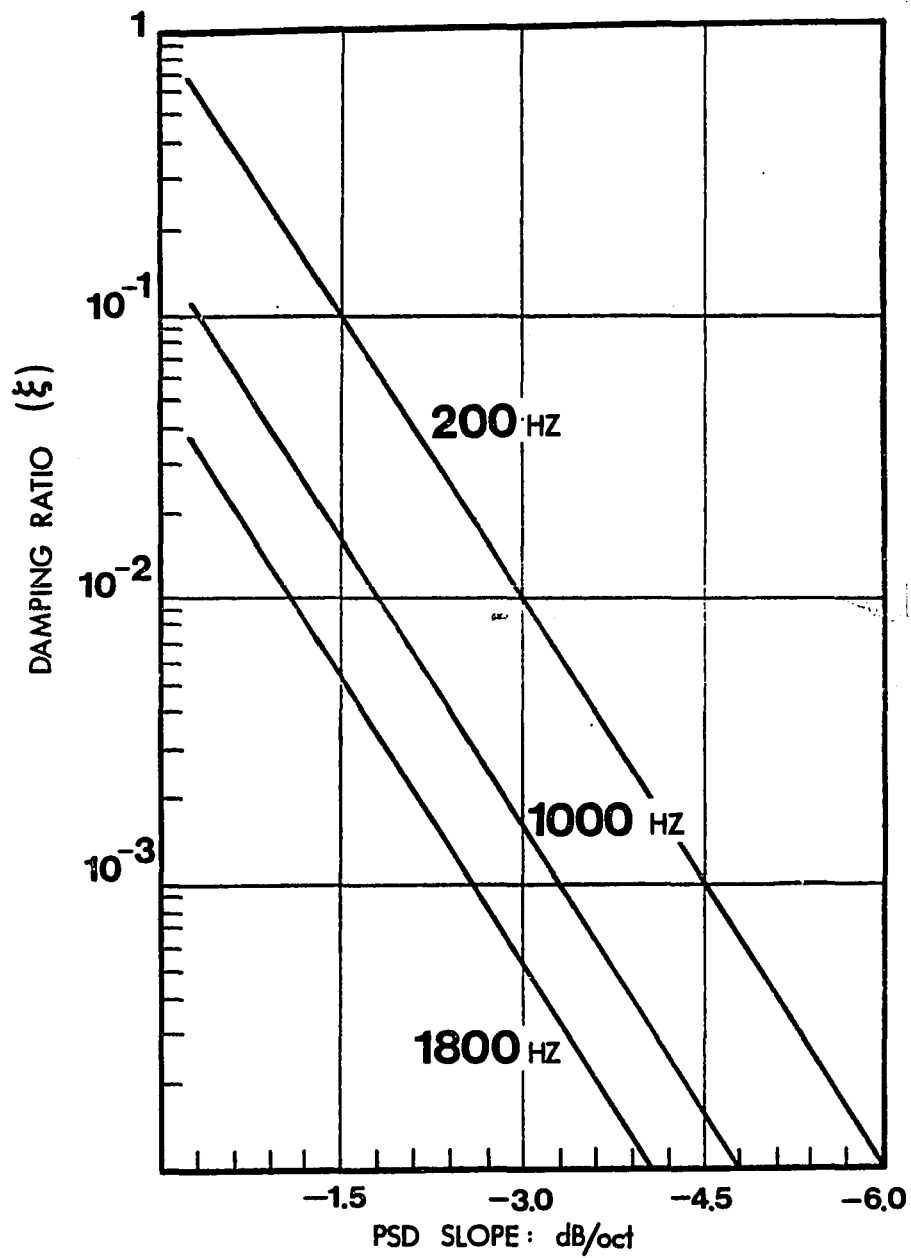


Figure 3.5b. Limitations of the Accuracy of the White Noise Approximation for PSD Inputs With Negative Slopes

Spectrum Method for a given slope of the PSD input and natural frequency.

To gain some insight as to the cause of the discrepancies between the two methods when the PSD input function is not uniform, it is instructive to examine sample PSD output functions from the Power Spectrum solutions with respect to a PSD output function which is generated by the white noise approximation. The mean-square of the response, which is the area under the PSD output curve, will be different for each of the cases which are shown in Figures 3.6a and 3.6b. Note that the fundamental frequency and critical damping ratio are the same for each of the curves.

For a PSD input function with a negative slope, a contribution to the total area can be found in the lower frequency range (Figure 3.6a). This area is not accounted for in the white noise approximation and the resulting approximation for the total area can be significantly less than the true value which is calculated by the Power Spectrum Method. For a PSD input function with a positive slope, the area under the PSD output curve that is computed by the white noise approximation can be greater than the area which is calculated by the Power Spectrum Method (Figure 3.6b).

The white noise approximation assumes that a constant PSD input function is defined at all frequencies

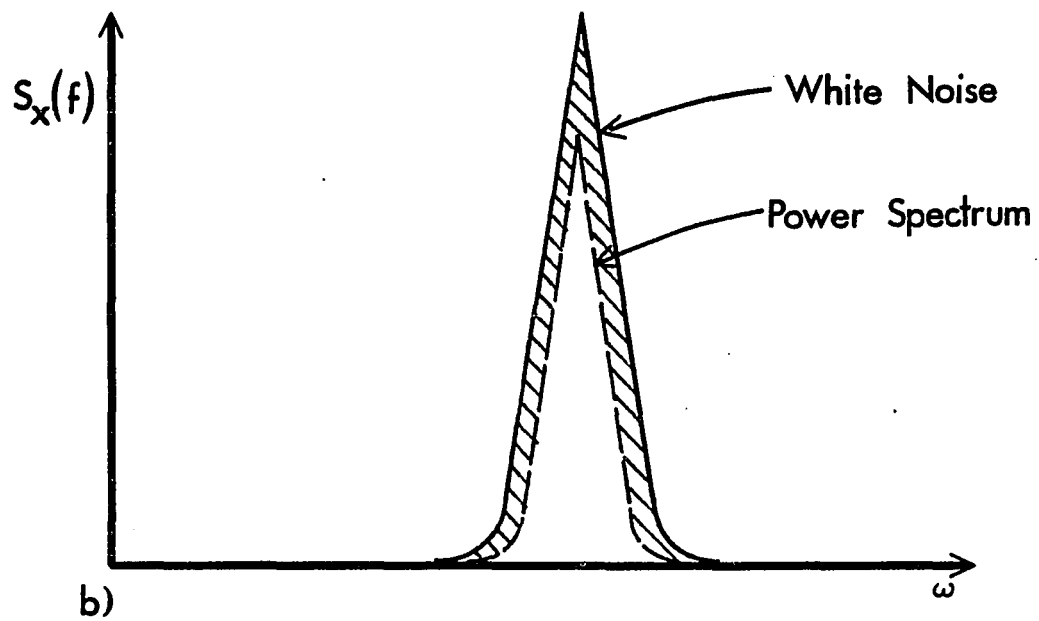
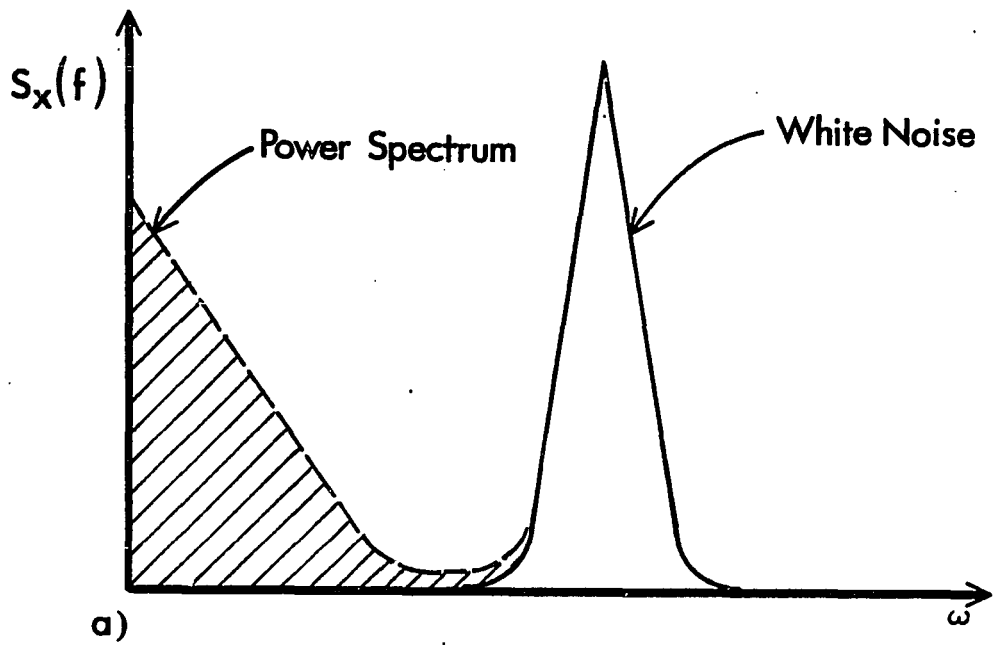


Figure 3.6. Comparison of PSD Output Functions Generated by the Power Spectrum Method and White Noise Approximation

Shown in Figure 3.7 are the errors which are inherent in the approximation when the PSD input function is not constant. The product of the gain function squared and a constant PSD input function between the limits of zero and the fundamental frequency of the system is shown in Figure 3.7a. For a PSD input function with a non-zero slope this same product, which is the area computed by the Power Spectrum Method, is shown in Figures 3.7b and 3.7c.

The magnitude of the differences in area calculated by the two methods becomes larger with an increase in the slope of the PSD input function. As shown in Figures 3.8a and 3.8b, the differences in the calculated area also increase with an increase in the fundamental frequency of the system. Therefore, the error of the white noise approximation for systems with relatively high frequency or those subjected to PSD input functions with large slopes can be significant.

In the development of the white noise approximation, the total area was defined by the integral in Equation 2.18 to be composed of three separate terms. The area defined by the first term exists primarily in the immediate vicinity of the fundamental frequency (Figure 3.9a). This is because for low levels of damping, the gain function is characterized by a sharp peak at the fundamental frequency. However, as the damping of the system is increased, the gain function becomes flatter

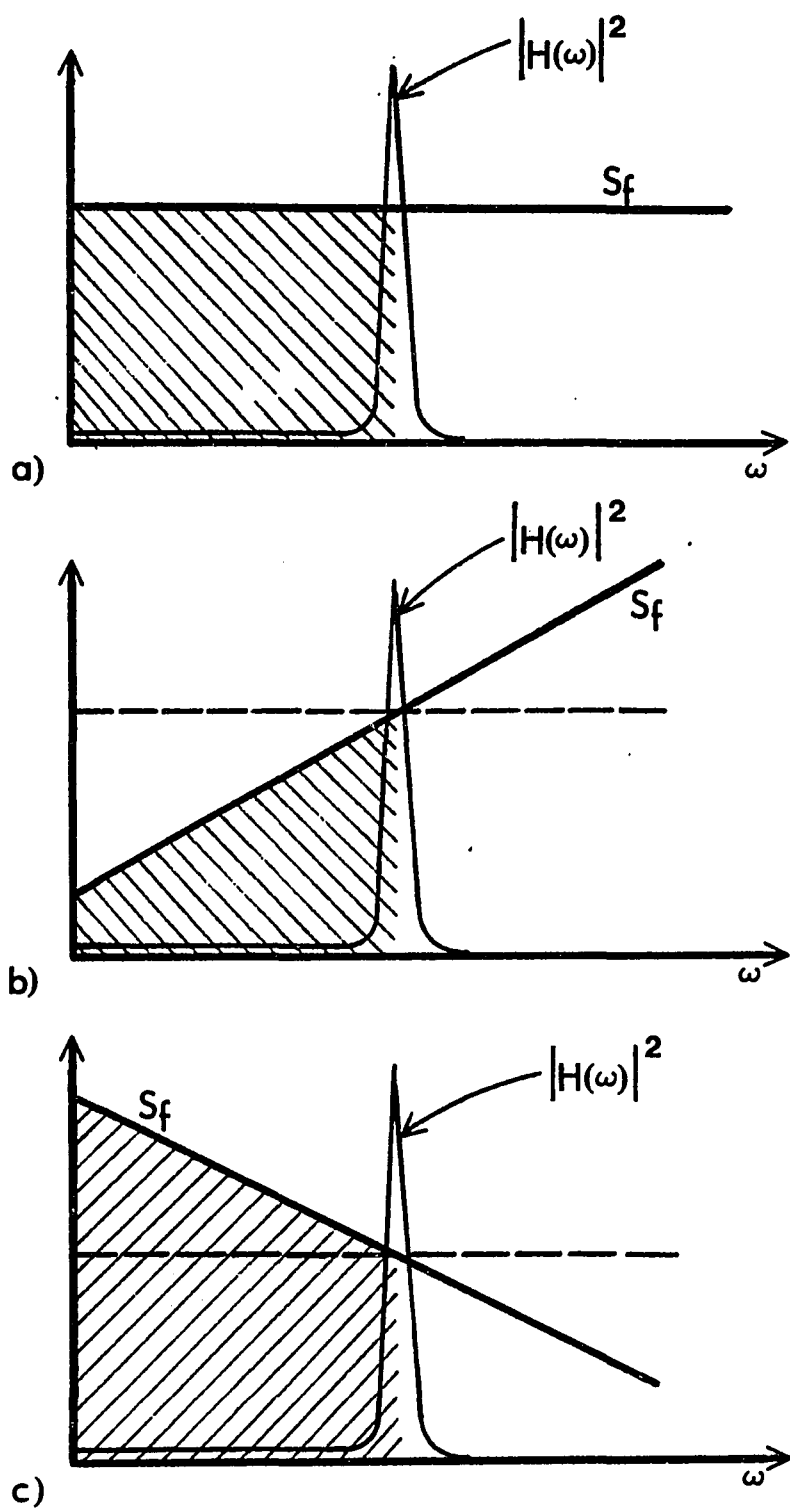


Figure 3.7. The White Noise Approximation for Non-Constant PSD Input Functions

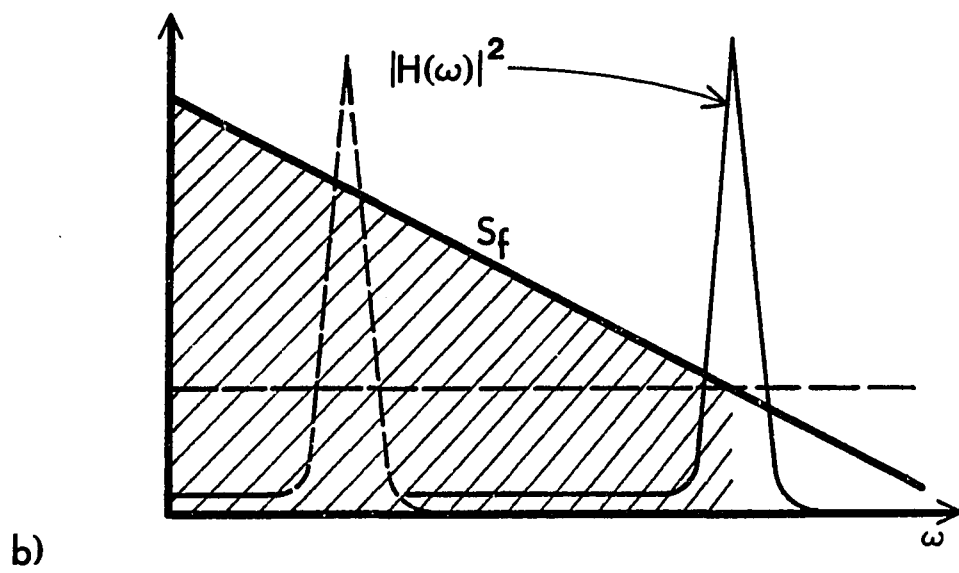
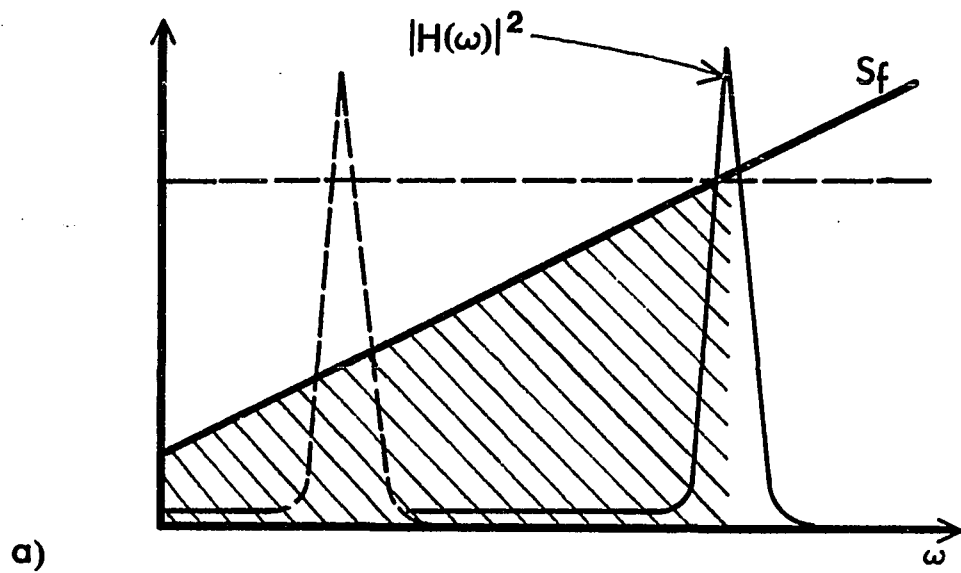


Figure 3.8. The White Noise Approximation for Large Fundamental Frequencies

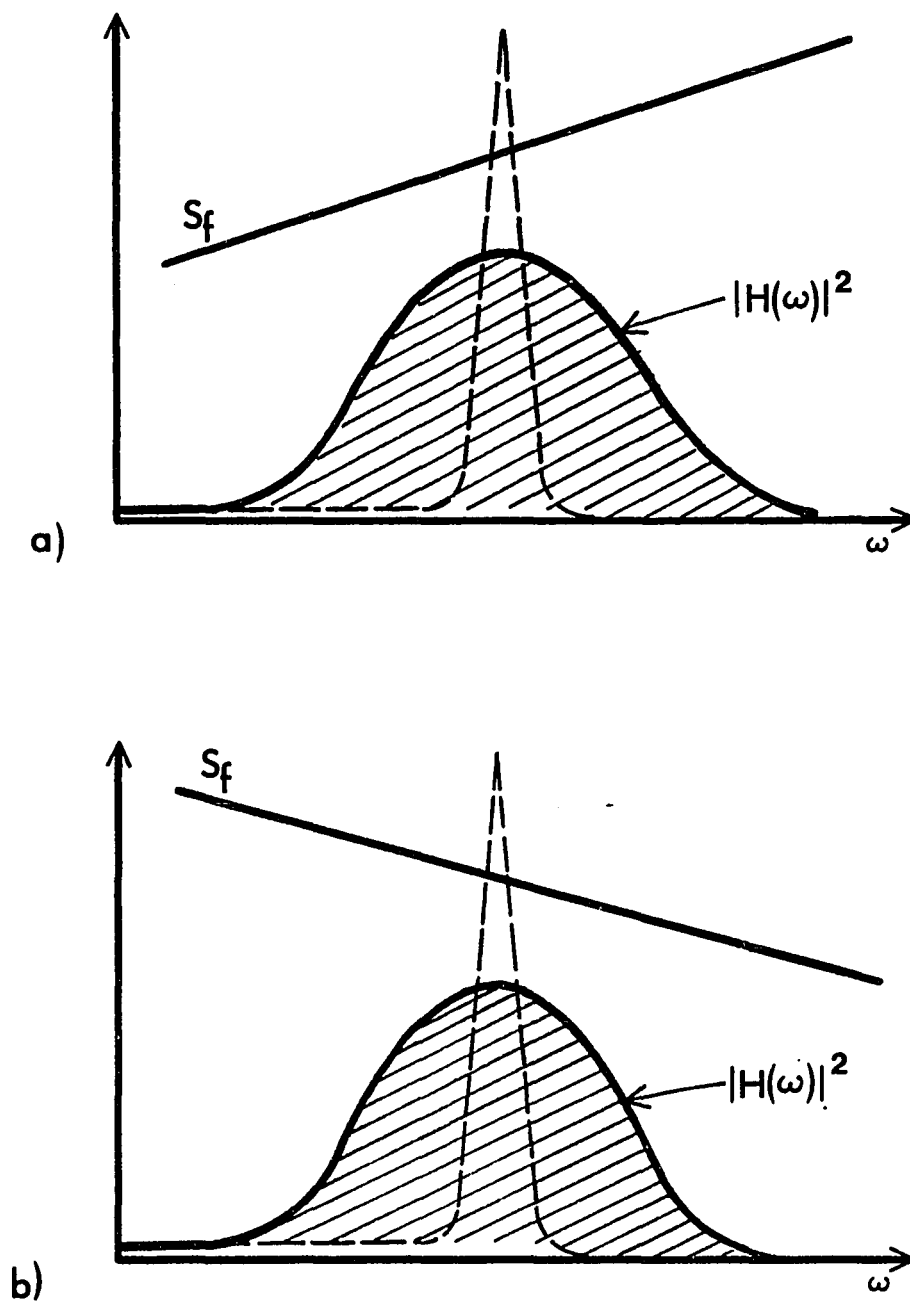


Figure 3.9. The White Noise Approximation for Large Damping Ratios

and an additional contribution to the total area arises. This additional area is not accounted for in the white noise equation (Figures 3.9b and 3.9c).

To compare the overall accuracy of the white noise approximation in relation to the Power Spectrum Method it is necessary to consider the total effects of damping, slope of the PSD input function, and the frequency. This has been given in graphical form by Figures 3.5a and 3.5b. The results shown in Figures 3.7 thru 3.9 may be summarized as follows:

Area Calculated by the White Noise Approximation

	Large Slope	High Frequency	High Damping
Positive Slope	> Power Spectrum Method	> Power Spectrum Method	< Power Spectrum Method
Negative Slope	< Power Spectrum Method	< Power Spectrum Method	< Power Spectrum Method

Therefore, a cancellation of errors may occur which results in more accurate solutions for the white noise approximation for PSD inputs with positive slopes than for PSD inputs with negative slopes. This is reflected by the pattern in the curves shown in Figures 3.5a and 3.5b.

CHAPTER 4

RESPONSE OF MDOF SYSTEMS TO RANDOM EXCITATIONS

When the response of a structure can be described by a single coordinate the equation of motion reduces to a single differential equation. Solutions to this equation for randomly applied loads were obtained in the previous chapter by the Response Spectrum and the Power Spectrum Methods.

In many instances, the motion of a structure cannot be adequately described in terms of a single-degree-of-freedom. Either the physical properties of the structure or the character of the response will require that the structural model be defined by a multiple-degree-of-freedom (MDOF) system. In this chapter, the Response Spectrum and Power Spectrum Methods will be expanded to determine the stresses and displacements of MDOF systems which are subjected to stationary and ergodic random excitations.

Modal Superposition Method for Decoupling MDOF Equations of Motion

Formulation of the random vibration response analysis for MDOF systems can be presented with matrix

notation in a similar manner to that which was used in the development of the SDOF analysis methods. For MDOF systems, the equation of motion can be re-written as:

$$[m]\{\ddot{x}\} + [c]\{\dot{x}\} + [k]\{x\} = \{p(t)\} \quad (4.1)$$

where:

$[m]$	=	structural mass matrix
$[c]$	=	structural damping matrix
$[k]$	=	structural stiffness matrix
$\{x\}$	=	vector of nodal displacements
$\{p(t)\}$	=	vector of nodal loads.

In general, the frequency response solution of equation 4.1 is obtained by either of two methods:

- 1) Direct frequency response analysis
- 2) Modal frequency response analysis.

In the modal method of analysis, the eigenvectors (mode shapes) are used to relate the physical degrees of freedom to a set of generalized coordinates which can reduce the number of degrees of freedom in the analysis. The direct method uses the displacements at the nodes as the degrees of freedom. The modal method will usually be more efficient in problems where a small fraction of the total number of modes is sufficient to produce the desired accuracy. All frequency response calculations in this dissertation were by modal frequency response analysis.

Equation 4.1 is a set of dependent, second-order, linear differential equations. To decouple this set of equations it is assumed that the displacement vector can be defined as the sum of each mode-shape vector multiplied

by a modal amplitude:

$$\{x\} = \sum_{i=1}^n \{\phi_i\} Y_i = [\phi] \{Y\} \quad (4.2)$$

where: $\{\phi_i\}$ = the i th mode shape vector
 Y_i = the i th modal amplitude.

Calculation of the mode shape vectors and frequencies is accomplished by assuming that the free-vibration response is a simple harmonic (Clough and Penzien). The frequency equation of the structure is:

$$|[k] - \{\omega_n\}^2 [m]| \{x\} = 0 \quad (4.3)$$

where: $\{\omega_n\}$ = vector of free-vibration frequencies.

Solution of equation 4.3 gives the eigenvalues and eigenvectors. The choice of the solution method used is governed by the size of the problem and the number of eigenvalues and eigenvectors to be extracted (Joseph). The two most commonly used methods are the Inverse Power Method which is primarily used when solving for a small number of eigenvalues and eigenvectors from a structural model with many degrees of freedom, and the Givens Method which extracts all of the eigenvalues and eigenvectors and is usually used for structural models with less than 100 degrees of freedom.

To decouple the equations of motion substitute equation 4.2 and its time derivatives (mode shapes do not change with respect to time) into equation 4.1 to produce:

$$[m][\phi]\{\ddot{Y}\} + [c][\phi]\{\dot{Y}\} + [k][\phi]\{Y\} = \{p(t)\} \quad (4.4)$$

If equation 4.4 is premultiplied by the transpose of the i th mode-shape vector, it becomes:

$$\begin{aligned} \{\phi_i\}^T [m][\phi]\{\ddot{Y}\} + \{\phi_i\}^T [c][\phi]\{\dot{Y}\} + \{\phi_i\}^T [k][\phi]\{Y\} \\ = \{\phi_i\}^T \{p(t)\} \end{aligned} \quad (4.5)$$

Because of the orthogonality of the mode shape vectors with respect to the mass and stiffness matrices, and if Rayleigh damping exists (Clough and Penzien), Equation 4.5 reduces to:

$$\begin{aligned} \{\phi_i\}^T [m]\{\phi_i\}\{\ddot{Y}\} + \{\phi_i\}^T [c]\{\phi_i\}\{\dot{Y}\} + \{\phi_i\}^T [k]\{\phi_i\}\{Y\} \\ = \{\phi_i\}^T \{p(t)\} \end{aligned} \quad (4.6)$$

Equation 4.6 is a set of n independent equations of the form:

$$M_i \ddot{Y}_i + C_i \dot{Y}_i + K_i Y_i = P_i(t) \quad (4.7)$$

where:

$M_i = \{\phi_i\}^T [m]\{\phi_i\}$ = generalized modal mass for mode i

$C_i = \{\phi_i\}^T [c]\{\phi_i\}$ = generalized modal damping for mode i

$$K_i = \{\phi_i\}^T [k] \{\phi_i\} = \text{generalized modal stiffness for mode } i$$

$$P_i = \{\phi_i\}^T \{p(t)\} = \text{generalized modal load for mode } i.$$

Power Spectrum Method for MDOF Systems

Frequency response solutions for equation 4.7 are well documented (Hurty and Rubinstein) and follow the procedures as were discussed in Chapter 2. To determine the amplitude of the modal response consider the forcing function, $p(t)$ to be defined as a simple harmonic

$$p(t) = p_0 f(t)$$

where: p_0 = amplitude of the forcing function

and $f(t) = e^{i\omega t}$
 = time dependence of the function.

The steady-state solution to equation 4.7 is then given by:

$$y_i(t) = \frac{p_0 \lambda_i}{\omega_i^2 M_i} H_i(\omega) f(t) \quad (4.8)$$

where λ_i is defined as the modal participation factor and is equal to:

$$\lambda_i = \{\phi_i\}^T [m] \{1\}$$

where:

$\{1\}$ = column vector with each element equal to 1.

Substitution of equation 4.8 into equation 4.2 yields the equation for the displacement

vector:

$$\{x\} = \sum_{i=1}^n \{\phi_i\} \frac{p_0 \lambda_i}{\omega_i^2 M_i} H_i(\omega) f(t) \quad (4.9)$$

Combining the results of equations 2.1 and 2.2 the mean-square value of this response variable can be given as:

$$\{\sigma_x^2\} = \lim_{T \rightarrow \infty} \frac{1}{2T} \int_{-T}^T \{x\}^2 dt \quad (4.10)$$

Substitution of equation 4.9 into equation 4.10 yields:

$$\{\sigma_x^2\} = \sum_{i=1}^n \sum_{j=1}^n \{\phi_i\} \{\phi_j\} \frac{p_o^2 \lambda_i \lambda_j}{\omega_i^2 \omega_j^2 M_i M_j} \lim_{T \rightarrow \infty} \frac{1}{2T} \int_{-T}^T H_i(\omega) H_j(\omega) f^2(t) dt \quad (4.11)$$

Using the relationship defined in equation 2.13d and disregarding the phase relations (Hurty and Rubinstein) the integral in equation 4.11 becomes:

$$\lim_{T \rightarrow \infty} \frac{1}{2T} \int_{-T}^T |H_i(\omega)| |H_j(\omega)| f^2(t) dt \quad (4.12)$$

When the forcing function $p(t)$ is a representative record of an ergodic random process, the limiting process in equation 4.12 can be transformed from the time domain to the frequency domain because the function $f(t)$ is then represented by frequency components in a continuous spectrum from zero to infinity (Hurty and Rubinstein). Equation 4.12 then becomes:

$$\frac{1}{2\pi} \int_0^\infty |H_i(\omega)| |H_j(\omega)| S_f(\omega) d\omega \quad (4.13)$$

where $S_f(\omega)$ is the power spectral density input function.

Substitution of equation 4.13 into equation 4.11 produces:

$$\{\sigma_x^2\} = \sum_{i=1}^n \sum_{j=1}^n \{\phi_i\} \{\phi_j\} \frac{p_o^2 \lambda_i \lambda_j}{\omega_i^2 \omega_j^2 M_i M_j} \frac{1}{2\pi} \int_0^\infty |H_i(\omega)| |H_j(\omega)| S_f(\omega) d\omega \quad (4.14)$$

Equation 4.14 represents the mean-square response of an n degree-of-freedom system which is excited by a random forcing function and forms the basis of the random vibration solution by the Power Spectrum Method in the NASTRAN finite element program. The calculation of the internal element forces by the Power Spectrum Method is discussed in the next section.

Calculating Internal Forces in the Power Spectrum Method

In the analysis of SDOF systems, the determination of the internal element forces is a straightforward calculation. If the relative displacement of the mass with respect to the support can be determined, the internal forces in a beam member with fixed ends can be calculated by one of the following relationships depending upon the type structural action:

1. Axial Force: $f_a = \frac{AE}{L} \delta_d$
2. Bending Moment: $f_{bm} = \frac{6EI}{L^3} \delta_d$
3. Shear Force (due to bending): $f_s = \frac{12EI}{L^3} \delta_d$

where: δ_d = relative displacement of the mass

A = area of the cross-section

E = Young's modulus

L = length of the member

I = moment of inertia of the cross-section.

When analyzing MDOF systems which are subjected to random excitations, it is necessary to compute the vector of maximum relative displacements. However, before the internal forces for the entire structure can be determined, an important clarification in the definition of the maximum relative displacement vector must be made.

Forces, moments, and shears are generally functions of the maximum relative displacements and their gradients. These maximum relative displacements and their gradients may not always occur at the same time or at the same frequency. However, the internal forces in a member are calculated with respect to a strain rate (deformation gradient) which occurs at a singularly defined time and frequency.

Calculation of the internal forces in a member of a MDOF system by the Power Spectrum Method requires that the displacement vector which is used in the equation of motion be re-defined. As an example, for the three-story "shear" building shown in Figure 4.1a, the three-degree-of-freedom model shown in Figure 4.1b may be used. For this structure the displacement vector is defined as:

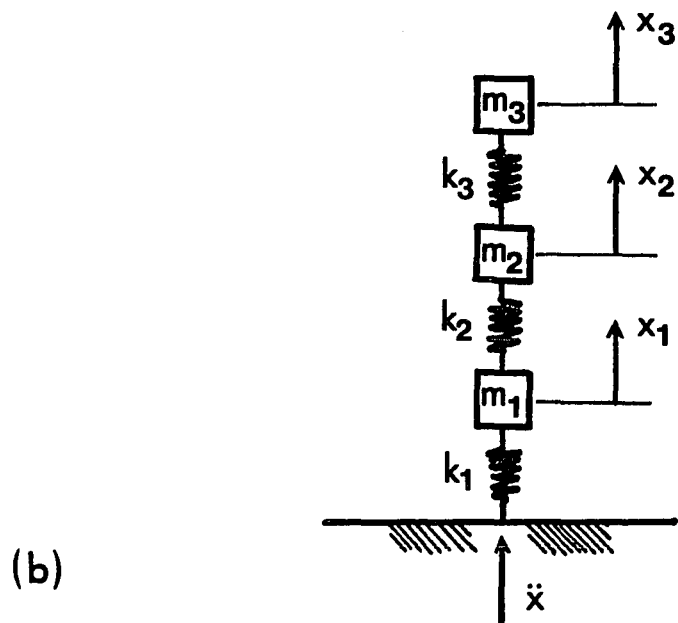
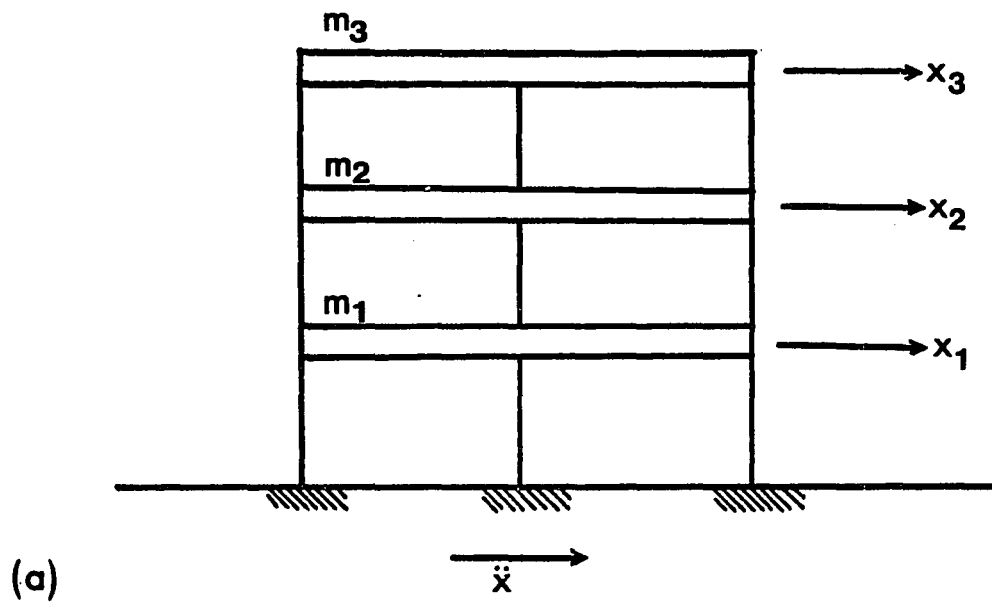


Figure 4.1. A Three-Story Building Excited by a Random Ground Acceleration

$$\{x\} = \begin{Bmatrix} x_1 \\ x_2 \\ x_3 \end{Bmatrix} \quad (4.15)$$

where x_i = relative displacement of node i with respect to the support.

To determine the deformation in each element which represents the relative floor displacements, the following coordinates are defined:

$$\begin{aligned} y_1 &= x_1 \\ y_2 &= x_2 - x_1 \\ y_3 &= x_3 - x_2 \end{aligned} \quad \begin{Bmatrix} y_1 \\ y_2 \\ y_3 \end{Bmatrix} = \begin{bmatrix} 1 & 0 & 0 \\ -1 & 1 & 0 \\ 0 & -1 & 1 \end{bmatrix} \begin{Bmatrix} x_1 \\ x_2 \\ x_3 \end{Bmatrix} \quad (4.16)$$

Inverting the matrix in 4.16 and substituting the result into 4.15 produces the following expression for $\{x\}$ which is in turn substituted into the equation of motion:

$$\begin{Bmatrix} x_1 \\ x_2 \\ x_3 \end{Bmatrix} = \begin{bmatrix} 1 & 0 & 0 \\ 1 & 1 & 0 \\ 1 & 1 & 1 \end{bmatrix} \begin{Bmatrix} y_1 \\ y_2 \\ y_3 \end{Bmatrix} \quad (4.17)$$

When $\{y\}$ has been calculated from the equation of motion, the internal forces in each member can be determined by the relationships which were given for SDOF systems. Generation of equations 4.16 and 4.17 will vary for the type of elements used to model the structure.

These constraint equations are internal to the NASTRAN program and can be very extensive when there are many degrees-of-freedom involved in the analysis of the structural displacements.

Response Spectrum Method for MDOF Systems

The solution of equation 4.14 can be very expensive and time consuming for MDOF structures. With the introduction of some approximations to equation 4.14, the Response Spectrum Method for the random vibration analysis of MDOF systems can be developed. For a lightly damped MDOF system, the gain functions have regions of pronounced peaks in the neighborhood of the corresponding natural frequencies (Figure 4.2). The products of these gain functions in equation 4.14 for $i \neq j$ are small in comparison with the same products of $i = j$. In addition, the contribution of products involving $\{\phi_i\}\{\phi_j\}$ and $\lambda_i \lambda_j$ for $i \neq j$ will be small since the sign of the product may be positive or negative and some terms will cancel (Hurty and Rubenstein).

Using these approximations, equation 4.14 reduces to:

$$\{\sigma_x^2\} = \sum_{i=1}^n \{\phi_i\}^2 \frac{p_o^2 \lambda_i^2}{\omega_i^4 M_i^2} \frac{1}{2\pi} \int_0^\infty |H_i(\omega)|^2 S_f(\omega) d\omega \quad (4.18)$$

The integrals in equation 4.18 can be approximated by replacing $S_f(\omega)$ by its discrete values $S_f(\omega_i)$ at the

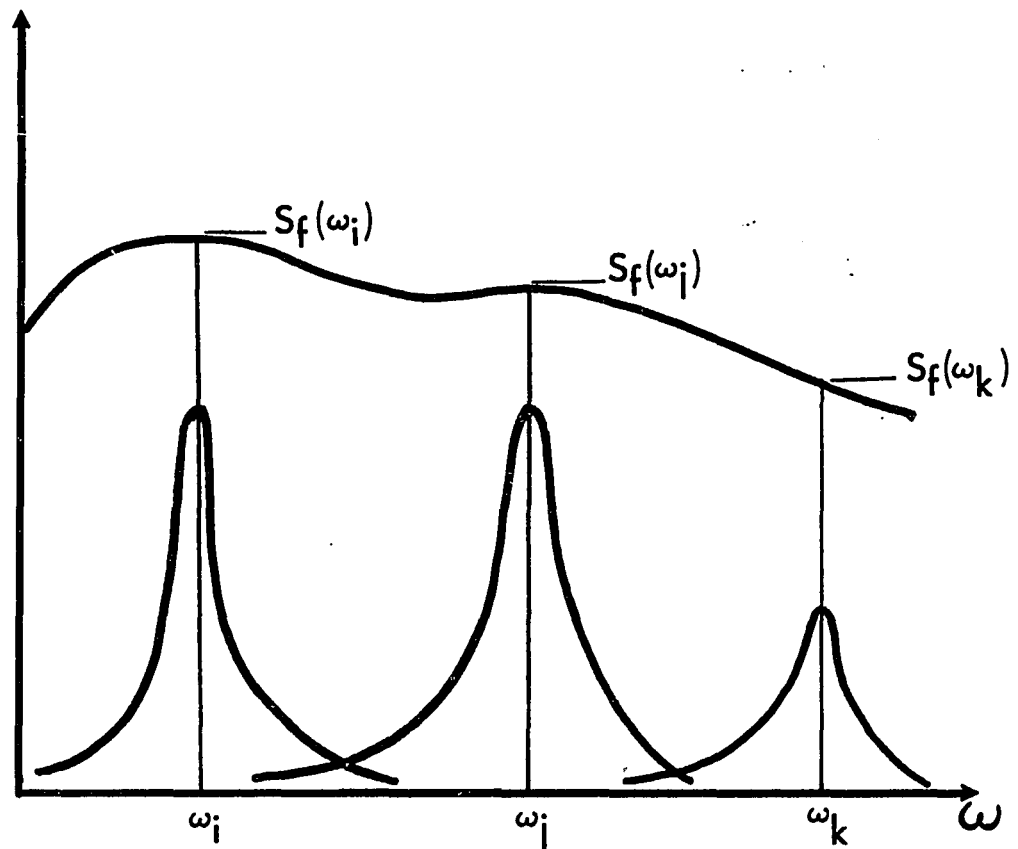


Figure 4.2. Gain Functions for a Lightly Damped MDOF System

natural frequencies (as was done in the SDOF approximation) and the substitution of the appropriate gain function. For the loading case of base acceleration input and relative displacement output, these approximations reduce equation 4.18 to:

$$\{\sigma_x^2\} = \sum_{i=1}^n \{\phi_i\}^2 \frac{p_o^2 \lambda_i^2}{\omega_i^4 M_i^2} \frac{S_f(\omega_i) \omega_i}{8\xi} \quad (4.19)$$

Equation 4.19 is an example of the MDOF form of the Response Spectrum Method. Using equation 4.8, this equation can also be written as:

$$\{\sigma_x^2\} = \sum_{i=1}^n [\{\phi_i\} Y_i]^2 \quad (4.20)$$

The vector of the RMS of the response variables (in this case the response variables are the relative displacements) is obtained by taking the square root of equation 4.20:

$$\{\sigma_x\} = \sqrt{\sum_{i=1}^n [\{\phi_i\} Y_i]^2} \quad (4.21)$$

Comparison of the Two Methods for Determining
the Relative Displacements of MDOF Systems

To illustrate the application of the Response Spectrum and the Power Spectrum Methods to the random vibration analysis of MDOF systems several example problems are presented. Through the use of examples, the important aspects of the methods are most easily demonstrated. In each example, the RMS relative displacement vector of a three-degree-of-freedom structure subjected to base acceleration input was calculated by each method.

The structure in Example 4.1 was subjected to the indicated white noise input spectral density function. Excellent correlation between the Response Spectrum and the Power Spectrum Methods was shown for damping ratios less than 0.10 (Example 4.1a). Even when the damping ratio was increased to 0.50 (Structures with damping ratios on the order of 50 percent represent systems designed with shock absorbers or energy dissipators. the relative displacement vector calculated by the two methods were accurate to within 15 percent of the total. The error occurs because the Response Spectrum Method does not account for the contributions which can arise due to the interaction between modes (Vanmarcke, 1976). This contribution is significant when the modal frequencies are close or the damping ratios are high.

A method of accounting for the effects of modal interaction in the Response Spectrum Method was proposed by Rosenblueth and Eldoruy (1969). Known as the Double-Sum Method, a modifying term is introduced which is added to equation 4.20 to produce a revised expression for the mean-square of the displacement vector:

$$\{\sigma_x\}^2 = \sum_{i=1}^n \{\sigma_x\}^2 + \sum_{i \neq j} \sum \frac{\{\sigma_{x_i}\}\{\sigma_{x_j}\}}{1 + \epsilon_{ij}^2} \quad (4.22)$$

where:

$$\epsilon_{ij} = \frac{\omega_i - \omega_j}{\xi_i \omega_i + \xi_j \omega_j}$$

A plot of $[(1 + \epsilon_{ij}^2)]^{-1}$ versus the modal frequency ratio ω_i/ω_j is presented in Figure 4.3 and demonstrates the effect of the modifying term in equation 4.22. For damping ratios of less than 0.01, only modal frequency ratios near unity will produce any appreciable interaction. As the damping is increased, the interaction between modes with larger differences in frequency also becomes greater. Shown in Example 4.1b, the Response Spectrum solution with the modifying terms of equation 4.22 reduced the differences in the RMS displacement vector which were calculated by the two methods to less than eight percent. In addition, the results of Example 4.1c demonstrate that for larger differences in frequency, the effects of modal interaction are reduced.

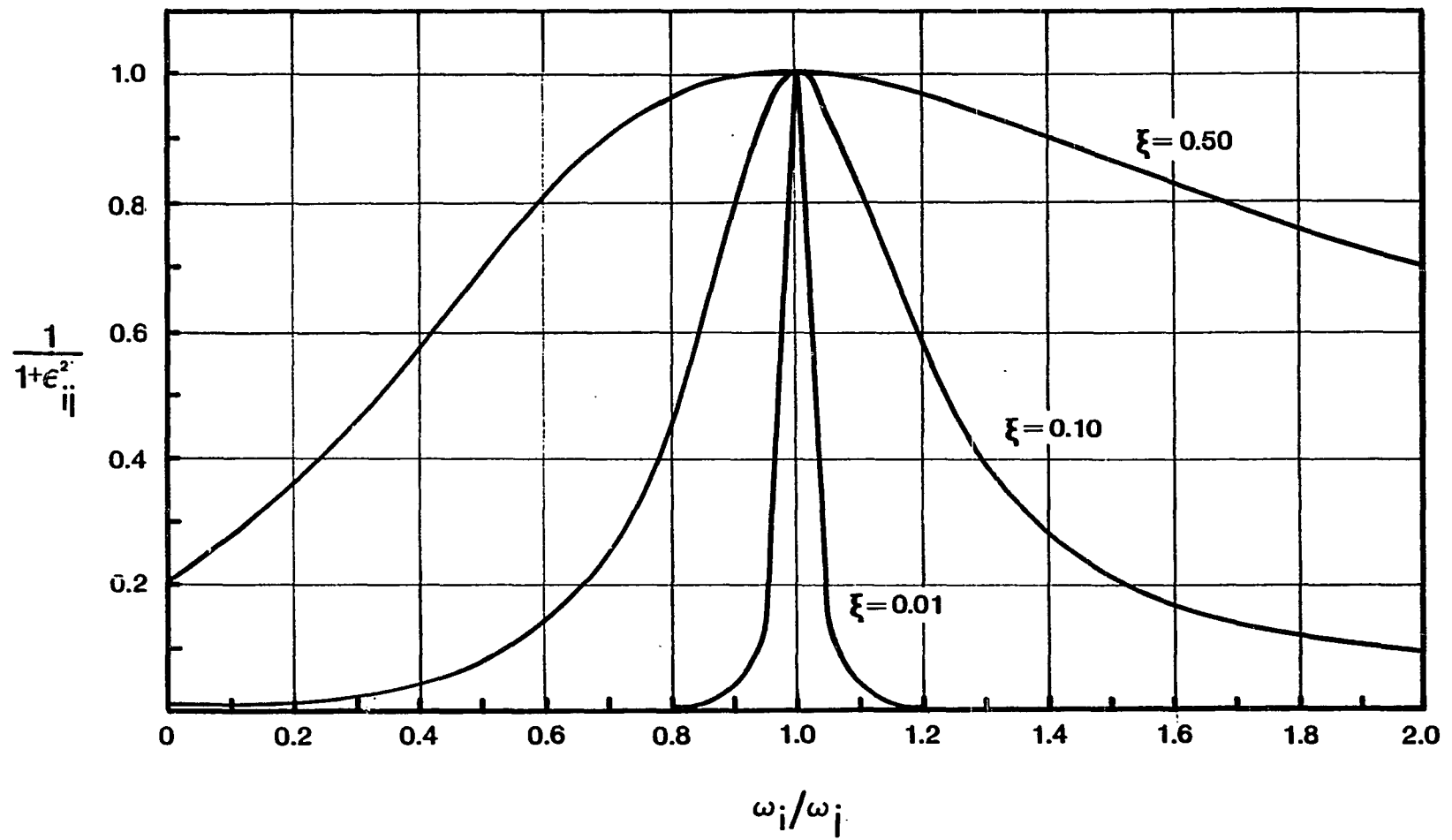


Figure 4.3. Correction Factor for Modal Interaction Using the RSS Method

In Example 4.2 a three-degree-of-freedom structure was subjected to a non-uniform PSD base acceleration input. The fundamental frequency of the system was within the limits of constant spectral density and the remaining two frequencies were located in the range of non-uniform spectral density.

For damping ratios less than 0.10 (Example 4.2a) modal contributions from the largest two frequencies were small. Because the first mode was the dominant mode in the total response and its frequency was within the limits of constant spectral density, excellent correlation between the two methods was obtained. As the damping ratio was increased to 0.50 (Examples 4.2b and 4.2c) the effects of modal interaction also increased and produced differences on the order of 10 to 50 percent between the RMS displacement vectors which were calculated by the two methods. Application of the modifying term in Equation 4.22 to the Response Spectrum Method reduced the differences in the calculated RMS displacements to less than eight percent.

The limitations of the Response Spectrum Method for predicting the response of MDOF systems become more apparent as demonstrated in Example 4.3. For this system, all three frequencies are located in the range of non-uniform spectral density. Good correlation between the results which were calculated by the Response Spectrum

and the Power Spectrum Methods was shown for damping ratios less than or equal to 0.0001 for this example. Because of the relatively low amount of damping in the structure, modal interaction was not an apparent influence to the total response (Example 4.3a).

Examination of Figure 3.5b shows that for a SDOF system with a natural frequency on the order of 400 Hz, the limiting damping ratio for accuracy of the Response Spectrum Method is on the order of 0.0001. Note that the fundamental frequency of the three-degree-of-freedom system in Example 4.3 is 400 Hz, and the Response Spectrum Method was accurate for a damping ratio of 0.0001. This suggests that for MDOF systems whose response is primarily governed in its first mode, the limiting values for the accuracy of the Response Spectrum Method which were predicted by the SDOF analysis can be considered to be a good approximation for the accuracy of MDOF systems.

Using the results of the preceding analyses, some basic conclusions regarding the limitations of the Response Spectrum Method for predicting the response of systems can be made.

1. In its general form, the Response Spectrum Method does not account for the effect of modal interactions which may occur at higher levels of damping ($\xi > 0.10$). A correction factor may be introduced which accounts for the effects of interaction and improves the

accuracy of the Response Spectrum Method (Examples 4.1b, 4.2b, and 4.3b).

2. At levels of damping which are low enough such that the effect of modal interaction becomes negligible, the response of the first mode predominates. In this case, the limitations in accuracy of the Response Spectrum Method for MDOF analysis correspond to the limitations which were derived for the SDOF analysis in Chapter 3. Therefore, for a MDOF system with its fundamental frequency in the range defined by a constant spectral density input, the response predicted by the Response Spectrum Method should be accurate for all levels of damping which ensure negligible contributions due to modal interaction. (Example 4.2a)

3. When a MDOF system has all of its dominant frequencies defined in the range of non-uniform spectral density, extreme care and judgement must be taken in application of the Response Spectrum Method. Contributions due to modal interaction and the limitations in accuracy which were derived in Chapter 3 must be observed. However, excellent results can be obtained for systems with low levels of damping and widely separated frequencies. (Example 4.3a)

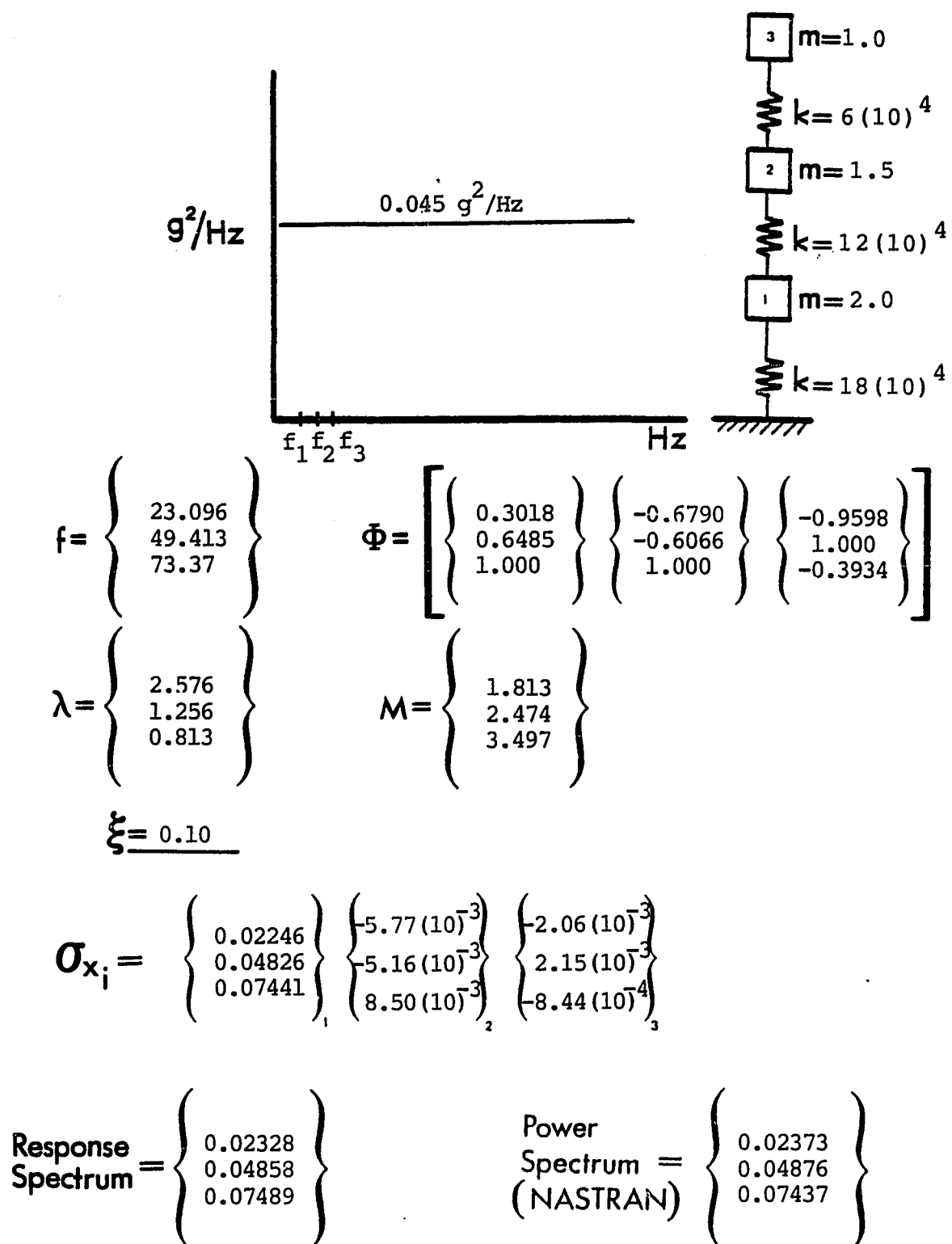


Figure 4.4. Example 4.1a

$$\underline{\xi = 0.50}$$

$$\sigma_{x_i} = \begin{Bmatrix} 0.0100 \\ 0.0216 \\ 0.0333 \end{Bmatrix}_1 \begin{Bmatrix} -2.89(10)^{-3} \\ -2.58(10)^{-3} \\ 4.25(10)^{-3} \end{Bmatrix}_2 \begin{Bmatrix} -9.21(10)^{-4} \\ 9.60(10)^{-4} \\ -3.78(10)^{-4} \end{Bmatrix}_3$$

$$\text{Response Spectrum} = \begin{Bmatrix} 0.0104 \\ 0.0218 \\ 0.0336 \end{Bmatrix}$$

$$\text{Power Spectrum (NASTRAN)} = \begin{Bmatrix} 0.0122 \\ 0.0226 \\ 0.0313 \end{Bmatrix}$$

$$\text{Response Spectrum with correction} = \begin{Bmatrix} 0.0115 \\ 0.0225 \\ 0.0338 \end{Bmatrix}$$

Figure 4.5. Example 4.1b

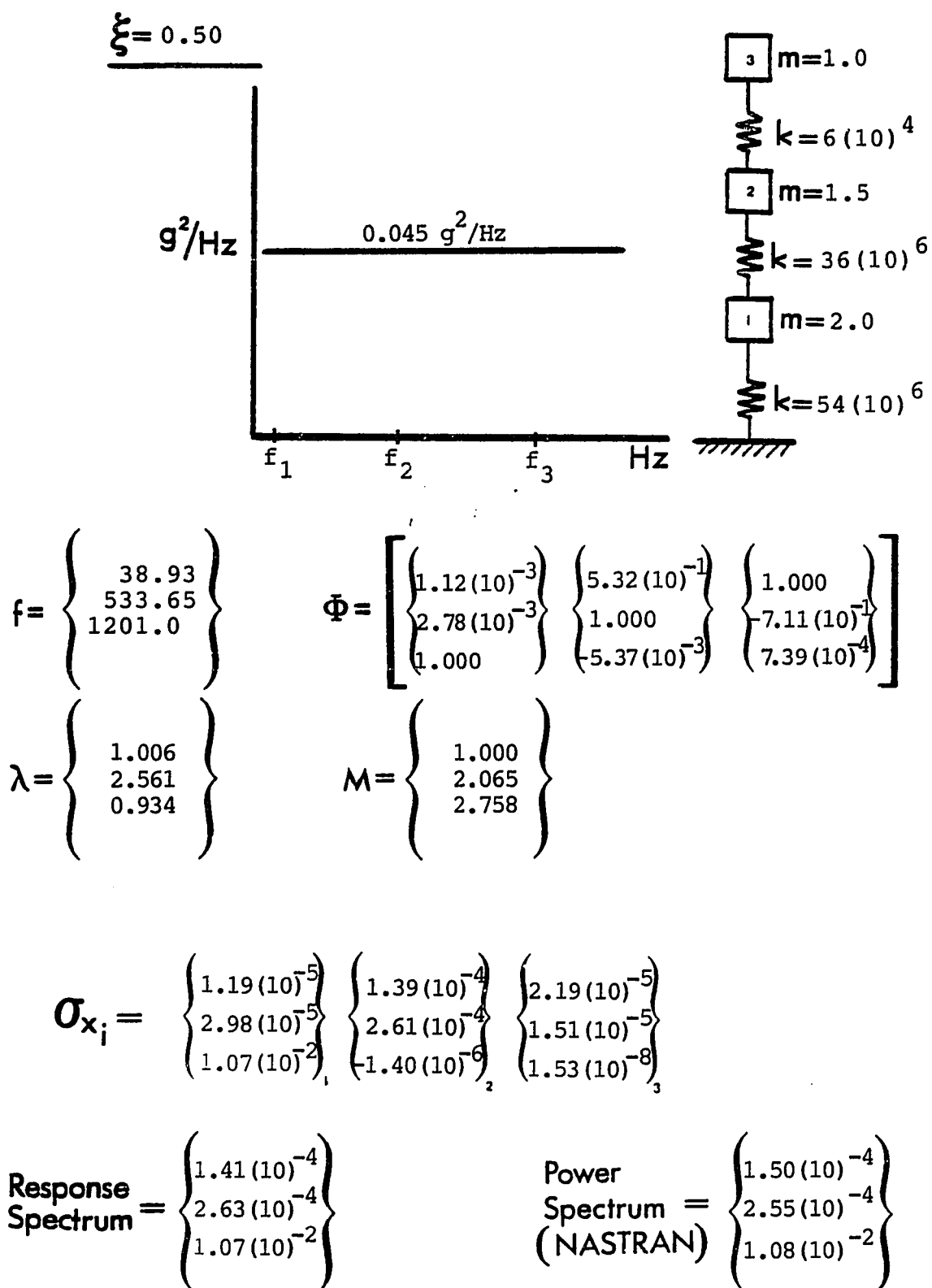
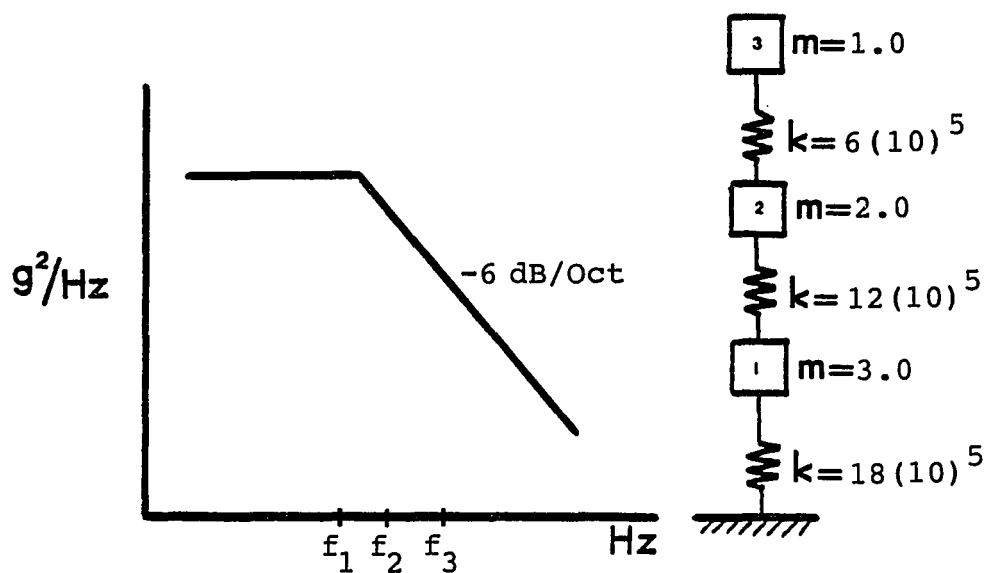


Figure 4.6. Example 4.1c



$$f = \begin{Bmatrix} 73.086 \\ 156.26 \\ 232.02 \end{Bmatrix} \quad \Phi = \begin{bmatrix} \begin{Bmatrix} 0.3018 \\ 0.6485 \\ 1.000 \end{Bmatrix} & \begin{Bmatrix} -0.6790 \\ -0.6066 \\ 1.000 \end{Bmatrix} & \begin{Bmatrix} -0.9598 \\ 1.000 \\ -0.3934 \end{Bmatrix} \end{bmatrix}$$

$$\lambda = \begin{Bmatrix} 2.576 \\ 1.256 \\ 0.813 \end{Bmatrix} \quad M = \begin{Bmatrix} 1.813 \\ 2.474 \\ 3.497 \end{Bmatrix}$$

$$\xi = 0.10$$

$$\sigma_{x_i} = \begin{Bmatrix} 3.99(10)^{-3} \\ 8.59(10)^{-3} \\ 1.32(10)^{-2} \end{Bmatrix}_1 \begin{Bmatrix} -8.21(10)^{-4} \\ -7.34(10)^{-4} \\ 1.21(10)^{-3} \end{Bmatrix}_2 \begin{Bmatrix} -1.97(10)^{-4} \\ 2.06(10)^{-4} \\ 8.09(10)^{-5} \end{Bmatrix}_3$$

$$\text{Response Spectrum} = \begin{Bmatrix} 4.08(10)^{-3} \\ 8.62(10)^{-3} \\ 1.33(10)^{-2} \end{Bmatrix} \quad \text{Power Spectrum (NASTRAN)} = \begin{Bmatrix} 4.16(10)^{-3} \\ 8.63(10)^{-3} \\ 1.32(10)^{-2} \end{Bmatrix}$$

Figure 4.7. Example 4.2a

$$\underline{\xi = 0.50}$$

$$\sigma_{x_i} = \begin{pmatrix} 1.79(10)^{-3} \\ 3.84(10)^{-3} \\ 5.92(10)^{-3} \end{pmatrix}_1 \begin{pmatrix} -3.67(10)^{-4} \\ -3.28(10)^{-4} \\ 5.41(10)^{-4} \end{pmatrix}_2 \begin{pmatrix} -8.83(10)^{-5} \\ 9.19(10)^{-5} \\ 3.62(10)^{-5} \end{pmatrix}_3$$

$$\text{Response Spectrum} = \begin{pmatrix} 1.83(10)^{-3} \\ 3.85(10)^{-3} \\ 5.94(10)^{-3} \end{pmatrix}$$

$$\text{Power Spectrum (NASTRAN)} = \begin{pmatrix} 2.12(10)^{-3} \\ 3.98(10)^{-3} \\ 5.53(10)^{-3} \end{pmatrix}$$

$$\text{Response Spectrum with correction} = \begin{pmatrix} 1.94(10)^{-3} \\ 4.08(10)^{-3} \\ 6.12(10)^{-3} \end{pmatrix}$$

Figure 4.8. Example 4.2b

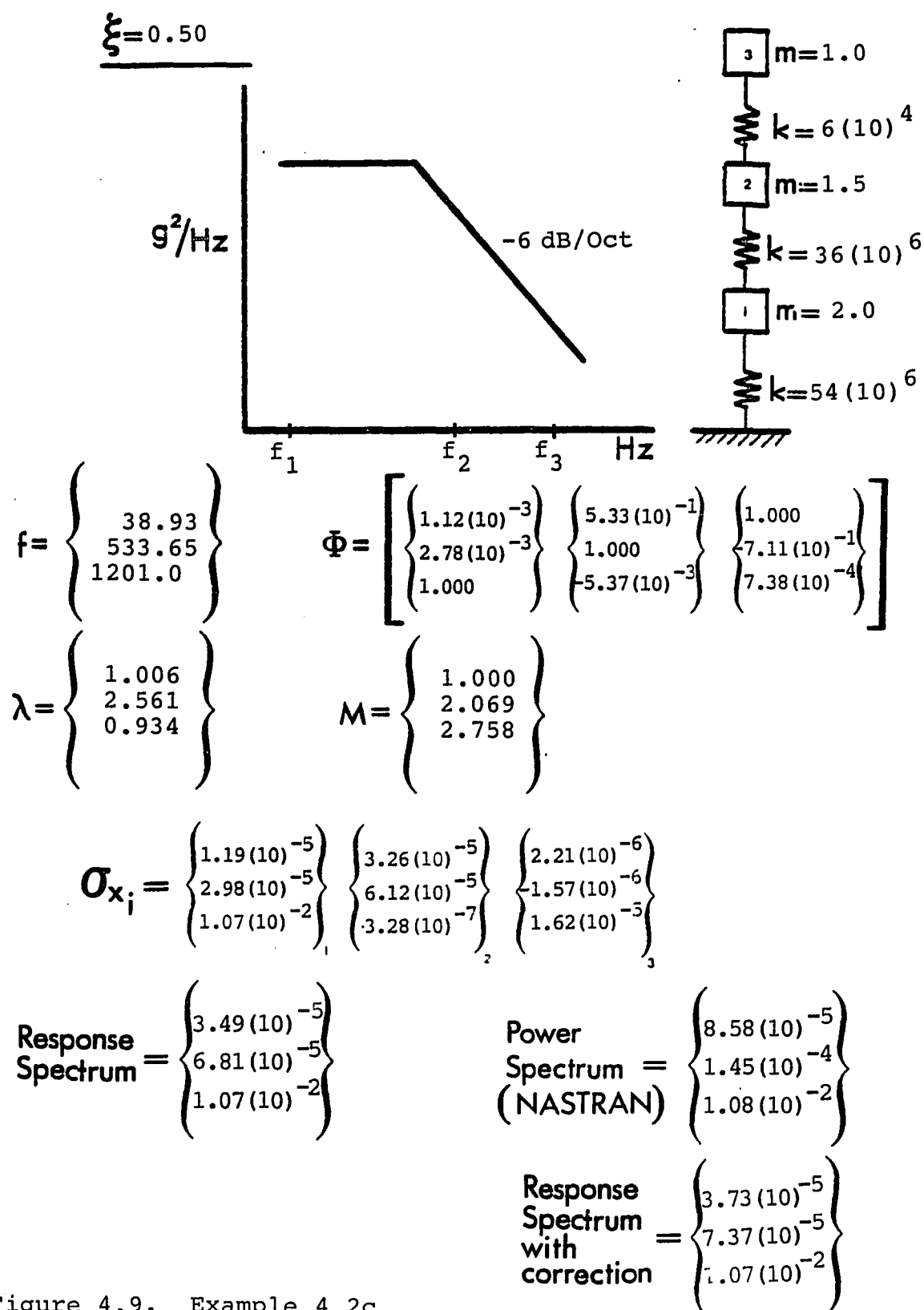
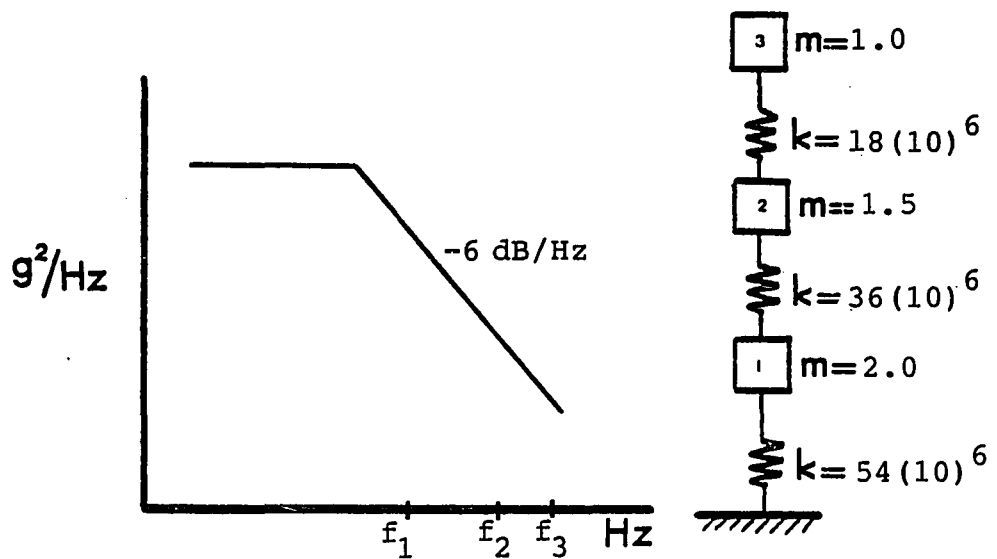


Figure 4.9. Example 4.2c



$$f = \begin{Bmatrix} 400.3 \\ 855.9 \\ 1270.8 \end{Bmatrix} \quad \Phi = \begin{bmatrix} \begin{Bmatrix} 0.3018 \\ 0.6485 \\ 1.000 \end{Bmatrix} & \begin{Bmatrix} -0.6790 \\ -0.6066 \\ 1.000 \end{Bmatrix} & \begin{Bmatrix} -0.9598 \\ 1.000 \\ -0.3934 \end{Bmatrix} \end{bmatrix}$$

$$\lambda = \begin{Bmatrix} 2.576 \\ 1.256 \\ 0.813 \end{Bmatrix} \quad M = \begin{Bmatrix} 1.813 \\ 2.474 \\ 3.497 \end{Bmatrix}$$

(a) $\xi = 0.0001$

$$\sigma_{x_i} = \begin{Bmatrix} 4.36(10)^{-4} \\ 9.34(10)^{-4} \\ 1.44(10)^{-3} \end{Bmatrix}_1 \quad \begin{Bmatrix} -5.23(10)^{-5} \\ -4.67(10)^{-5} \\ 7.70(10)^{-5} \end{Bmatrix}_2 \quad \begin{Bmatrix} -1.26(10)^{-5} \\ 1.31(10)^{-5} \\ -5.15(10)^{-6} \end{Bmatrix}_3$$

$$\text{Response Spectrum} = \begin{Bmatrix} 4.38(10)^{-4} \\ 9.36(10)^{-4} \\ 1.44(10)^{-3} \end{Bmatrix} \quad \text{Power Spectrum (NASTRAN)} = \begin{Bmatrix} 4.54(10)^{-4} \\ 9.61(10)^{-4} \\ 1.48(10)^{-3} \end{Bmatrix}$$

Figure 4.10. Example 4.3a

$$\underline{\xi = 0.10}$$

$$\sigma_{x_i} = \begin{Bmatrix} 9.72(10)^{-5} \\ 2.09(10)^{-4} \\ 3.22(10)^{-4} \end{Bmatrix}_1 \begin{Bmatrix} -1.17(10)^{-5} \\ -1.05(10)^{-5} \\ 1.72(10)^{-5} \end{Bmatrix}_2 \begin{Bmatrix} -2.81(10)^{-6} \\ 2.93(10)^{-6} \\ 1.15(10)^{-6} \end{Bmatrix}_3$$

$$\text{Response Spectrum} = \begin{Bmatrix} 9.80(10)^{-5} \\ 2.09(10)^{-4} \\ 3.23(10)^{-4} \end{Bmatrix}$$

$$\begin{matrix} \text{Power} \\ \text{Spectrum} = \\ \text{-(NASTRAN)} \end{matrix} \begin{Bmatrix} 14.52(10)^{-5} \\ 2.86(10)^{-4} \\ 4.18(10)^{-4} \end{Bmatrix}$$

$$\begin{matrix} \text{Response} \\ \text{Spectrum} \\ \text{with} \\ \text{correction} \end{matrix} = \begin{Bmatrix} 10.17(10)^{-5} \\ 2.13(10)^{-4} \\ 3.28(10)^{-4} \end{Bmatrix}$$

Figure 4.11. Example 4.3b

CHAPTER 5

APPLICATIONS

Design of the Support System For the SIRTf Primary Mirror

Success in the design of the Infrared Astronomical Satellite System in solving the technical problems associated with thermal and contamination control has demonstrated the feasibility of the proposed Space Infrared Telescope Facility (SIRTf). Fused silica, which has excellent figure stability at cryogenic temperatures, is a candidate for the material of the primary mirror of the telescope. Interfacing fused silica with structural metals (such as titanium or aluminum) requires an innovative design because of the large differential thermal contraction that occurs when the system is cooled to cryogenic temperatures.

For a 50 cm double-arch primary mirror design, a mirror mounting system was developed at the University of Arizona that incorporates clamp and flexure assemblies (Iraninejad). Three clamp and parallel spring guide flexure assemblies are attached to the back of the mirror 120 degrees apart (Figure 5.1). This design permits the

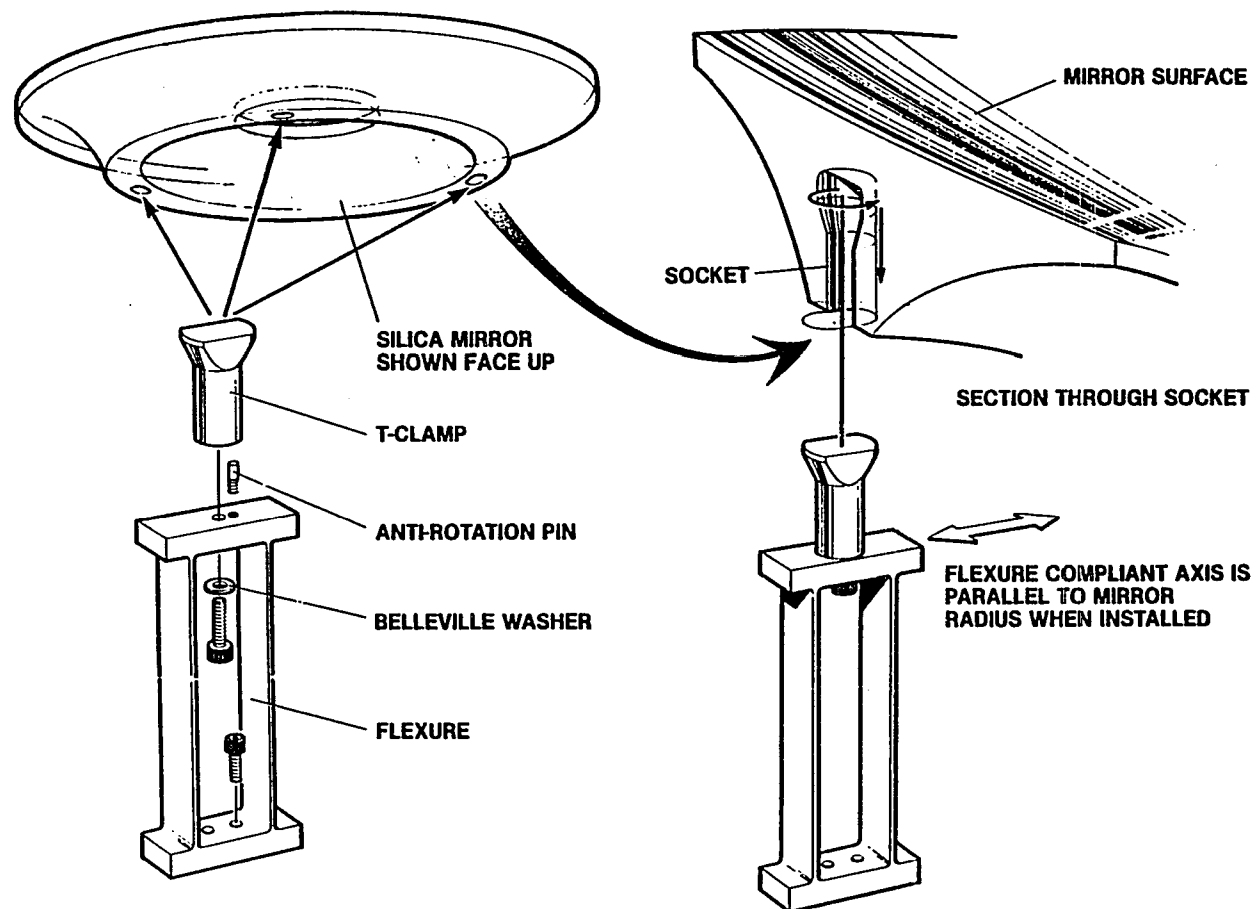


Figure 5.1. Mounting the SIRTf Primary Mirror

supporting structure to contract and transmit only acceptable intensities of bending moment and shear force to the mirror.

In addition to the cryogenic loading effects, the flexures must be designed to ensure survivability of the system during the launch of the space shuttle. A random loading environment has been prescribed to define launch conditions. Excitation loadings have been determined in the form of power spectral densities (PSD) in the three mutually orthogonal directions (Figures 5.2 and 5.3). Assuming that cross-correlations do not exist between these loadings, the responses can be determined independently and superimposed when appropriate.

Modeling the Structure

A finite element model was constructed to evaluate the RMS displacements and stresses in the half-meter primary mirror, the titanium flexures and the aluminum baseplate. A plot of the element mesh is shown in Figure 5.4. It is comprised of 925 nodes (3150 degrees of freedom), 384 solid hexahedron elements, and 60 plate bending elements.

The four lowest free vibration frequencies and their mode shapes were determined and are shown in Figures 5.5a thru 5.5d. The mode shapes comprise:

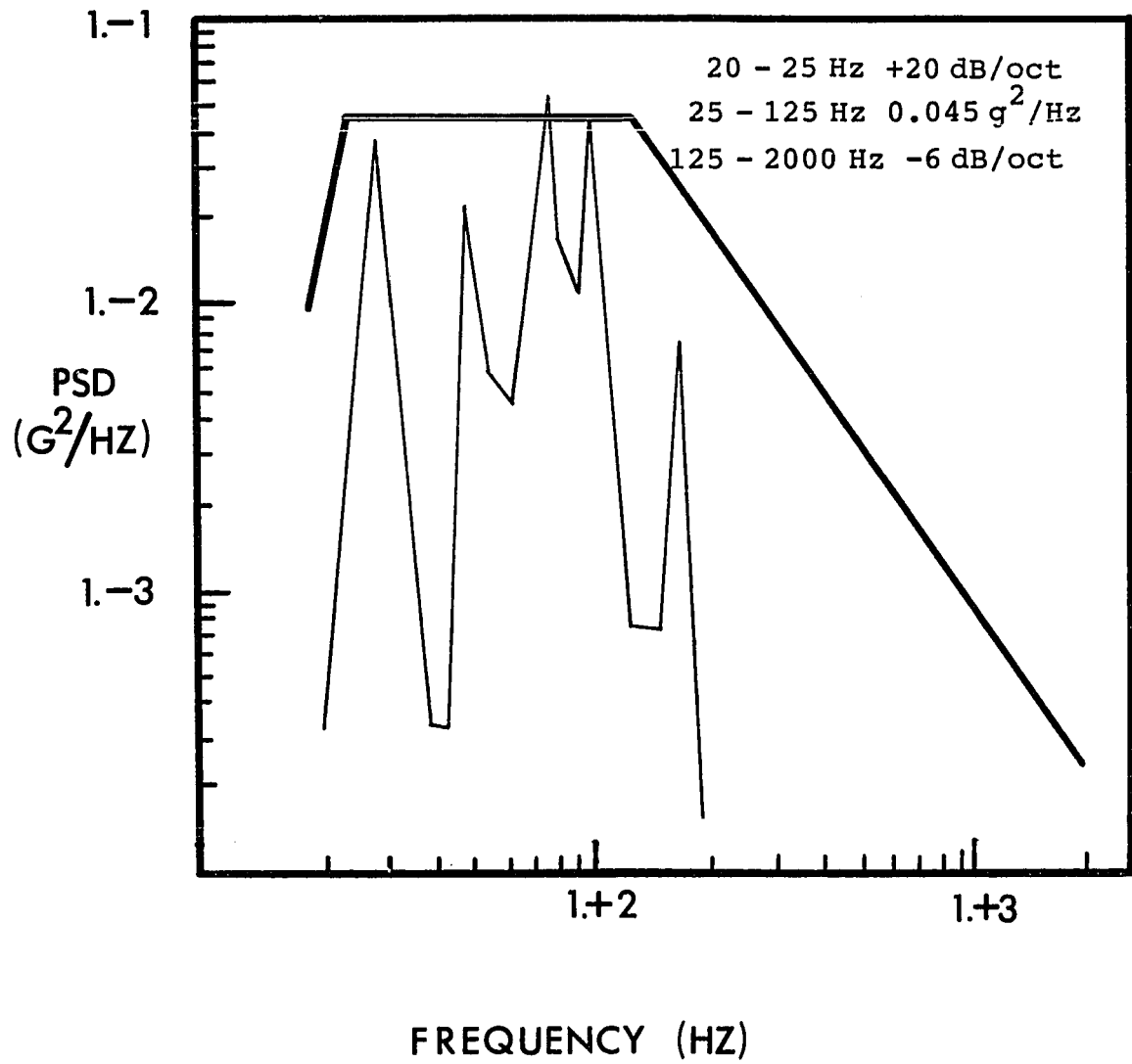


Figure 5.2. Random Vibration y-axis and z-axis Interface Levels

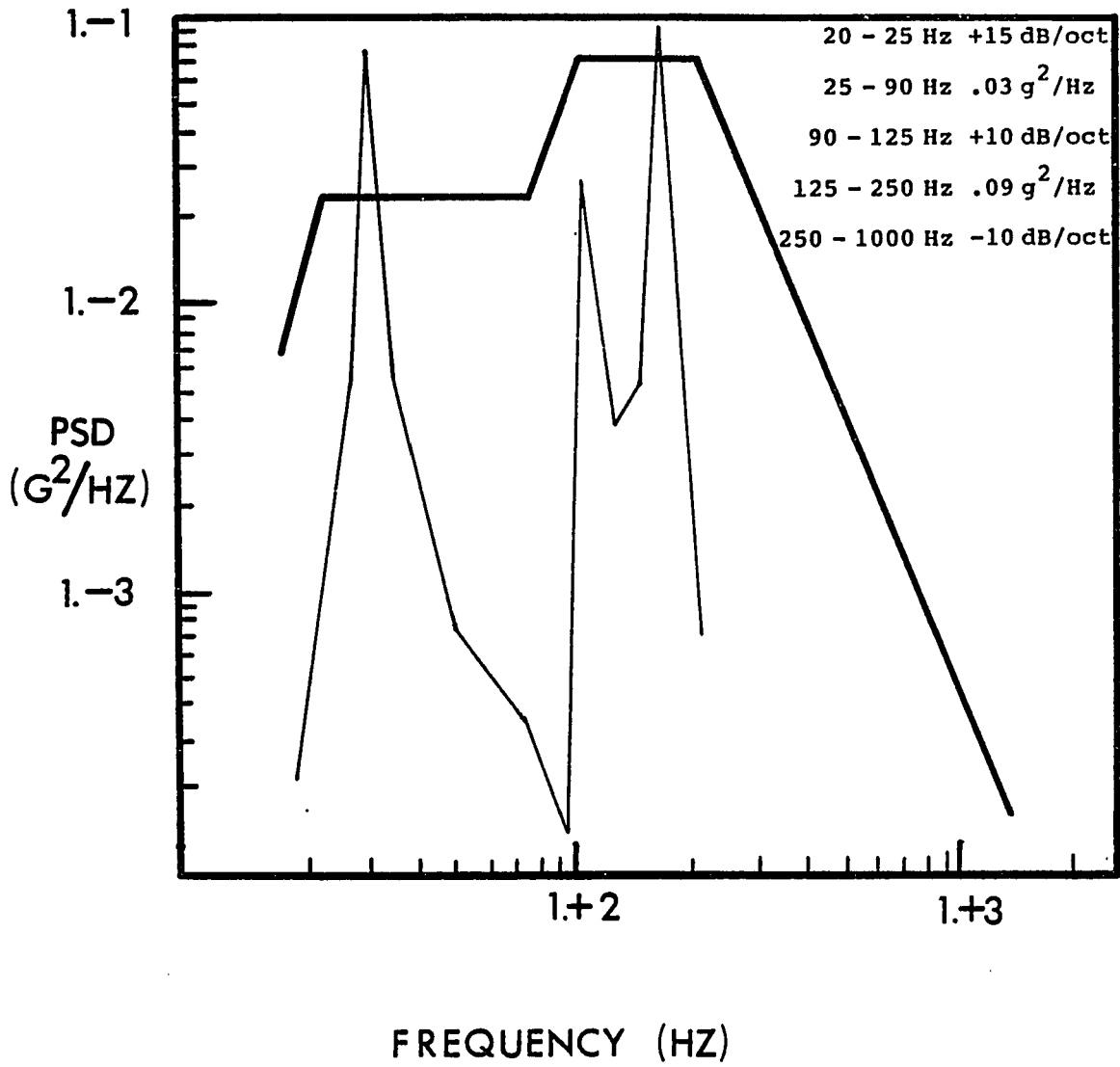


Figure 5.3. Random Vibration x-axis Interface Levels

- 1a. translation in the y-direction
- 1b. translation in the z-direction
2. twist about the x-axis
3. translation in the x-direction.

Because the relative stiffnesses of the mirror and the baseplate are an order of magnitude greater than the stiffness of the flexures for these displacement patterns, the free-vibration frequencies are almost entirely dependent upon the stiffness of the flexures.

Execution of a dynamic analysis with a large model such as that shown in Figure 5.4 can be very time consuming and expensive. The time required of a single eigenvalue solution for this model is on the order of 900 CPU seconds on a CYBER 175. Shown in Figure 5.6 is a simplified model (342 degrees of freedom) which was used for the Power Spectrum analysis of the primary mirror support system. The mirror has been replaced by rigid elements and beam bending elements model the flexures. Execution time of an eigenvalue extraction using this simplified model was on the order of 30 CPU seconds.

A further simplified model of the support structure was developed wherein the translational flexibility of the system is completely described by bending of the flexures. Shown in Figure 5.7, the bending stiffness of each flexure is represented by two springs, corresponding to each of the principal directions. Application of a unit displacement in the y-direction

demonstrates that the stiffness in that direction can be expressed in terms of a single combination of all of the stiffnesses. The entire structure can then be assumed to be a single-degree-of-freedom system when translated in either the y-direction or z direction.

By similar analyses, it was proved that each of the other 3 mode shapes could also be approximated by single-degree-of-freedom models. As shown in Table 5.1, this model was accurate enough for design purposes. Because of the assumption of no cross-correlation between the loadings, each excitation can be analyzed separately.

Summary of Results

Design of the flexural support system for the SIRT primary mirror requires the calculation of the shear force V , and the bending moment M , which occur in the flexures (Figure 5.8). When their maximum values have been determined, the maximum stresses in the flexures and in the mirror can be calculated. These values can be compared to allowable values so that a feasible design can be generated.

A parametric analysis was made to determine the RMS shear forces and bending moments in the flexures for various frequencies and damping ratios. Using the Response Spectrum Method and the input power spectral density functions, a response spectrum of the RMS relative

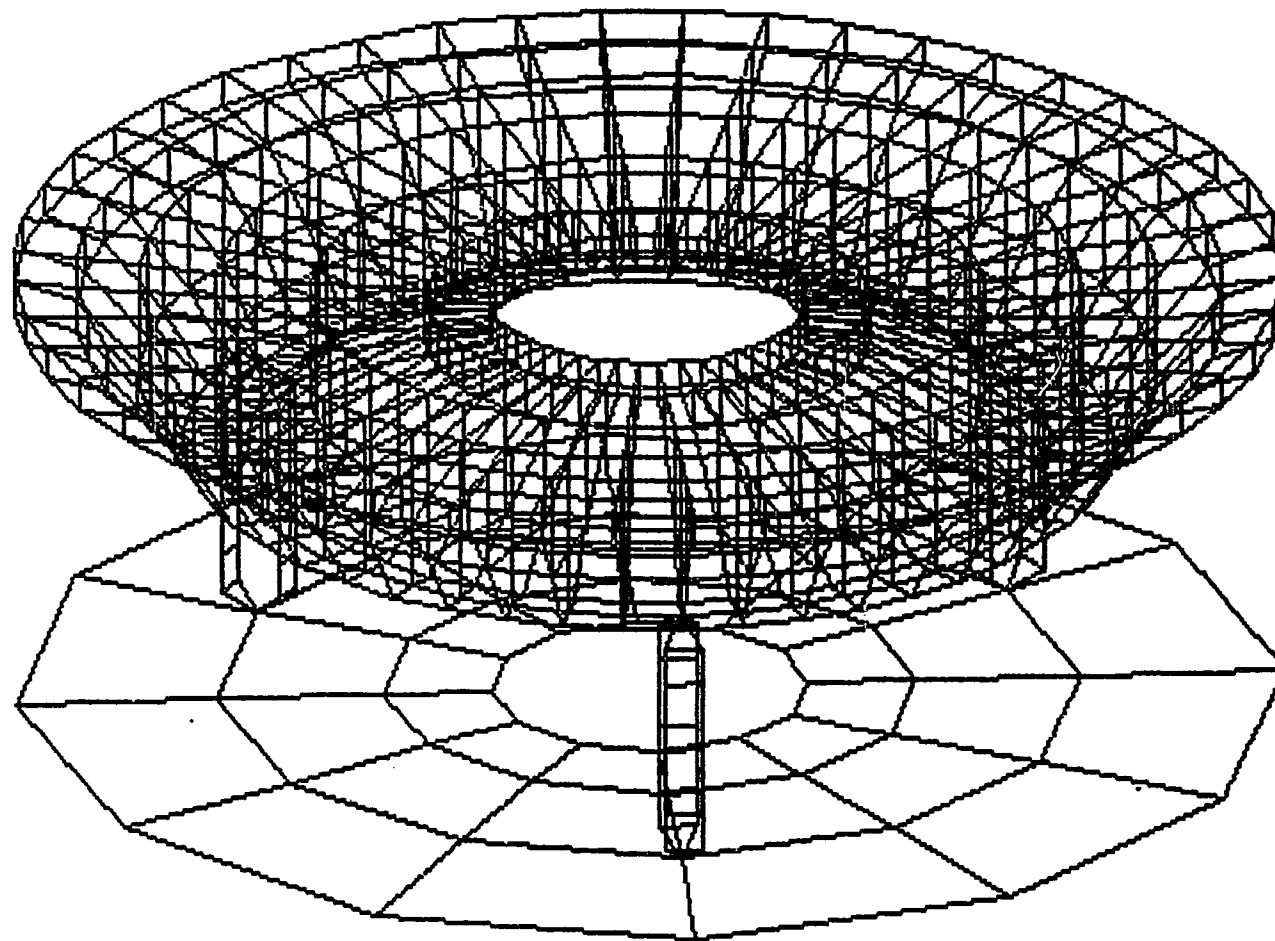
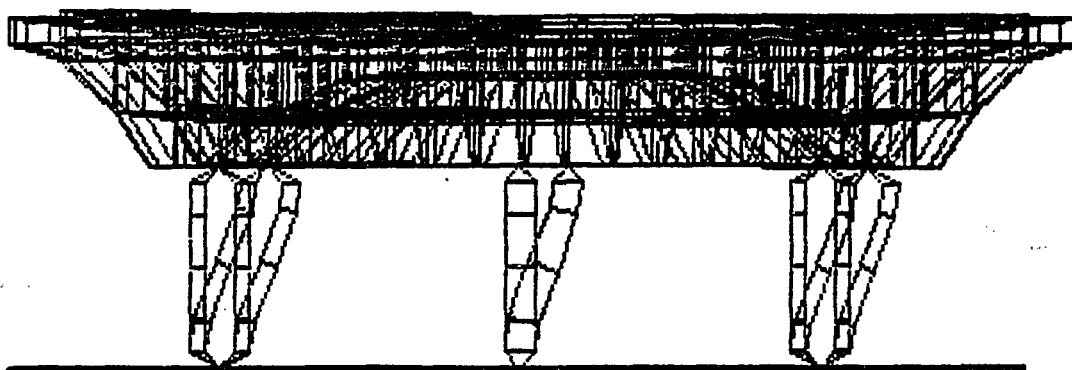
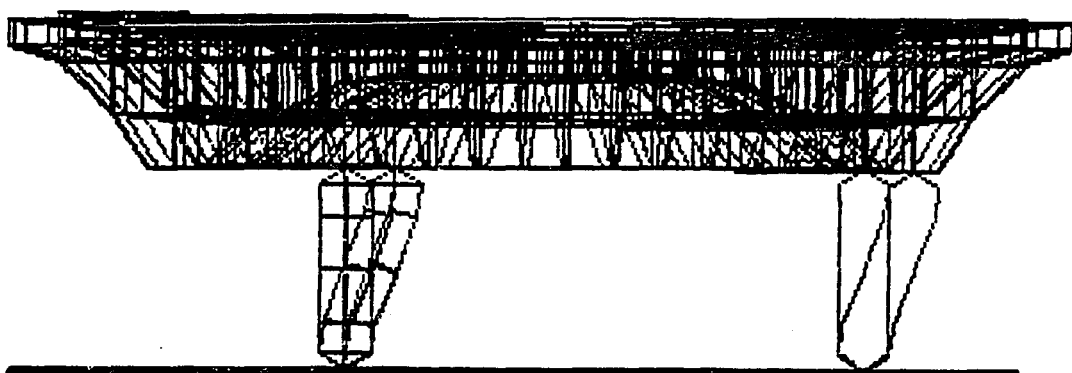


Figure 5.4. Complex Finite Element Model of the SIRTf Primary Mirror Support System

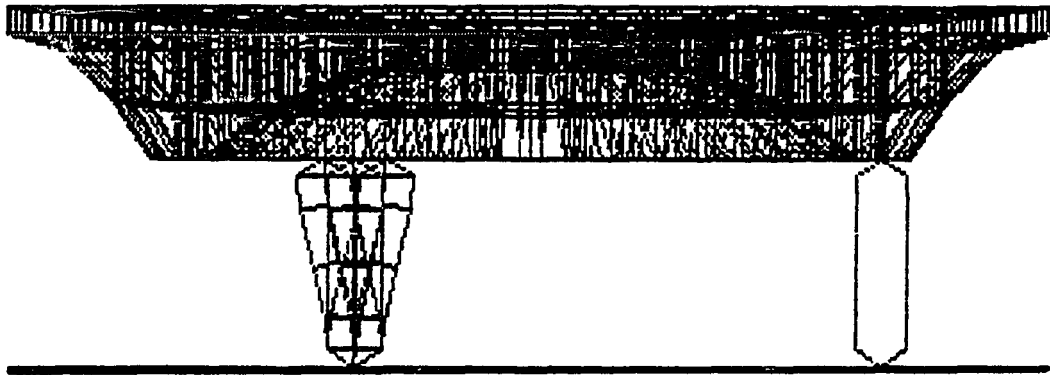


(a)

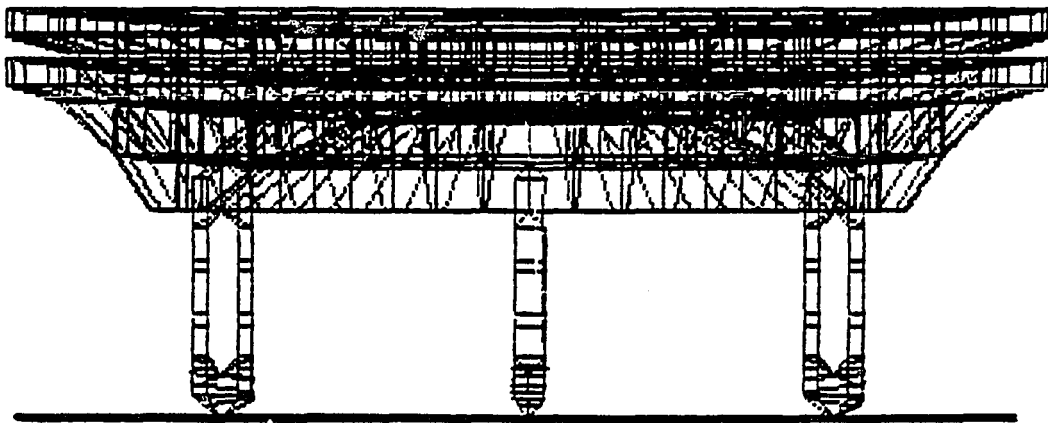


(b)

Figures 5.5a and 5.5b. Free-vibration Mode Shapes of the SIRTf Primary Mirror Support System



(c)



(d)

Figures 5.5c and 5.5d. Free-vibration Mode Shapes of the SIRTf Primary Mirror Support System

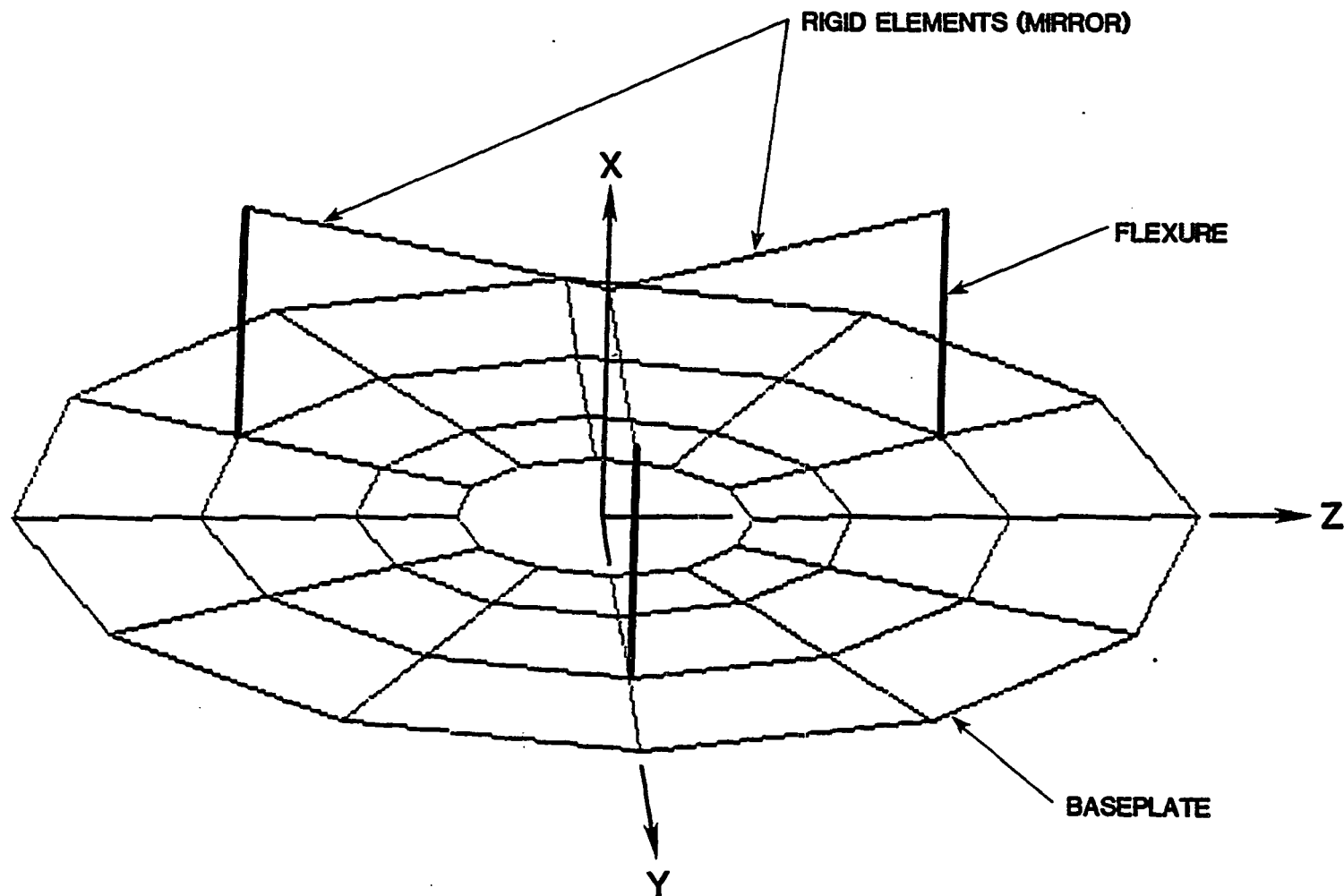


Figure 5.6. Simplified Finite Element Model of the SIRTf Primary Mirror Support System

displacement of the center of gravity of the mirror was calculated. Shear forces and bending moments which are a result of this relative displacement were determined from the following:

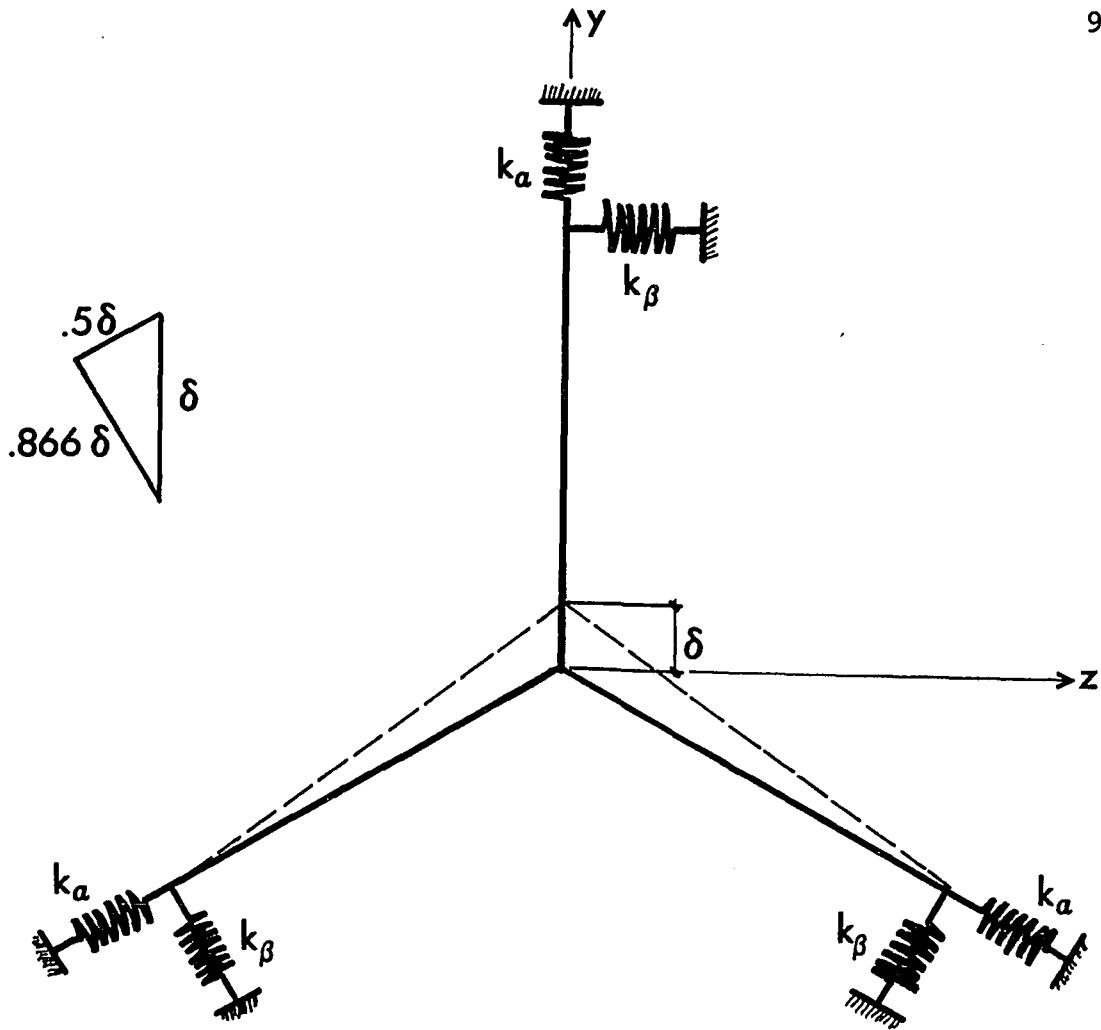
$$V = \frac{12EI}{L^3} \sigma_x \quad (5.1)$$

$$M = \frac{6EI}{L^3} \sigma_x \quad (5.2)$$

where: E = Young's Modulus (18×10^6 psi for titanium)
 I = effective moment of inertia
 L = length of the flexure
 σ_x = RMS relative displacement.

Note that equations 5.1 and 5.2 are the fixed-end forces for a flexural member.

Application of equations 5.1 and 5.2 with the Response Spectrum Method produced the response spectra shown in Figures 5.9 and 5.10 for a flexure length of 3 inches. These values of shear force and bending moment are the total values for the system. Shear forces and bending moments in the individual flexures are easily determined from the geometry of the structure (Figure 5.7). The response to the excitation in the x-direction does not produce an increase in the shear force or bending moment in the flexures because of the small lateral displacements which were of the order of 0.00001 of the flexure length.



$$\begin{aligned}\sum F_y &= \delta \left\{ k_a + 2(.5k_a \sin 30^\circ) + 2(.866k_\beta \cos 30^\circ) \right\} \\ &= \delta (k_a + k_\beta) 1.5 \\ \therefore \omega &= \sqrt{\frac{k}{m}} = \sqrt{\frac{1.5(k_a + k_\beta)}{m}}\end{aligned}$$

Figure 5.7. SDOF Idealization of the SIRTf Primary Mirror Support System

TABLE 5.1
Free-Vibration Frequencies of the
SIRTF Primary Mirror Support System

	Mode 1a y-translation	Mode 1b z-translation	Mode 2 Twist about x	Mode 3 x-translation
1. NASTRAN complex finite element model (Figure 5.4)	57.62	57.62	78.3	463.2
2. NASTRAN simplified finite element model (Figure 5.6)	57.61	57.61	78.2	461.2
3. SDOF model (Figure 5.7)	57.6	57.6	78.2	461.1

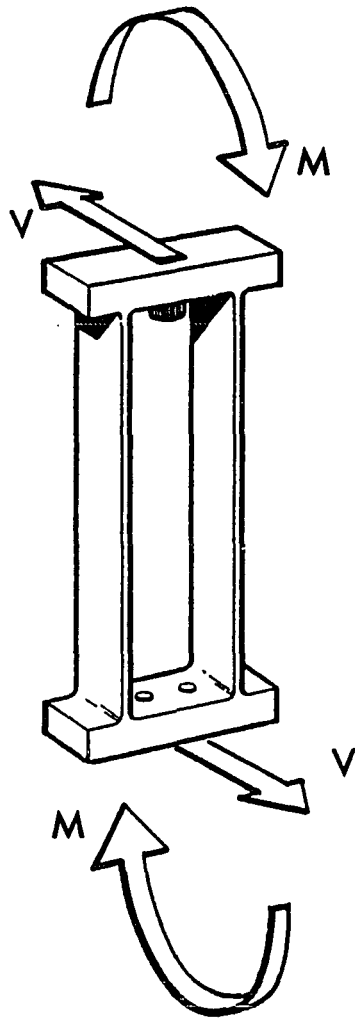


Figure 5.8. Shear Forces and Bending Moments Applied to the Flexures About Strong Axis

Analysis of the structure was also made by the Power Spectrum Method using the model shown in Figure 5.6. Shear forces and bending moments in the flexures were determined at discrete frequencies and are indicated in Figures 5.9 and 5.10. Excellent correlation with the Response Spectrum Method was demonstrated in the lower ranges of damping and frequency.

Additional calculations were made using the shear force and bending moments to determine the RMS stresses in candidate flexure cross-sections. These are presented in Figure 5.11. For a limiting value of maximum RMS stress and a given damping ratio the fundamental frequency of the system can be obtained. Cross-sectional dimensions of flexures which produce this frequency are readily determined from the calculations shown in Figure 5.7.

Example 5.1

Design the cross-section of the flexures subjected to the -6 dB/Oct loading as shown in Figure 5.3:

$$\text{Damping ratio} = 0.001$$

$$\text{Effective flexure length } L = 3 \text{ inches}$$

$$\text{Mass of mirror} = 0.0908 \frac{\text{lb}}{\text{in}} \text{sec}^2.$$

To determine an allowable RMS stress for the flexures, the 3σ criteria (Robson) was applied to the limiting material stress. For 6Al - 4V titanium, this limiting stress was

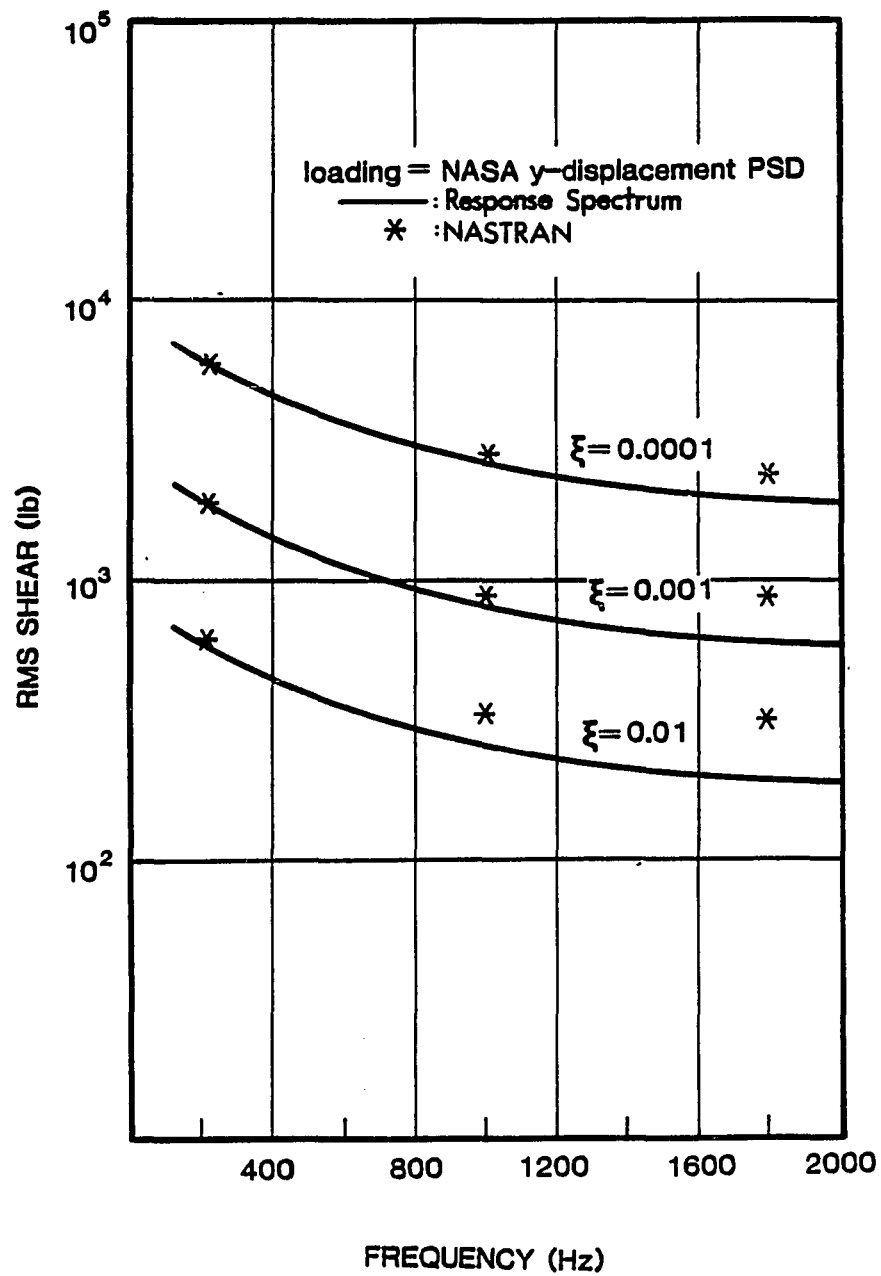


Figure 5.9. Shear Force Response Spectrum for y-axis Random Vibration

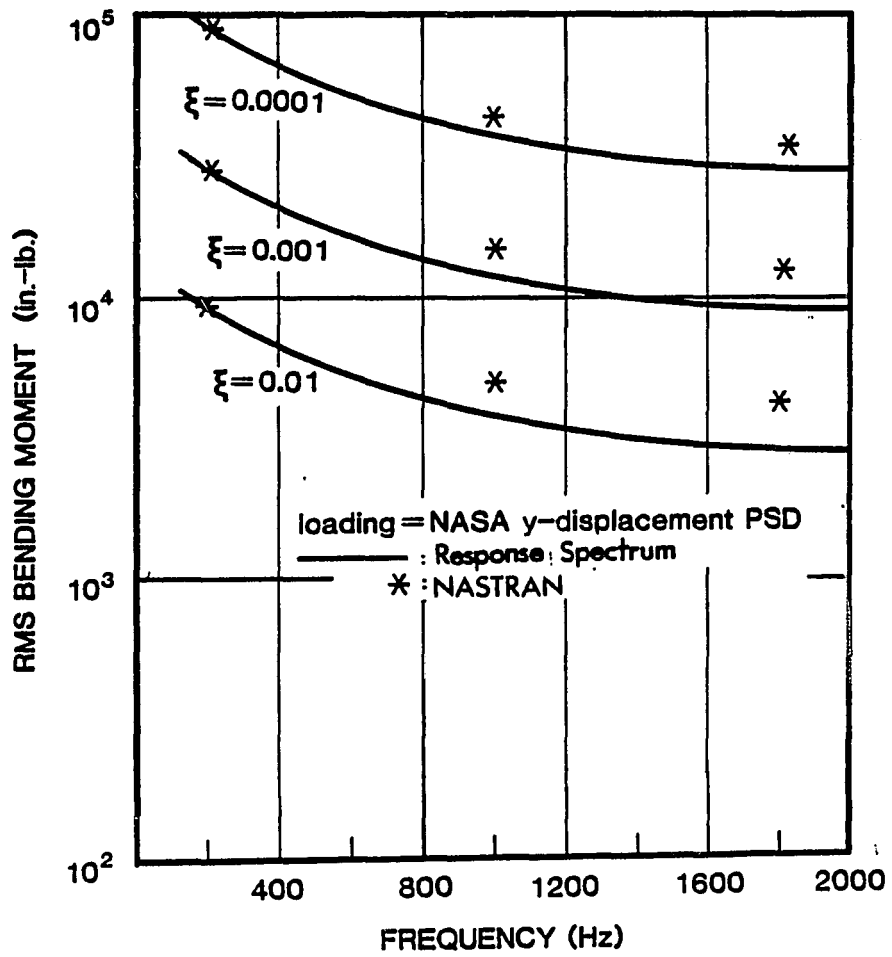


Figure 5.10. Bending Moment Response Spectrum for y-axis Random Vibration

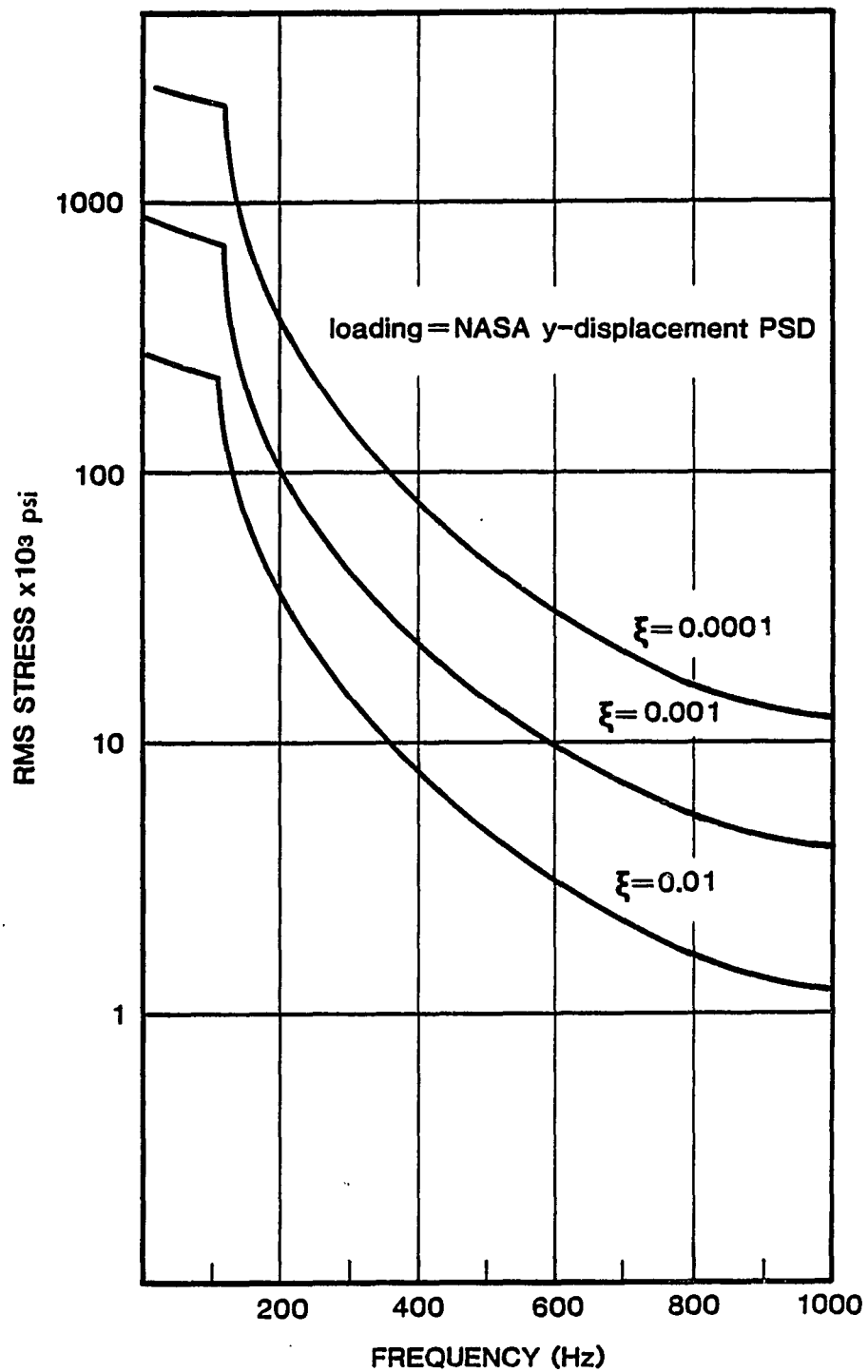


Figure 5.11. Maximum RMS Stress in the Flexures for Combined y-axis and z-axis Random Vibration

the microcreep stress level of 120,000 psi (Marschall). Therefore, by setting the RMS design stress at 40,000 psi, the probability that the limiting value of 120,000 psi will be exceeded is 0.3%. Referring to Figure 5.12, for a damping ratio of 0.001 and a limiting RMS allowable stress of 40,000 psi, the fundamental frequency of the system is 320 Hz. From Figure 5.8,

$$\omega^2 = \frac{k}{m} = \frac{12EI_{\text{eff}}}{mL^3} \quad I_{\text{eff}} = 1.5(I_1 + I_2)$$

$$\omega^2 = (320 * 2\pi)^2 = \frac{12(18)10^6 I_{\text{eff}}}{0.0908(3)^3}$$

$$\text{solving for } I_{\text{eff}} = 0.0459 \text{ in}^4$$

Therefore, a support system of three flexures, each having an effective moment of inertia of its cross-section of 0.0459 in^4 , has a maximum RMS stress of 40,000 psi for the combination of random excitations in the y and z directions as shown in Figure 5.3. As a check, a Power Spectrum analysis using a finite element model with the cross-sectional dimensions of each flexure blade as $b = 1.10 \text{ in.}$ and $h = 0.12 \text{ in.}$ ($I_{\text{eff}} = 0.041$) produced a maximum RMS stress of 41,486 psi.

Damping Evaluation with the
White Noise Equation

To calculate the stresses and displacements which occur in a structure when subjected to random excitation the importance of the transfer function has been demonstrated. It has also been shown (Clough and Penzien) that for damping ratios less than 0.10 the maximum response of a structure to random excitation occurs at or very near resonant frequency ($\omega = \omega_n$) which simplifies the equation for the transfer function to:

$$H(\omega) = \frac{1}{2\xi\omega_n^2} \quad (5.3)$$

As shown in Figure 5.12, the effect on the response of varying the damping can be substantial. However, the damping can be difficult to quantify in most problems as it may be a combination of several factors (e.g., air damping or intergranular friction damping).

Application of the white noise equation together with a laboratory experiment can be useful in determining the damping ratio of a SDOF system. Rearrangement of equation 2.23 yields:

$$\xi = \frac{S_f \pi f_n}{4\sigma_a^2} \quad (5.4)$$

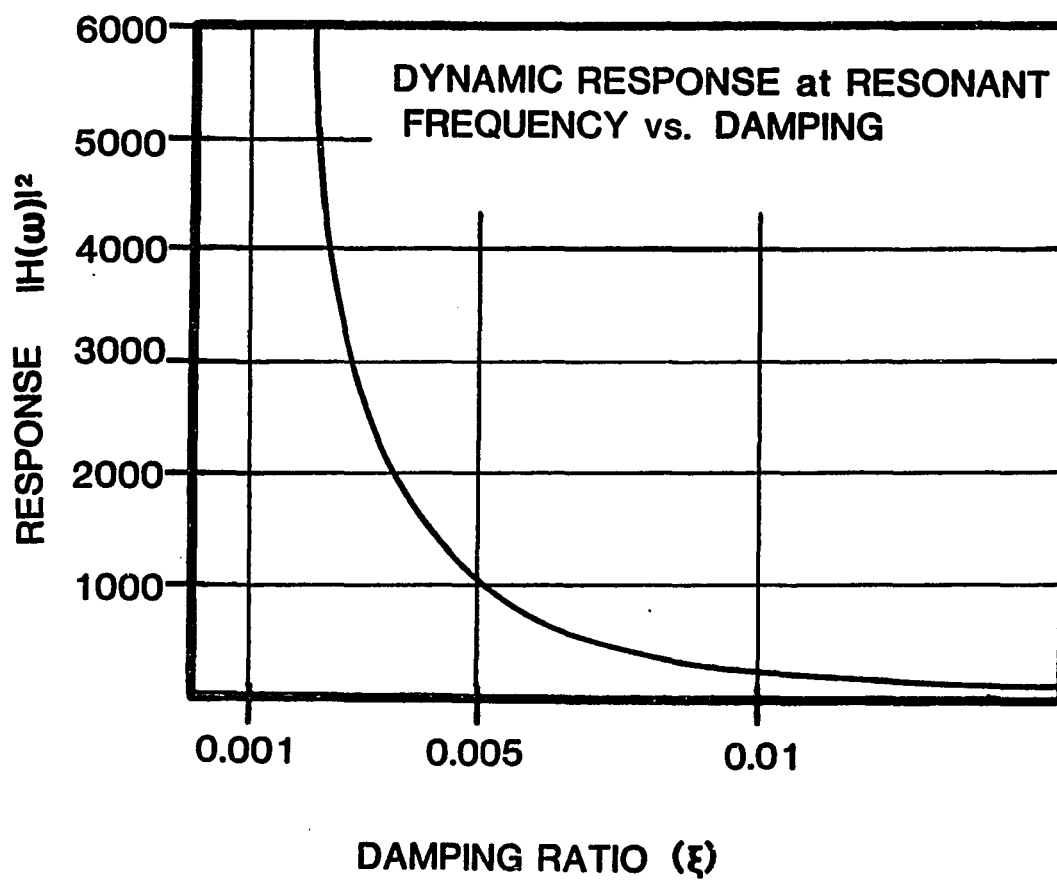


Figure 5.12. Dynamic Response at Resonant Frequency vs. Damping

where: σ_a^2 = mean-square of the relative acceleration response

S_f = white noise PSD input

f_n = fundamental frequency

(Values of σ_a^2 and S_f could be obtained from laboratory tests equipment.)

Example 5.2

As an example, if the damping ratio for a SDOF system with a fundamental frequency of 120 Hz subjected to a white noise PSD input of $0.01 \text{ g}^2/\text{Hz}$, the mean-square of relative acceleration response is 18.49 g^2 . So that the damping ratio of 0.05 is given by:

$$\xi = \frac{0.01(\pi)120}{4(4.3)^2} = 0.05$$

CHAPTER 6

SUMMARY AND CONCLUSIONS

Development of the Response Spectrum and the Power Spectrum Methods for the analysis of SDOF and MDOF structures subjected to random excitations has been presented. Accuracy of the Power Spectrum Method can be limited by the accuracy of its numerical integration procedure. Approximations which have been made in the formulation of the Response Spectrum Method (which is based upon the white noise solution for SDOF systems) limit its application to specified ranges of damping, frequency and input spectral density envelopes.

The limitations to the accuracy of the Response Spectrum Method for the analysis of SDOF systems have been determined by comparing the solutions which were obtained by the white noise equation to the solutions which were obtained by the NASTRAN finite element program which uses the Power Spectrum Method. From the comparison of the solutions, the curves in Figures 3.5a and 3.5b were generated. Using these figures, the maximum value of the damping ratio can be estimated for which the white noise

approximation produces a difference of less than 5 percent with the Power Spectrum Method for a given slope of the PSD input and natural frequency. As shown in Chapter 4, these figures may also be used for MDOF systems in which the response of the structure is primarily in its first mode.

In the analysis of MDOF systems, each of the methods was formulated using modal analysis to decouple the set of differential equations. Example problems were presented to demonstrate the application of each method to MDOF problems. Effects of modal interaction were not accounted for in the Response Spectrum Method and can be substantial for systems with closely-spaced frequencies. However, a modification term which was added to the Response Spectrum Method to account for modal interaction was shown to increase its accuracy to within acceptable limits for certain problems.

When the Power Spectrum Method is used, calculation of internal forces and stresses in MDOF systems requires the re-formulation of the unknown displacement vector. This procedure is transparent to the analyst when the NASTRAN finite element program is used. Stresses and internal forces are calculated using a root-sum-square procedure for the Response Spectrum Method.

The cost of execution of the Power Spectrum Method can be very expensive. Each curve which was generated in Figures 3.4a thru 3.4h required the calculation of the RMS relative displacement at each of several distinct frequencies, each of which used about 30 CPU seconds of CYBER 175 computer time. The resulting eight sets of curves required about 500 CPU seconds per set. By comparison, the entire set of curves generated by the Response Spectrum Method required less than 5 CPU seconds.

In conclusion, the Response Spectrum Method has been shown to be a very economical and accurate analytical technique which can be used for the random vibration analysis of a large class of structures. Care and judgment must be used in its application to problems which contain high levels of damping, high frequency or large slopes of the PSD input function. However, as is demonstrated in this dissertation, the white noise approximation can provide a reasonable estimate of the response of heavily damped systems to random excitations.

REFERENCES

- BENDAT, J. S. Principles and Applications of Random Noise Theory, Wiley, 1957.
- BLACKMAN, R. B. and J. TUKEY, "The Measurement of Power Spectra," Bell System Technical Journal, Vol. 37, 1958.
- CLARKSON, B. L. "The Design of Structures to Resist Jet Noise Fatigue," Journal Royal Aerospace Society, Vol. 66, 1962.
- CLOUGH, R. W. AND J. PENZIEN, Dynamics of Structures, McGraw Hill, New York, 1975.
- COOK, ROBERT D. Concepts and Applications of Finite Element Analysis, Wile and Sons, New York, 1974.
- CRAMER, H. Mathematical Models of Statistics, Princeton University Press, Princeton, 1946.
- CRANDALL, STEPHEN H. Random Vibration, The Massachusettes Institute of Technology, Cambridge, Massachusettes, 1958.
- . Random Vibration, Volume Two, The Massachusettes Institute of Technology, Cambridge, Massachusettes, 1963.
- DAVENPORT, W. B. and W. L. ROOT, An Introduction to the Theory of Random Signals and Noise, McGraw-Hill, New York, 1958.
- DYER, I. and P. SMITH, "Sonic Fatigue Resistance of Structural Designs," ASD TR 61-262, Wright-Patterson Air Force Base, Ohio, 1961.
- FELLER, W. Probability Theory and its Applications, Wiley, New York, 1950.

- GALLAGHER, RICHARD H. Finite Element Analysis Fundamentals. Prentice-Hall, Englewood Cliffs, New Jersey, 1975.
- GOCKEL, M. A. MSC/NASTRAN Handbook for Dynamic Analysis, The MacNeal-Schwendler Corporation, Los Angeles, 1983.
- HECKEL, M. A. "Vibrations of Print-Driven Cylindrical Shells," Journal of Acoustic Society, Vol. 34, 1962.
- HURTY, W. C. and M. RUBINSTEIN, Dynamics of Structures, Prentice-Hall, New Jersey, 1964.
- IRANINEJAD, B. "Double Arch Mirror Study," NASA Ames Engineering Analysis Report, Optical Sciences Center, University of Arizona, 1983.
- JOSEPH, JERRARD A. "MSC/NASTRAN Application Manual," CDC Version, The MacNeal-Schwendler Corporation, Los Angeles, 1986.
- KAPUR, K. K. and C. IP, "Random Vibration Using the Finite Element Approach," Shock and Vibration Bulletin, 38, 1968.
- LANING, J. H. and R. BATTIN, Random Processes in Automatic Control, McGraw-Hill, 1957.
- LYON, R. H. "Sound Radiation From a Beam Attached to a Plate," Journal of Acoustic Society, Vol. 34, 1962.
- MILES, J. W. "On Structural Fatigue under Random Loading," Journal of Acoustic Society, Vol. 21, 1954.
- MINER, M. A. "Cumulative Damage in Fatigue," Journal of Applied Mechanics, Vol. 12, 1945.
- NEWMARK, N. M. and E. ROSENBLUETH, Fundamentals of Earthquake Engineering, Prentice-Hall, Englewood Cliffs, New Jersey, 1971.
- POWELL, A. "On the Fatigue Failure of Structures Due to Vibrations Excited by Random Pressures Fields," Journal of Acoustic Society, Vol. 30, 1958.
- RICE, S. O. "Mathematical Analysis of Random Noise," Bell Systems Technical Journal, Vol. 23, 1945.

- ROBSON, J. D. An Introduction to Random Vibration, University Press, Edinburgh, 1963.
- ROSENBLUETH, E. "A Basis for Aseismic Design," Thesis, University of Illinois, 1951.
- ROSENBLUETH, E. and J. ELDORDUY, "Responses of Linear Systems to Certain Transient Disturbances," Proceedings 4th WCEE, Santiago, 1969.
- SCHAEFFER, HARRY G. MSC/NASTRAN Primer: Static and Normal Modes Analysis, Wallace Press, Milford, 1982.
- STEARN, S. M. "Spatial Variation of Stress, Strain and Acceleration in Structures Subject to Broad Frequency Band Excitation," Journal of Sound and Vibration, 12, May 1970.
- TACK, D. H. and R. LAMBERT, "Response of Bars and Plates to Boundary Layer Turbulence," Journal of Aerospace Science, Vol. 29, 1962.
- THOMSON, W. T. and M. BARTON, "The Response of Mechanical Systems to Random Excitation," Journal of Applied Mechanics, Vol. 24, 1957.
- THOMSON, WILLIAM T. Theory of Vibration with Applications, Prentice-Hall, Englewood Cliffs, New Jersey, 1981.
- VANMARCKE, ERICK H. "Structural Response to Earthquakes", Seismic Risk and Engineering Decisions, Elsevier, Amsterdam, 1976.
- _____. "Seismic Safety Assessment", Random Excitation of Structures by Earthquakes and Atmospheric Turbulence, International Centre for Mechanical Sciences, Udine, Italy, 1977.
- ZIENKIEWICZ, O. C. The Finite Element Method, McGraw-Hill, London, 1977.